Order Number 9009736

Chemical, physical and spectroscopic studies of two clostridial-type 2(4Fe-4S) ferredoxins

Gluck, Martin Ronald, Ph.D.

City University of New York, 1989

U·M·I
300 N. Zeeb Rd.
Ann Arbor, MI 48106

A

CHEMICAL, PHYSICAL AND SPECTROSCOPIC STUDIES OF TWO CLOSTRIDIAL-TYPE 2(4Fe-4S) FERREDOXINS

by

MARTIN R. GLUCK

A dissertation submitted to the Graduate Faculty in Biochemistry in partial fulfillment of the requirements for the degree of Doctor of Philosophy, The City University of New York

1989

This manuscript has been read and accepted for the Graduate Faculty in Biochemistry in satisfaction of the dissertation requirement for the degree of Doctor of Philosophy.

October 2, 1989
Date

Chair of Examining Committee

October 2, 1989
Date

Executive Officer

Supervisory Committee

The City University of New York

ABSTRACT

CHEMICAL, PHYSICAL AND SPECTROSCOPIC STUDIES OF TWO CLOSTRIDIAL-TYPE 2(4Fe-4S) FERREDOXINS

by

Martin R. Gluck

Advisor: Dr. William V. Sweeney

The clostridial-type 8Fe ferredoxins contain two 4Fe-4S centers, and are responsible for the oxidation-reduction properties of these proteins. Although it was originally thought for many clostridial-type 8Fe ferredoxins, particularly from Clostridium pasteurianum, the apparent midpoint reduction potential (E_m) was pH dependent, evidence is presented in the first part of this thesis that demonstrates the absence of such a pH dependent midpoint reduction potential.

The central portion of this thesis describes some physical, chemical and spectroscopic studies of reductively methylated Clostridium pasteurianum 8Fe ferredoxin. The results show that the N-terminal amine in this protein is in an ion pair in both the oxidized and reduced forms of the protein, and that this ion pair is likely to be homologous to the one observed in Peptococcus aerogenes, another 8Fe ferredoxin for which an x-ray structure is known. Disruption of the normal ion pair by

methylation appears to substantially decrease the intrinsic stability of the protein. Also presented is a spectroscopic analysis of the optical purity ratio, A_{390}/A_{280}, that characterizes the quantitative meaning of this widely used ratio. By the methods described it is possible to correlate the extent of protein denaturation with the change in the purity ratio as the protein undergoes degradation.

The latter part presents a thorough investigation of the products formed when 8Fe ferredoxin from either Clostridium pasteurianum or Clostridium acidi-urici is reacted with potassium ferricyanide. The results indicate that a variety of products are formed which contain varied amounts of peptide, iron and sulfide. The different iron and sulfide content reflects the presence of various iron-sulfur centers including the 3Fe and 4Fe types. However, a more homogeneous protein is formed if the native protein is allowed to degrade under aerobic conditions.

The final part examines the uptake of isotopically prepared alpha-^{2}H-L-cysteine into the 8Fe ferredoxin from Clostridium acidi-urici so that assignments can be made for these resonances in the ^{1}H-NMR spectrum of this protein. NMR analysis revealed that three of the eight alpha-cysteinyl resonances are downfield shifted while the remaining five appear to be buried within the aliphatic envelope.

Acknowledgement

I wish to extend special thanks to Dr. William V. Sweeney, my thesis advisor, for his help and guidance throughout my undergraduate and graduate career. I would also like to thank the members of my thesis committee, Prof. Peter Lipke, Prof. Klaus Grohmann, Prof. Jacqueline Barton and Prof. Fred Nadar. I am particularly thankful to Prof. Klaus Grohmann for his help in the synthesis of isotopically labelled cysteine and his useful discussions concerning chemical modification of proteins. Credits are due to Prof. Michelle Broido and Dr. Michael Blumenstein at Hunter College for their very useful NMR discussions. Additionally, credits are also due to Dr. Micheal Adams at the University of Georgia for his helpful advice in the purification of hydrogenase proteins, and to Dr. Micheal Johnson , also at the University of Georgia, for his collaborative contributions in helping me complete my work on the characterization of ferricyanide treated 8Fe ferredoxins. Finally, I wish to thank Laura Vinson for providing gas phase calculations and computer simulations of various ion pair conformations.

TABLE OF CONTENTS

LIST OF ABBREVIATIONS

ala	alanine
asp	aspartate
CAU	Clostridium acidi-urici
CD	circular dichroism
CP	Clostridium pasteurianum
cys	cysteine
DMSO	dimethyl sulfoxide
DSS	sodium 2,2-dimethyl-2-silapentane-5-sulfonate
DTNB	5,5'-dithiobis-(2-nitrobenzoic acid)
E_{mdpt} or E_m	midpoint reduction potential
EPR	electron paramagnetic resonance
E_{soln}	solution potential
Fd	ferredoxin
Fd_{ox}	oxidized ferredoxin
Fd_{red}	reduced ferredoxin
Fd_{apo}	apoferredoxin
Fe-S	iron-sulfur
8Fe Fd	ferredoxin containing 2(4Fe-4S) centers
3Fe Fd	ferredoxin containing 3Fe-4S centers
HIPIP	High Potential Iron-Sulfur Protein
$K_3Fe(CN)_6$	potassium ferricyanide
lys	lysine
MCD	magnetic circular dichroism
mV	millivolts

LIST OF ABBREVIATIONS (continued)

MW	molecular weight
NMR	nuclear magnetic resonance
PA	Peptococcus aerogenes
pK_{red}	pK of ferredoxin protein in reduced form
pK_{ox}	pK of ferrdoxin protein in oxidized form
pK_{apo}	pK of protein in apoferredoxin
Rd	rubredoxin protein
SDS	sodium dodecyl sulfate
TMS	tetramethylsilane
w/v	weight to volume
w/w	weight to weight

LIST OF TABLES

List of Figures

INTRODUCTION

Ferredoxins are non-heme iron-sulfur proteins that have been isolated from a variety of organisms including bacteria, plants and mammals (1). Ferredoxins belong to a larger class of proteins, the iron-sulfur proteins, which are now recognized as among the main types of electron transferring proteins in biological systems, together with heme and flavoproteins (2). The iron-sulfur proteins contain, in addition to the polypeptide chain an inorganic cofactor, the iron-sulfur center, which is required for redox activity. The iron-sulfur center, composed of iron and sulfide, is covalently attached to the peptide through cysteinyl sulfur ligands (3). The x-ray crystallographic structures of several ferredoxins have revealed the presence of different types of iron-sulfur centers (Figure I). Structure A represents the 2Fe-2S centers representative of bacterial ferredoxins such as Halobacterium halobium and plants such as spinach or parsely, and spirulina blue green algae (4-8). Structure B, the 3Fe-4S center, a relatively recent finding , is found in bacterial proteins from E. coli, Thermus thermophilus and Azotobacter vinelandii , among others (9-11). This type of center is also found in mammalian aconitase, a long-known citric acid cycle enzyme (12). Structure C , the 4Fe-4S center, is characteristic of the clostridial-type ferredoxins and the iron-sulfur proteins found in hydrogenase, NADH dehydrogenase and High

Figure I. Common recognized types of known Fe-S centers

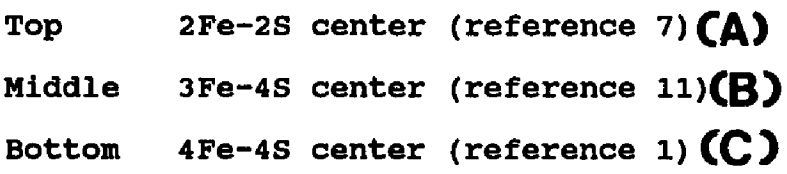

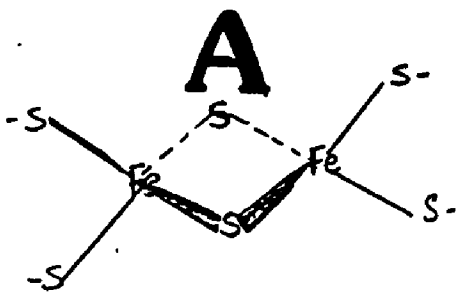
A
S-
S
-S
Fe
Fe
S
S-
-S

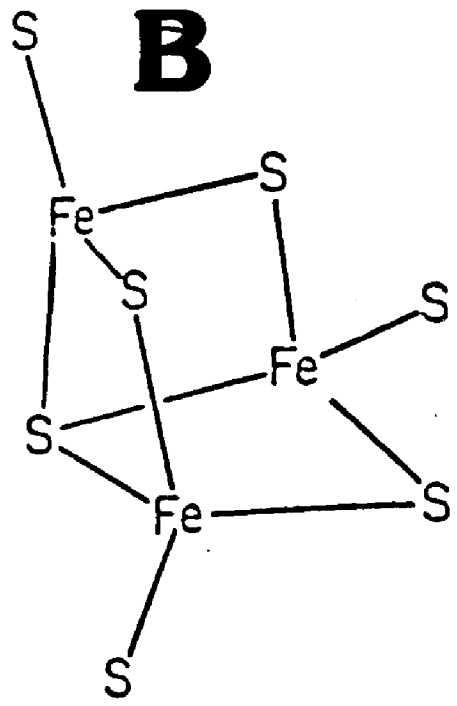
B
S
S
Fe
S
S
Fe
S
S
Fe
S
S

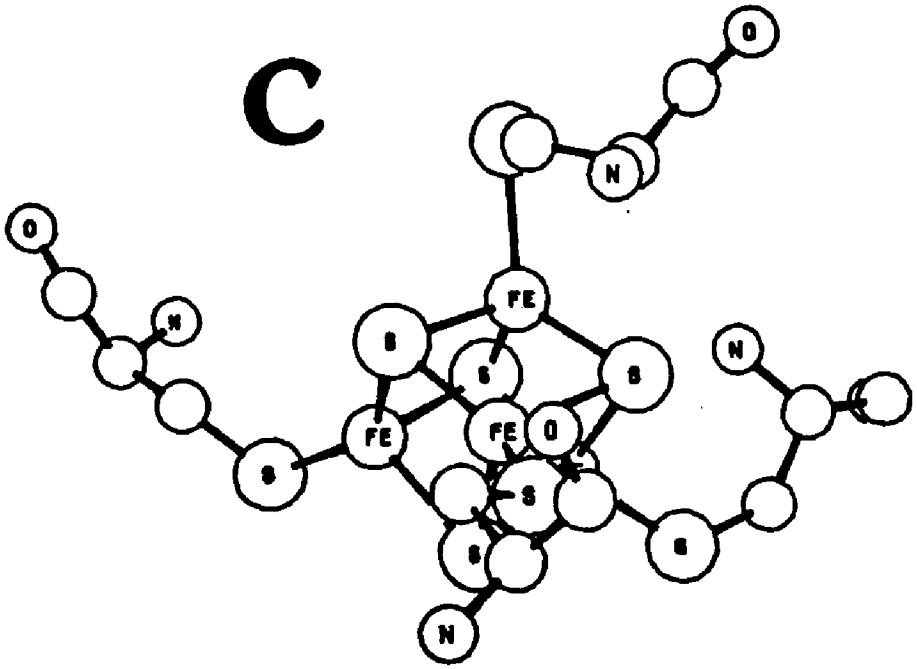
C
O
N
FE
S
FE
FE
O
S
N
N

Potential Iron-Sulfur protein (HIPIP) from Chromatium vinosum (13-16). The nomenclature (XFe-YS) refers only to the composition of the cofactor itself and not its ligands. However, x-ray data has shown that the 2Fe-2S center is covalently bound to the polypeptide chain by four cysteinyl thiol ligands whereas the 3Fe-4S and 4Fe-4S centers have three and four thiol ligands, respectively.

Iron-sulfur proteins can function as single electron transfer centers or in complex protein assemblies (2). These assemblies can include flavins, hemes, thiamine pyrophosphate and even other metals such as molybdenum (Table I). Iron-sulfur proteins are ubiquitous in living organisms and have been the focus of a large number of investigations. The clostridial-type ferredoxins are the most well-characterized iron-sulfur protein. This is due in part to their small size, as many iron-sulfur proteins are associated into complex subunits , and their readily available sources from bacteria such as Clostridium pasteurianum and Clostridium acidi-urici. It has been shown that the spectroscopic properties of the complex iron-sulfur proteins in many cases display significant similarities to the simpler ferredoxin-type iron-sulfur proteins. Thus, it is apparent that the study of ferredoxins should lead to a better understanding of the more complex iron-sulfur proteins by providing simpler paradigms for modeling the more complex protein systems.

Table I. Diversity of iron-sulfur proteins in various enzymes

PROSTHETIC GROUP	Enzymes
Iron-sulfur group(s)	Hydrogenase, aconitase, ferredoxin, glutamine amidoribosyl transferase, w-hydroxylase, photosystem I
Iron-sulfur-flavin	succinate dehydrogenase, NADH dehydrogenase, glutamine synthase, dihydroorotate dehydrogenase, formate dehydrogenase, enolate reductase
Iron-sulfur-heme	sulfite reductase, nitrate reductase, ubiquinone-cytochrome C reductase
Iron-sulfur-heme-flavin	sulfite reductase, nitrate reductase
Iron-sulfur-molybdenum	nitrogenase, formate dehydrogenase CO_2 reductase, nitrate reductase
Iron-sulfur-flavin molybdenum	xanthine oxidase, xanthine dehydrogenase , aldehyde oxidase
Iron-sulfur-thiamine pyrophosphate	pyruvate-ferredoxin oxidoreductase 2-oxoglutarate-ferredoxin oxido-reductase, 2-oxobutyrate ferredoxin oxidoreductase

This importance is underscored, for instance, by nitrogenase - a complex iron-sulfur protein containing a 3Fe-1Mo-4S center - which is the only known protein that is able to enzymatically convert atmospheric nitrogen into ammonia.

The studies herein described concern the chemical, physical and spectroscopic properties of the 2(4Fe-4S) ferredoxins from Clostridium pasteurianum and Clostridium acidi-urici.

A. Clostridium pasteurianum and Clostridium acidi-urici 2(4Fe-4S) ferredoxin

1. Structure

Clostridium pasteurianum 2(4Fe-4S) ferredoxin, first isolated by Mortenson in 1962, was the first reported iron-sulfur protein (17). Subsequently, ferredoxin from other bacteria including Clostridium acidi-urici was isolated (18). The amino acid sequences of the two ferredoxins are shown in Table II, along with that of an analogous ferredoxin from Peptococcus aerogenes for which an x-ray structure has been published (19-21). The close sequence homology between the three ferredoxins (80%-90%) is likely to indicate homologous structural features and chemical behavior. Accordingly, any discussions presented here regarding the structure of CP or CAU ferredoxin is

Table II. Comparison of amino acid sequences and composition of 8Fe ferredoxins from *C. pasteurianum*, *C. acidi-urici* and *P. aerogenes*

TABLE II

										10		
1.	ala	tyr	lys	ile	ala	asp	ser	cys	val	ser	cys	gly
2.	ala	tyr	val	ile	asn	glu	ala	cys	ile	ser	cys	gly
3.	ala	tyr	val	ile	asn	asp	ser	cys	ile	ala	cys	gly
								20				
1.	ala	cys	ala	ser	glu	cys	pro	val	asn	ala	ile	ser
2.	ala	cys	asp	pro	glu	cys	pro	val	asp	ala	ile	ser
3.	ala	cys	lys	pro	glu	cys	pro	val	asn		ile	gln
						30						
1.	gln	gly	asp	ser	ile	phe	val	ile	asp	ala	asp	thr
2.	gln	gly	asp	ser	arg	tyr	val	ile	asp	ala	asp	thr
3.	gln	gly		ser	ile	tyr	ala	ile	asp	ala	asp	ser
				40								
1.	cys	ile	asp	cys	gly	asn	cys	ala	asn	val	cys	pro
2.	cys	ile	asp	cys	gly	ala	cys	ala	gly	val	cys	pro
3.	cys	ile	asp	cys	gly	ser	cys	ala	ser	val	cys	pro
		50										
1.	val	gly	ala	pro	val	gln	glu					
2.	val	asp	ala	pro	val	gln	ala					
3.	val	gly	ala	pro	asn	pro	glu	asp				

Ferredoxin	hydrophobic residues	neutral residues	acidic residues	basic residues
C. pasteurianum	27	20	7	1
C. acidi-urici	28	17	9	1
P. aerogenes	26	20	7	1

based on the assumption that they are likely to be closely related to the x-ray structure of PA ferredoxin. This also includes comparison of spectroscopic and magnetic properties, iron and acid-labile sulfur content and chemical reactivity.

The clostridial-type 8Fe ferredoxins contain two 4Fe-4S centers that are covalently bound to the polypeptide through cysteinyl sulfur ligands. Because the peptide is small most of it is used to make up the hydrophobic binding cavity for the 4Fe-4S centers. The amino acid sequences of CP and CAU ferredoxin show sequence homology within the protein between amino acids 1-28 and 29-55 (Figure II). This sequence homology gives the native holoprotein an approximate two-fold axis of symmetry. Unlike many proteins, ferredoxins do not contain any disulfides or free sulhydryls. Instead, the cysteines are used to bind the Fe-S center. For PA, CP and CAU 2(4Fe-4S) ferredoxin cysteines 8, 11, 14 and 45 are used to bind one of the 4Fe-4S centers. The other center is held by cysteines 35, 38, and 41 (cys-37 , 40 and 43 for the homologous CP and CAU ferredoxin) and cysteine 18 . A schematized diagram is presented in Figure III.

Each cysteinyl sulfur becomes covalently bonded to one iron in the 4Fe-4S center , where the irons in the cluster only approximate tetrahedral geometry, and the cubane-like structure is actually distorted into D_{2d} symmetry. The distance between the two centers is about

Figure II. Sequence homology of *Clostridium pasteurianum* ferredoxin between amino acids 1-27 and 28-55

(adapted from reference 19)

ala <-> ile-29

tyr <-> phe

lys val

ile <-> ile

ala asp

asp ala

ser asp

8-cys <-> cys-37

val <-> ile

ser asp

11-cys <-> cys-40

gly <-> gly

ala asn

14-cys <-> cys-43

ala <-> ala

ser <-> asn

glu val

18-cys <-> cys-45

pro <-> pro

val <-> val

asn gly

ala <-> ala

Ile <-> pro

ser val

gln <-> gln

gly glu-55

asp

28-ser

Figure III. Relative positions of cysteine residues in Clostridium pasteurianum 8Fe ferredoxin used in forming the binding domains for the 2(4Fe-4S) centers

(adapted from reference 1)

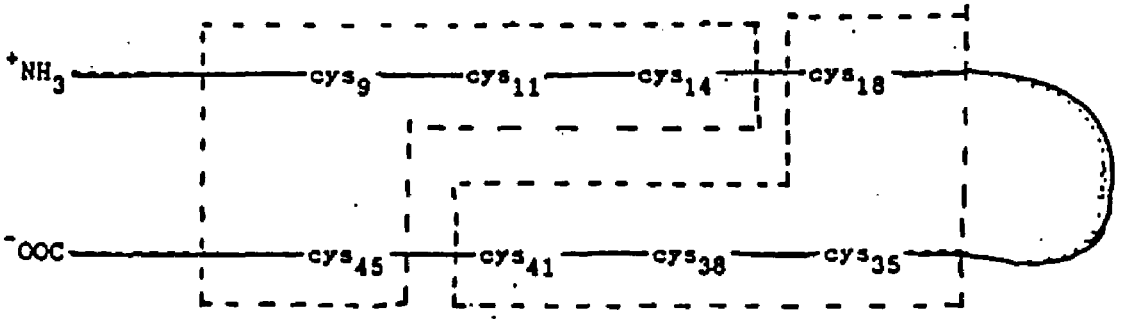
+NH3
cys9
cys11
cys14
cys18
-OOC
cys45
cys41
cys38
cys35

twelve angstoms and they are buried within hydrophobic cavities in each domain of the polypeptide (Figure IV). However, one cysteinyl sulfur atom from each Fe-S center , Cys-11 and 38, is solvent exposed. Piercing into the hydrophobic domain around the 4Fe-4S centers are several amino acid side chains that hydrogen bond with the sulfurs in the cluster or the cysteinyl sulfurs bound to the cluster. The only two aromatic residues in PA ferredoxin, Tyr-2 and Tyr-28, each lie about 3.5 angstoms from one of the sulfurs of each cluster. Several angstroms from Tyr-2 lies the N-terminal amine, which is in close proximity to the carboxyl groups of Asp-37 and the carboxy-terminus (1).

2. Metabolism

The roles of ferredoxin in the oxidation-reduction linked metabolic reactions of CP and CAU have been characterized and are shown schematically in Figures V and VI, respectively (3,22,23). Besides carbohydrate chemistry, CP ferredoxin is also important in nitrogenase linked electron transport reactions as illustrated in Figure VII. It can also be used to transfer electrons to the hydrogenase catalyzed reaction $Fd_{red} + 2H^{+} \longrightarrow Fd_{ox} + H_2$. Ferredoxin can transfer electrons to cytochrome C as well (3,24,25).

Figure IV. Stereodiagrams of Peptococcus aerogenes oxidized 8Fe ferredoxin including peptide backbone, iron-sulfur centers and hydrophobic binding cavities

(Taken from reference 1)

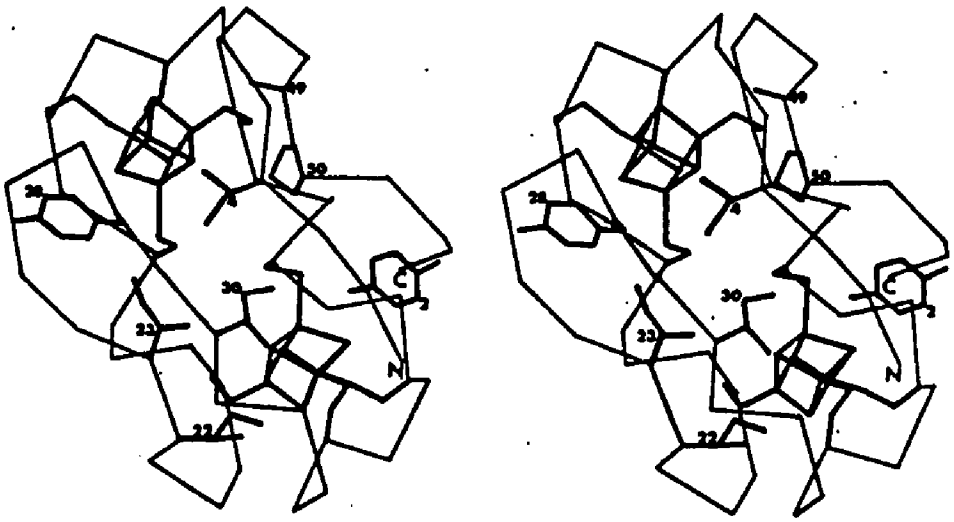

Figure V. *In vivo* and *in vitro* reactions catalyzed by *Clostridium pasteurianum* 8Fe ferredoxin

(adapted from reference 3)

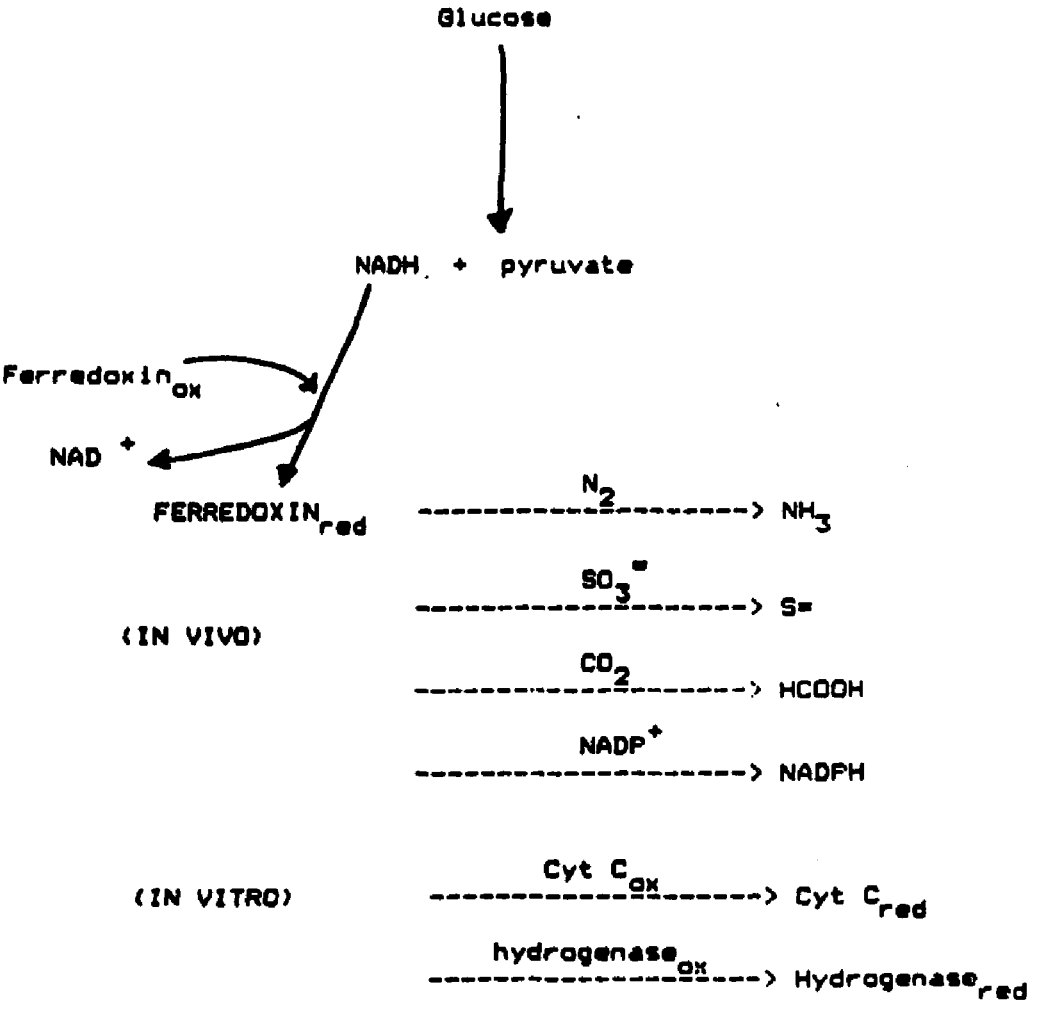
Glucose
NADH + pyruvate
Ferredoxin ox
NAD +
FERREDOXIN red
N2
NH3
SO3=
S=
(IN VIVO)
CO2
HCOOH
NADP+
NADPH
(IN VITRO)
Cyt C ox
Cyt C red
hydrogenase ox
Hydrogenase red

Figure VI. Role of Clostridium acidi-urici 8Fe ferredoxin in uric acid and pyruvate metabolism

(adapted from reference 23)

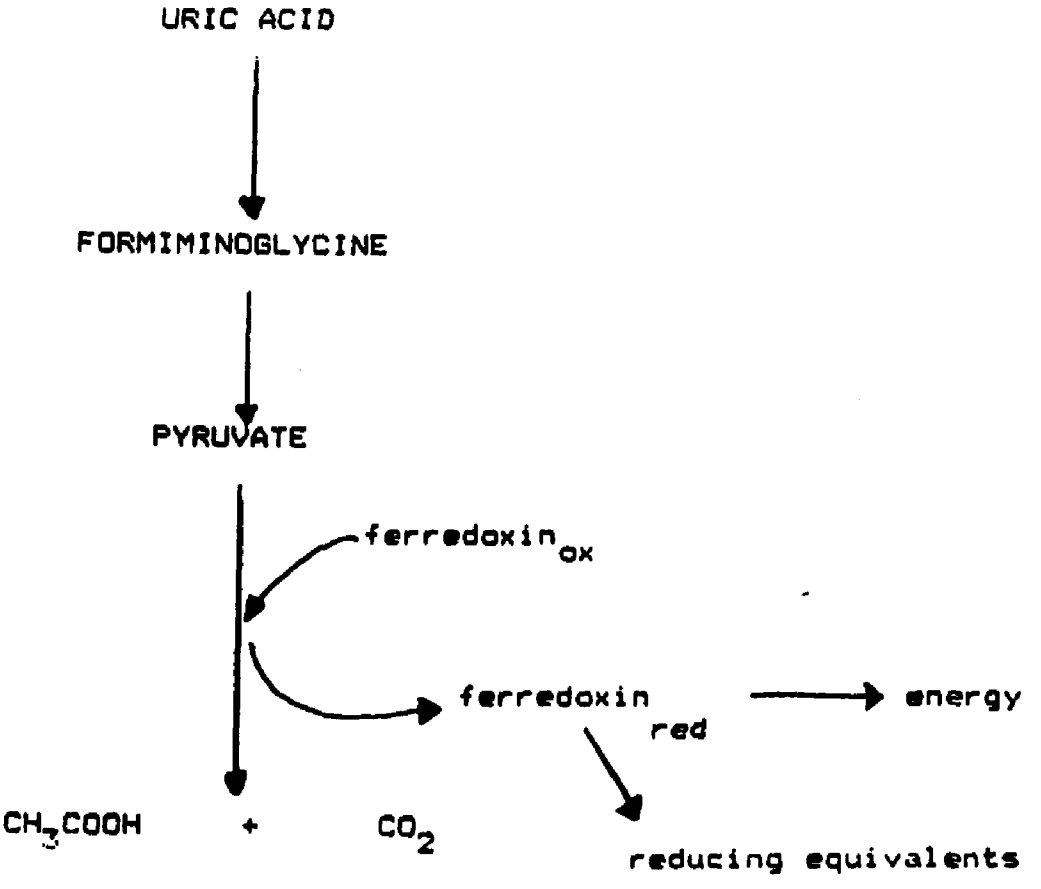
URIC ACID
FORMIMINOGLYCINE
PYRUVATE
ferredoxin ox
ferredoxin red
energy
CH3COOH
+
CO2
reducing equivalents

Figure VII. Nitrogen linked metabolism involving Clostridum pasteurianum nitrogenase protein

(adapted from reference 3)

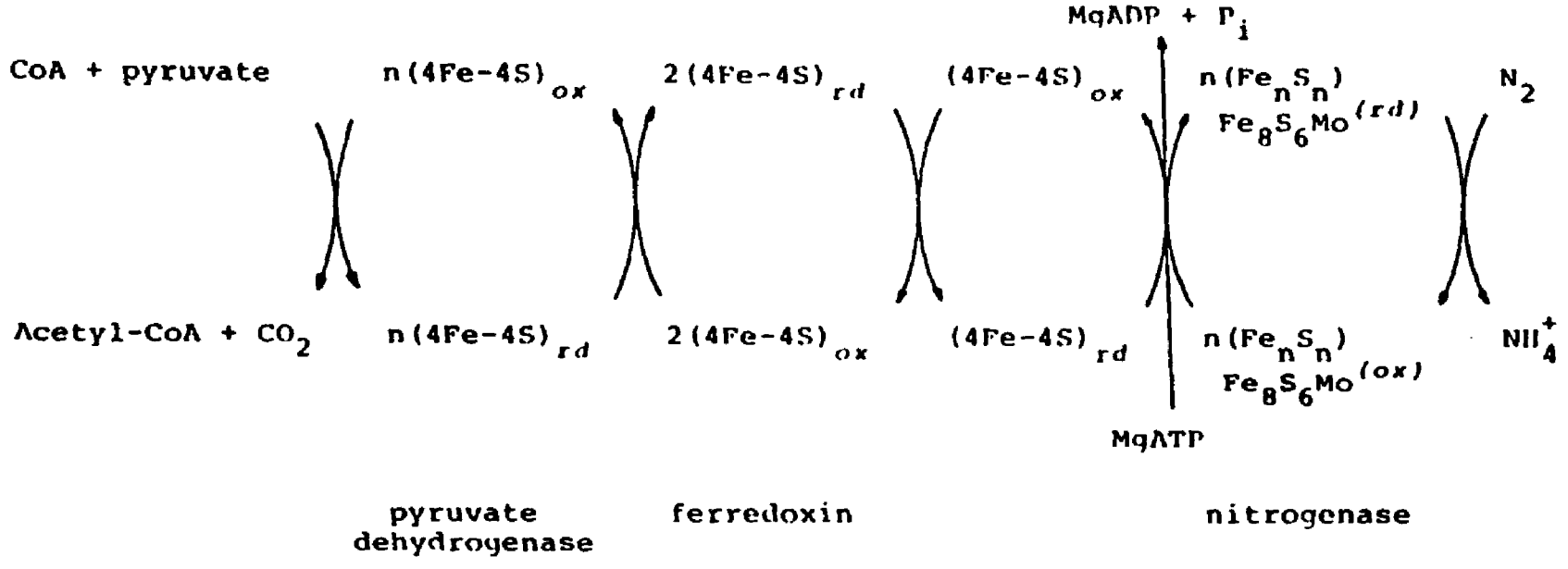
MgADP + P_i
CoA + pyruvate
$n(4Fe\text{-}4S)_{ox}$
$2(4Fe\text{-}4S)_{rd}$
$(4Fe\text{-}4S)_{ox}$
$n(Fe_nS_n)$
$Fe_8S_6Mo^{(rd)}$
N_2
Acetyl-CoA + CO_2
$n(4Fe\text{-}4S)_{rd}$
$2(4Fe\text{-}4S)_{ox}$
$(4Fe\text{-}4S)_{rd}$
$n(Fe_nS_n)$
$Fe_8S_6Mo^{(ox)}$
NH_4^+
MgATP
pyruvate dehydrogenase
ferredoxin
nitrogenase

3. Spectroscopic properties

a. UV-visible

The UV-visible absorption spectra for native oxidized and reduced ferredoxin from CP and CAU are presented in Figures VIII and IX. For the oxidized protein spectra , the broad absorption centered near 390 nm, with a molar extinction coefficient of around 30,600, is characteristic of the clostridial-type 2(4Fe-4S) ferredoxins. The absorption arises from a Fe ---> S charge transfer band between the iron in the cluster and a cysteinyl sulfur from the peptide. The absorbance around 280 nm is due to both the charge transfer band , and to a smaller extent , the aromatic side groups in the peptide . The ratio of A_{390}/A_{280} is used to assess to purity of ferredoxin with a ratio of 0.81 and 0.79 being pure for CP and CAU ferredoxin, respectively. When the 4Fe-4S center is degraded and the protein denatures the 390 nm absorption disappears, and therefore, serves as a good indicator of protein purity. A similar effect is seen when ferredoxin becomes reduced. Upon reduction, the UV-visible spectrum undergoes bleaching . The greatest difference in absorbances between the oxidized and reduced protein is observed at 425 nm where A_{red}/A_{ox} equals 0.435 (26). This absorbance difference has been extensively used in determining the midpoint reduction potential of the protein (27).

Figure VIII. UV-visible absorption spectrum of native oxidized and reduced *Clostridium acidi-urici* 8Fe ferredoxin

Conditions: .20 mg/ml protein in 0.050M potassium phosphate buffer/0.10M NaCl , pH 8.5 . Sample reduced with hydrogenase protein.

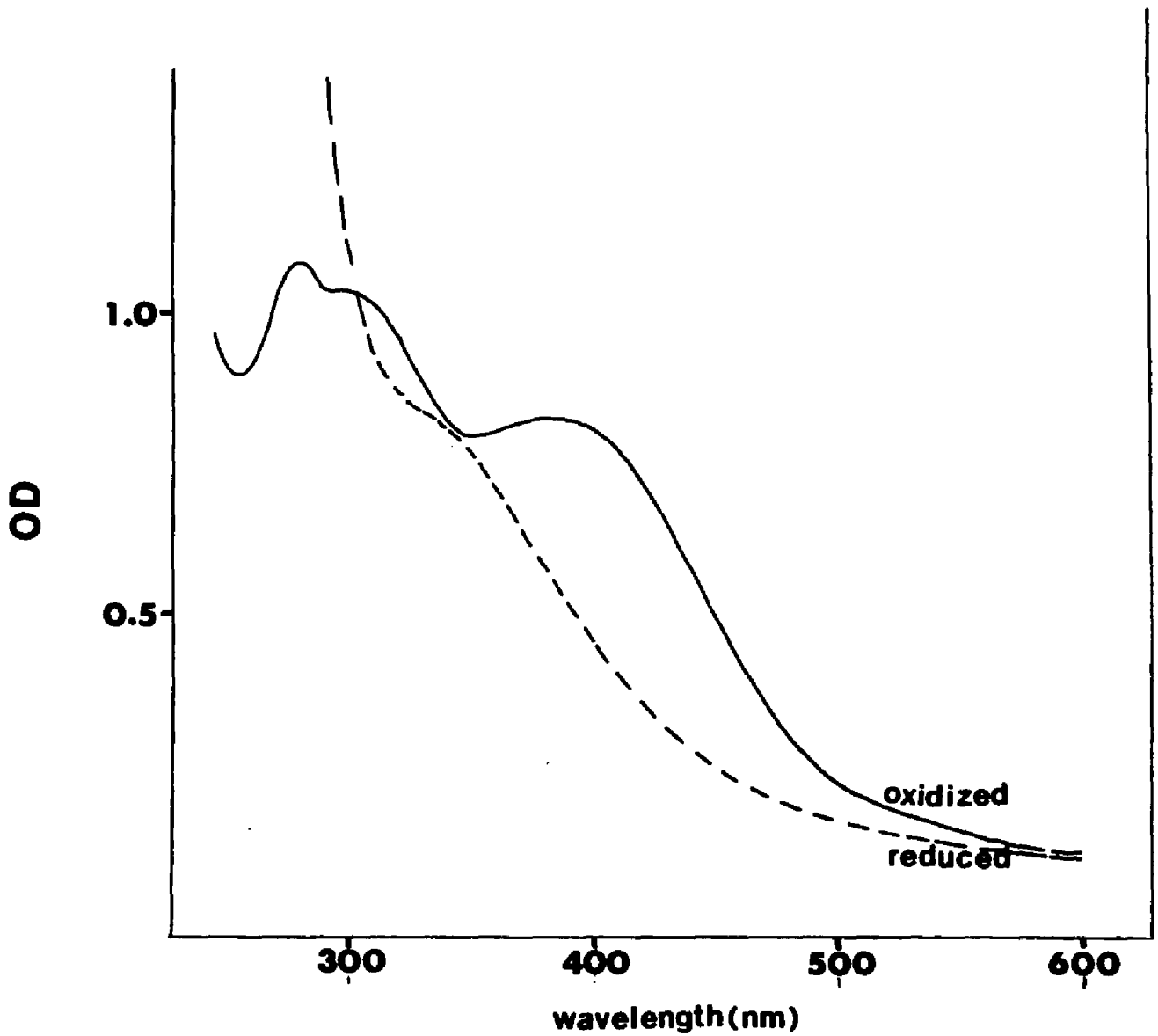
OD
1.0
0.5
300
400
500
600
wavelength(nm)
oxidized
reduced

Figure IX. UV-visible absorption spectrum of native oxidized and reduced Clostridium pasteurianum 8Fe ferredoxin

Conditions: .20 mg/ml protein in 0.050M potassium phosphate buffer/0.10M NaCl , pH 8.5 . Sample reduced with hydrogenase protein

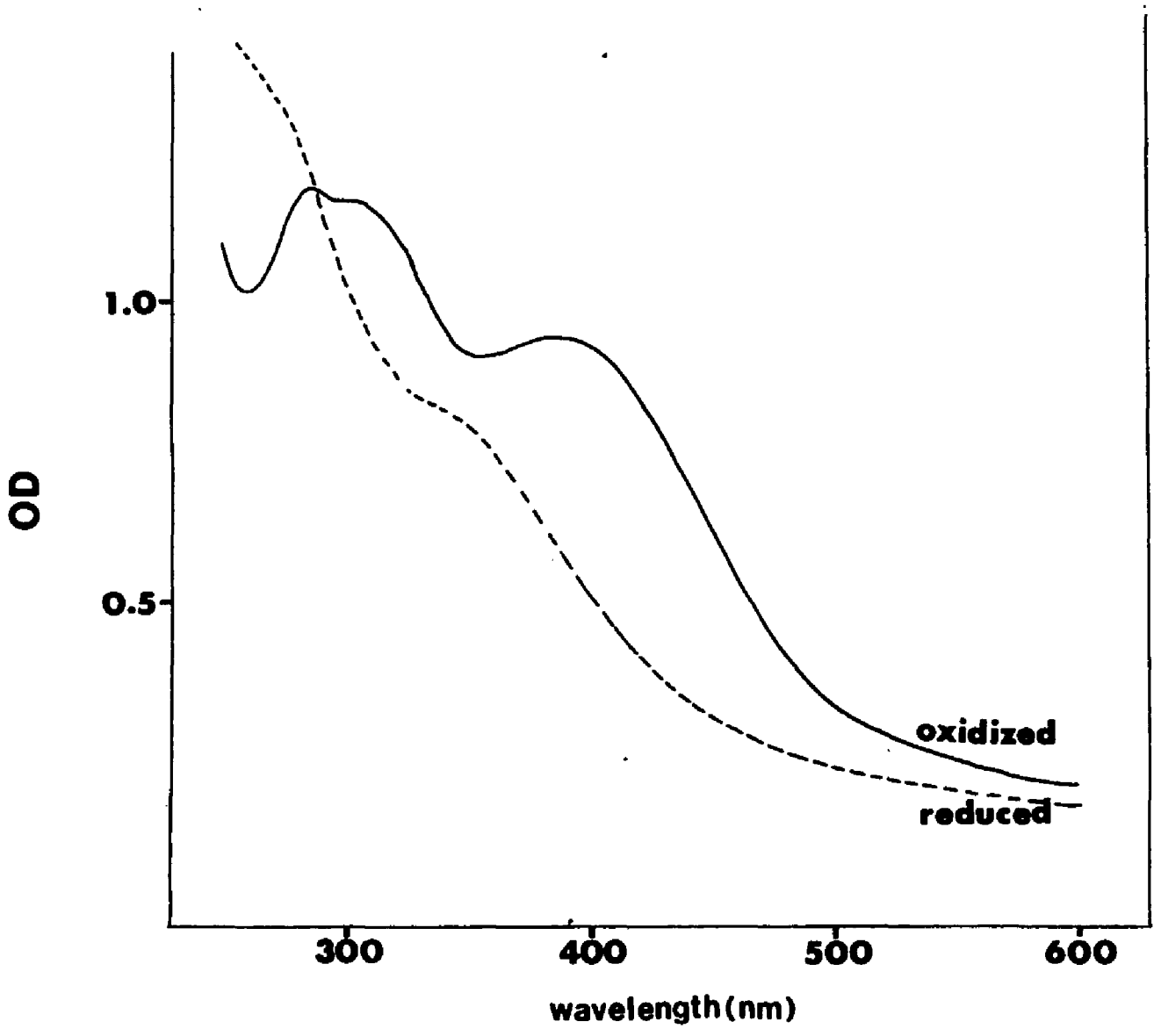
OD
1.0
0.5
oxidized
reduced
300
400
500
600
wavelength (nm)

b. Resonance Raman

The broad electronic absorption around 390 nm results in the detection of lower energy vibrational transitions when the oxidized ferredoxin is pulsed with 457.5 nm laser light. The active Raman vibrational bands arise from Fe-sulfur bonds between the 4Fe-4S center and the cysteinyl thiol ligands (28). Resonance Raman spectroscopy on 2Fe and 3Fe ferredoxins have revealed that the relative intensities and frequency positions are characteristic of the type of Fe-S center under study (29,30). Thus, it is possible to discern different Fe-S centers present in a mixture using resonance Raman spectroscopy.

c. Magnetic circular dichroism (MCD)

Many ferredoxins have characteristic low temperature MCD spectra (31,32). Like resonance Raman spectroscopy, the spectra are characteristic of the type of Fe-S center present. Therefore, as with resonance Raman spectroscopy, MCD finds application here because it is useful in discerning different types of Fe-S centers present in a mixture of iron-sulfur proteins.

d. Electron paramagnetic resonance (EPR)

The low temperature EPR spectrum of two electron reduced CP ferredoxin appears in Figure X. This complex signal, exhibiting g_{av} = 1.96, is typical of the

Figure X. Low temperature EPR spectrum of two electron reduced Clostridium pasteurianum 8Fe ferredoxin

Conditions: 3 mg/ml in 0.10M Tris/ 0.10M NaCl , pH 8.3 , Temperature, 15°K

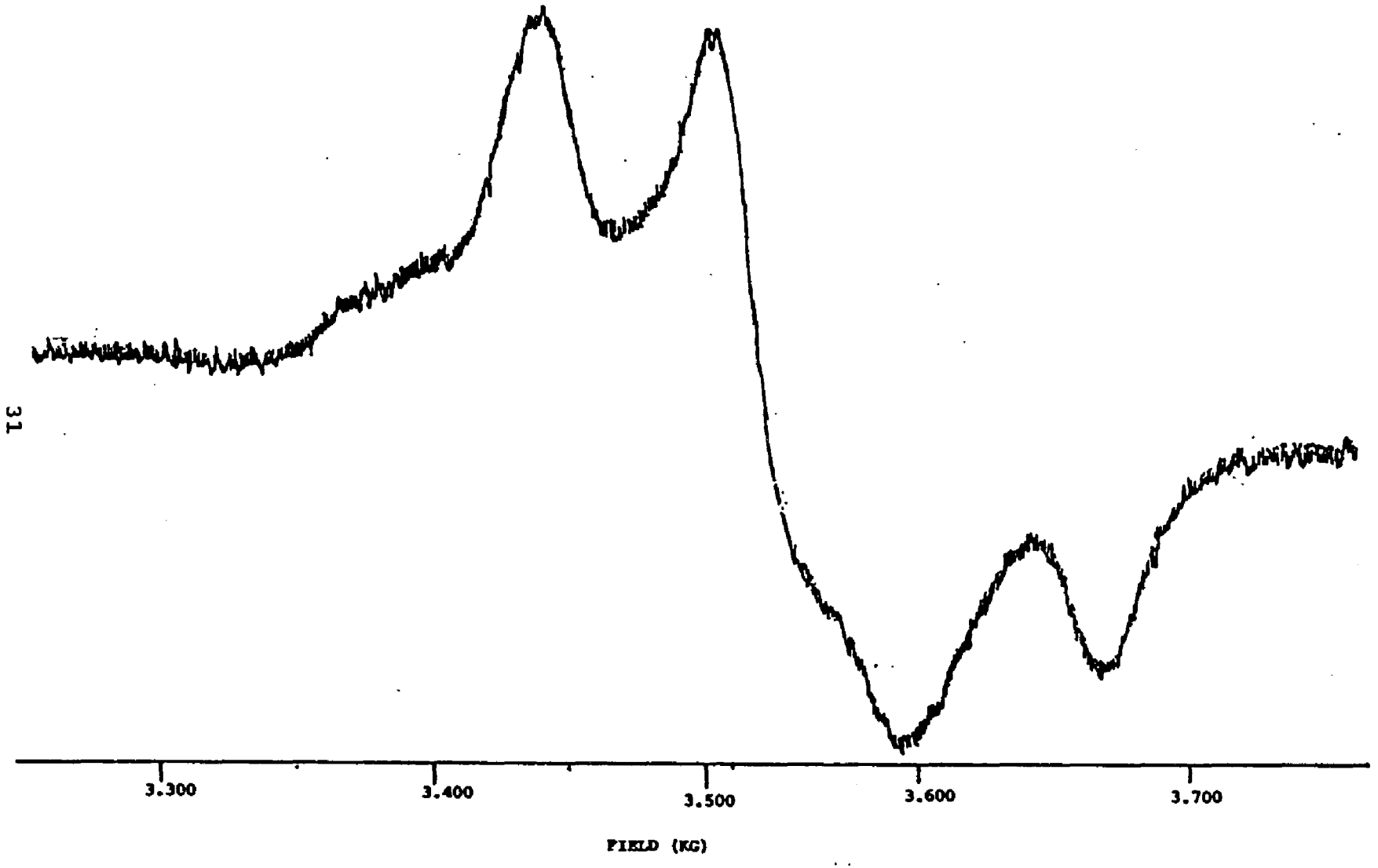
31
3.300
3.400
3.500
3.600
3.700
FIELD (KG)

clostridial 8Fe reduced ferredoxins and is believed to be due to spin-spin coupling between the two reduced centers in the protein. Oxidized clostridial ferredoxin is EPR silent because of anti-ferromagnetic exchange coupling between iron atoms in the oxidized centers that result in an S = 0 ground state at low temperature (33). EPR spectroscopy is useful because the g-values and linewidths can be used in the detection of 8Fe ferredoxin, as well as being a probe for studying geometric changes around these paramagnetic centers.

e. Proton nuclear magnetic resonance (^{1}H-NMR)

The ^{1}H-NMR spectra of oxidized CP and CAU ferredoxin are shown in Figures XI and XII. The downfield region between 8-20 ppm is of most interest. The broad resonances downfield of 10 ppm arise from beta-cysteinyl protons, whereas the narrow peaks around 10 ppm arise from alpha-cysteinyl hydrogens (34). The resonances are shifted downfield because of their proximity to the paramagnetic 4Fe-4S clusters. These resonances are particularly sensitive to changes around the 4Fe-4S center, and therefore, can be used as probes to assess changes around it. The NMR spectra are also useful in monitoring changes in protein conformation.

3. Midpoint reduction potential

The 4Fe-4S center in CP and CAU formally contains two

Figure XI. 400 MHz ^{1}H-NMR spectrum of oxidized Clostridium pasteurianum 8Fe ferredoxin

Conditions: 3 mg/ml protein in 0.050M K_2DPO_4/ .040M NaCl in 99.9% D_2O, pH 7.8, 1000 scans , pulse repeat time 0.607 sec.

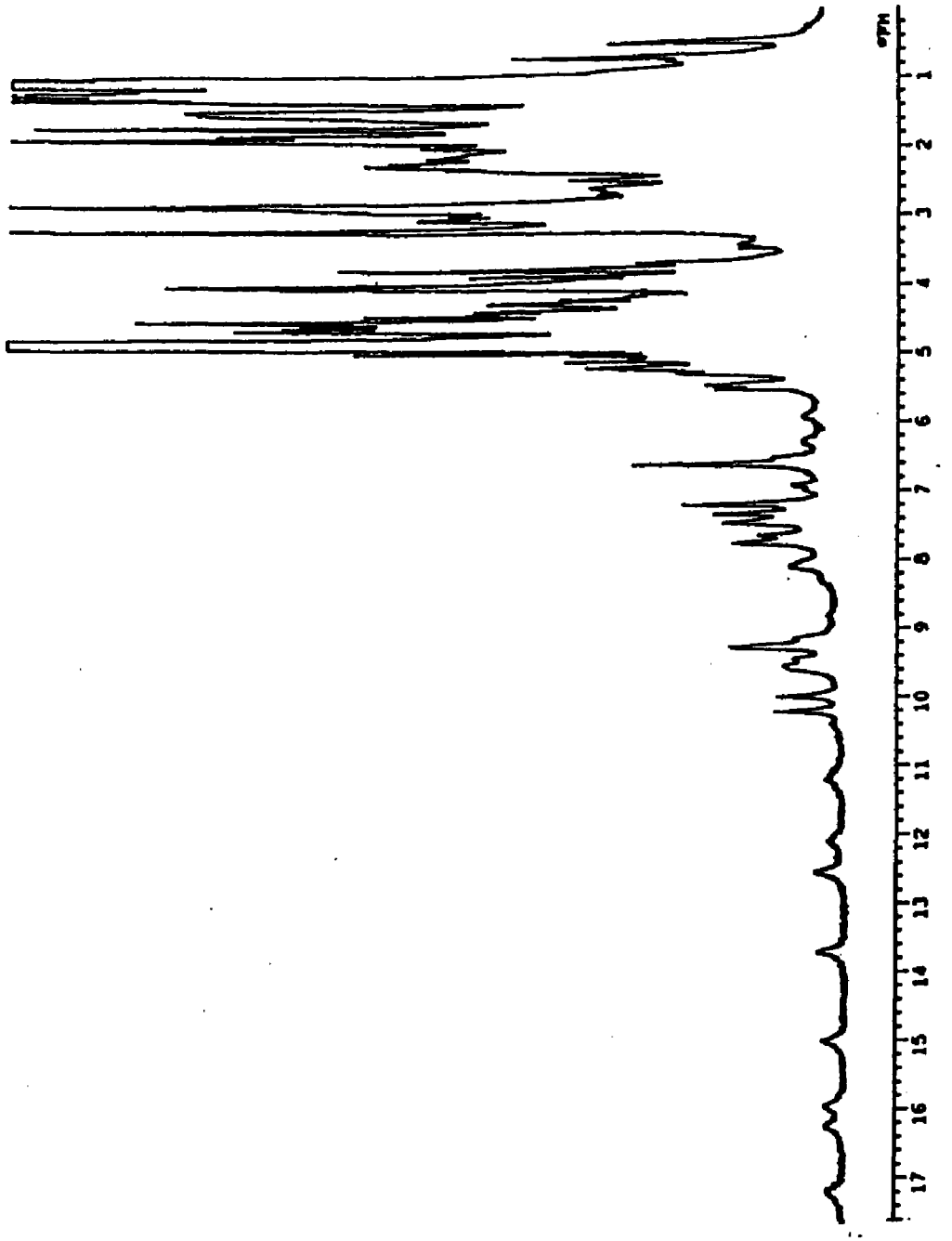
PPM
1
2
3
4
5
6
7
8
9
10
11
12
13
14
15
16
17

Figure XII. 400 MHz ^{1}H-NMR spectrum of oxidized *Clostridium acidi-urici* 8Fe ferredoxin

Conditions: 5 mg/ml protein in 0.050M K_2DPO_4/ .030M NaCl in 99.9% D_2O, pH 7.6, 1000 scans , pulse repeat time 0.607 sec

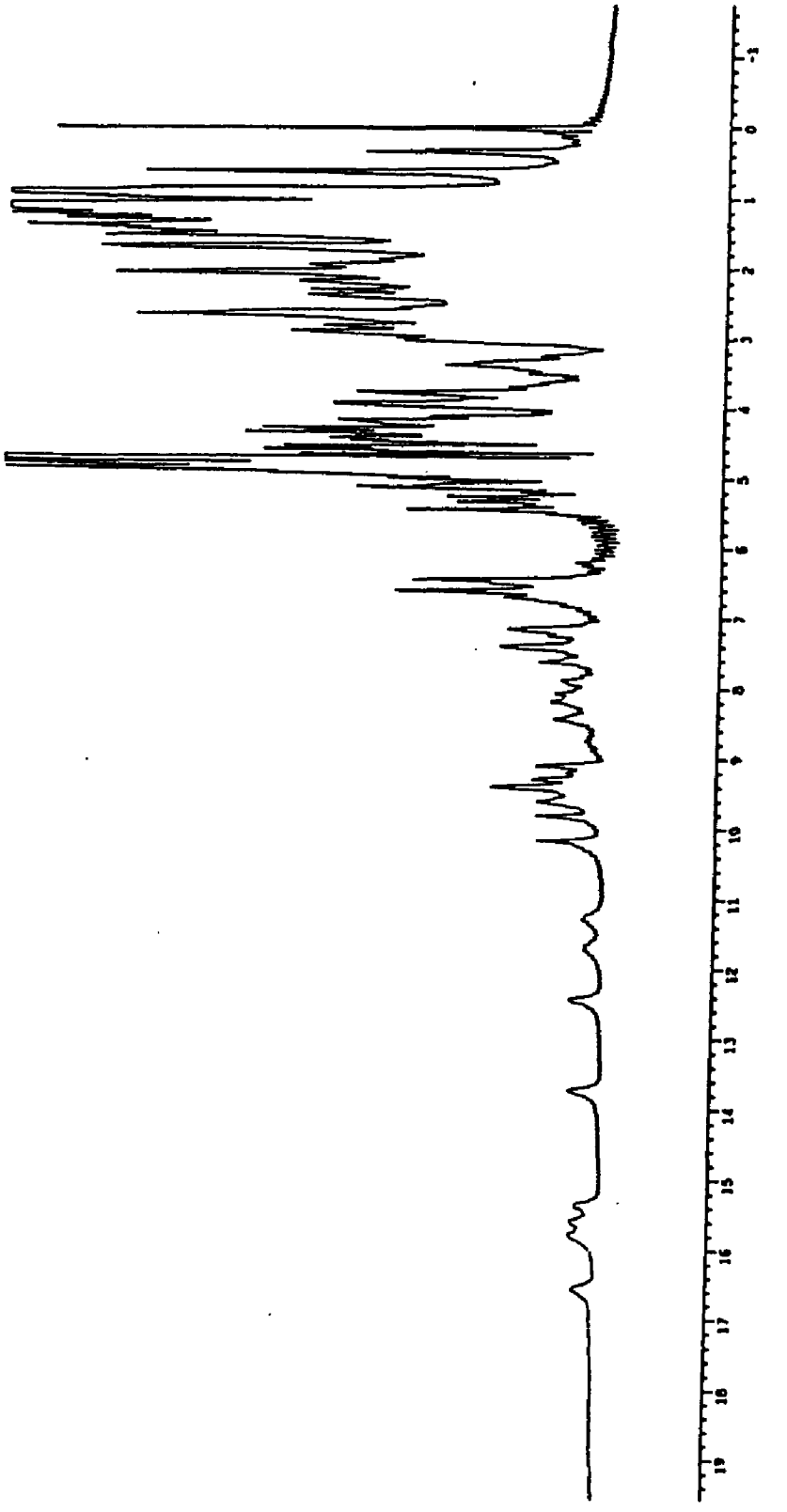

ferrous and two ferric ions (+10 total charge), four sulfides (-8 total charge) and four cysteinyl thiol ligands (-4 total charge) giving the Fe-S cluster a formal oxidation state of -2 (the "C" state). Although the formal charge on the atoms in the as isolated Fe-S center can be evaluated by conventional oxidation state assignments (one Fe^{3+} and three Fe^{2+} atoms) the actual electron densities in the clusters are delocalized and the individual iron atoms are nearly equivalent (35). Each cluster in the molecule can undergo a one electron reduction giving the cluster a formal charge of -3 (the "C^{-}" state), which corresponds to the EPR active reduced ferredoxin. Alternately, the "C" state can undergo oxidation to the corresponding -1 charge (the "C^{+}" state). The latter state is typical of the EPR active state seen in various HIPIP-type ferredoxins (36). The HIPIP-type ferredoxins are differentiated from clostridial-type ferredoxins because the former undergoes oxidation-reduction involving the C <---> C^{+} interconversion, whereas the latter undergoes C <---> C^{-} conversions. The C <---> C^{-} reduction occurs typically at around -400 mV to -500 mV, but the C <---> C^{+} reduction occurs at much higher potentials, around +350 mV (37,38). The differences in these potentials may arise from differences is solvent accessibility of the Fe-S centers, and in addition, from changes in hydrogen bonding around the 4Fe-4S centers ; PA ferredoxin has nearly twice as many

hydrogen bonds per cluster than does HIPIP ferredoxin from Chromatium vinosum. Although there are two 4Fe-4S centers in the clostridial 8Fe ferredoxins , for Clostridium pasteurianum they show no cooperativity (39). The midpoint reduction potentials of the two clusters in Clostridium pasteurianum differ by about 10 mV whereas for Clostridium acidi-urici ferredoxin they are nearly the same (40).

4. Chemical reactivity

8Fe clostridial-type ferredoxins can be converted into the corresponding apoprotein by the removal of the 4Fe-4S centers. The protein is easily denatured under mildly acidic conditions (pH < 6) or slowly in the presence of oxygen. In both cases the 4Fe-4S center is degraded into ferric ion and sulfide. The apoprotein can be reconstituted by treating it with a ferrous salt and sulfide in the presence of urea and mercaptoethanol (40). The biological activity of reconstituted ferredoxin has been shown to be identical to that of native protein. The 4Fe-4S center is also susceptible to ferricyanide oxidation which leads to the formation of a new Fe-S center having spectroscopic properties of a 3Fe center (42). Similarly, there are reported conversions of 3Fe centers to 4Fe centers as well (43).

5. Clostridium pasteurianum hydrogenase

Clostridium pasteurianum contains two hydrogenases. These extremely oxygen sensitive iron-sulfur proteins catalyze the oxidation and production of hydrogen gas (44,45). CP hydrogenase I catalyzes both H_2 oxidation and H_2 production, whereas CP hydrogenase II preferentially catalyzes H_2 oxidation. CP hydrogenase I is a 60000 M.W. protein that contains 3(4Fe-4S) centers , whereas CP hydrogenase II , a 53000 M.W. protein, contains 2(4Fe-4S) centers (14). Hydrogenase finds application here because it can be used as a general biological reductant for ferredoxin in experiments involving studies of ferredoxin in the reduced state.

6. Rubredoxin protein

Rubredoxin, another electron transport protein, is a 6000 dalton protein containing a single iron. Rubredoxin, found in Clostridium pasteurianum has been characterized through x-ray crystallography. Its function remains obscure (46). The importance of rubredoxin, as it finds application here, will be presented subsequently on discussions involving its isolation and characterization from Clostridium acidi-urici.

GENERAL METHODS

A. Growth of Clostridium pasteurianum

Clostridium pasteurianum cultures ATCC strain 6013, were initially grown from lyophilized cells using a potato medium (47). One ml of freshly grown cells were added to 18 cm X 1.5 cm borosilicate disposable test tubes containing 9 ml of autoclaved media. Cells were grown anaerobically by adding small amounts of solid sodium dithionite after inoculation. The tubes are anaerobically sealed with sterile non-absorbent cotton plugs containing alkaline pyrogallol (15% w/v pyrogallic acid in 12.5 M NaOH), or chromous chloride solution. Cells were grown at 30°C for about 18-20 hours. Cultures of less than 1 liter were grown using volumetric flasks, whereas florence flasks were used for one and two liter cultures. For larger batches of 20L or more autoclavable Nalgene plastic carboys were employed. The following recipe was used when 50 liters of bacteria were grown.

carboy autoclave time	90 minutes
sucrose (table sugar)	1.0 kg
$MgCl_2 \cdot 6H_2O$	7.5 g
NaCl	5.0 g
Biotin	0.25 mg
Para-aminobenzoic acid	0.25 mg
Na_2MoO_4 (10% w/v)	2.50 ml
NH_4Cl	80.0 g

Na_2SO_4	4.50 g
$CaCO_3$	75.0 g

The ingredients above were added to a 50 L Nalgene carboy that contained 44 liters of distilled water and autoclaved. Prior to inoculation a sterile solution containing 5% by weight $K_2HPO_4 \cdot 3H_2O$ and 7% KH_2PO_4 (10 ml phosphate/liter medium) was added to the carboy followed by 200 ml of ethanol containing 8g $FeCl_3$. 5 liters of actively growing cells were used as an innoculum. After inoculation the pH was adjusted to 7.4-7.6 using about 40 ml of 10N NaOH, a small amount of dithionite was added and the top of the container was loosely sealed with a rubber stopper. If cells that were not rigorously evolving hydrogen gas were used as innoculum it was necessary to bubble the carboy containing fresh medium for at least 15 minutes prior to innoculation with nitrogen or argon gas. The cell growth was followed by monitoring the Klett turbidity reading (green filter). When this reading reached 450-475 the cells were harvested using a CEPA cell harvester and stored at $0^{o}C$. 50 liters of freshly grown cells yielded approximately 300 grams of wet cells.

B. Growth of Clostridium acidi-urici

Clostridium acidi-urici bacteria were grown according to the methods described by Rabinowitz (47). The media used for the growth of this bacteria is shown below.

	For 1 liter	For 50 L
Uric acid	2.0 g	115 g
KOH (pellets)	0.68 g	34 g
distilled H_2O	750 ml	45 L
$K_2HPO_4 \cdot 3H_2O$	0.91 g	46 g
$MgSO_4 \cdot 7H_2O$	35.0 mg	1.8 g
$FeSO_4 \cdot 7H_2O$	2.5 mg	125 mg
$CaCl_2 \cdot 2H_2O$	4.5 mg	225 mg
Difco yeast extract	1.0 g	50 g

The growth media was prepared in the following way: the uric acid, KOH and water are brought to a boil. The $K_2HPO_4 \cdot 3H_2O$ was added and boiling was continued until all the uric acid had dissolved. Discontinue heating , allow the solution to cool to about 40-50^oC and add yeast extract, iron , magnesium and calcium salts. For initial growths mercaptoacetic acid was added to the medium (1.6 g/liter medium). The containers were cooled and the pH was adjusted to between 7.4-7.6 using HCl or KOH. For 50L growths, prior to inoculation, a sterile solution containing 150 g of Na_2CO_3 in 500 ml of distilled water was added to the carboy. 5 liters of freshly grown cells were used as an innoculum for large growths. After inoculation, the pH of the medium is readjusted to about 7.4, the top of the carboy flushed with argon or nitrogen gas and the container was fitted with a sterile anaerobic

plug and sealed with a rubber stopper. The cells were incubated at 37°C for approximately 20 hours. Bacterial growth was monitored by following the uptake of uric acid at 290 nm. Initially an absorbance of about 1.4 is observed at 290 nm for a 1:100 dilution, but as growth proceeded this absorbance decreased. When this value decreased to 0.0350 or less the cells were harvested in a centrifuge. Typically, 50 liters of freshly grown cells yielded approximately 30 grams of wet cells. The freshly harvested cells were frozen and stored at 0°C.

C. Growth of Clostridium acidi-urici for uptake studies and rubredoxin isolation

A modified growth medium was used for amino acid uptake studies and rubredoxin isolation from Clostridium acidi-urici.

	For 1 liter	For 50 L
Uric acid	2.0 g	115 g
KOH (pellets)	0.68 g	34 g
distilled H_2O	750 ml	45 L
$K_2HPO_4 \cdot 3H_2O$	0.91 g	46 g
$MgSO_4 \cdot 7H_2O$	35.0 mg	1.8 g
$FeSO_4 \cdot 7H_2O$	2.5 mg	125 mg
$CaCl_2 \cdot 2H_2O$	4.5 mg	225 mg
NaCl	50.0 mg	2.5 g
DL-cystine	24.0 mg	1.2 g

D. Isolation and purification of 8Fe ferredoxin from Clostridium acidi-urici or Clostridium pasteurianum

The purification of the 8Fe ferredoxin from Clostridium acidi-urici or Clostridium pasteurianum was identical and based on the procedure described by Rabinowitz (47). Typically, 2000g of frozen CP cells, thawed overnight at 4°C, are dissolved in buffer at room temperature by adding the thawed cells with gentle stirring into 2000 ml of 0.10M Tris·HCl pH 8.5 . After the cells are dissolved the pH of the solution is adjusted to 7.5 using 12N HCl or 10N NaOH. 4.0 grams of chicken egg white lysozyme is added and the solution is allowed to incubate for two hours at room temperature. Occasional pH adjustment was sometimes necessary during this incubation period. After lysozyme treatment the cells are sonicated in 200 ml batches for a total of six minutes using a Branson W-180 sonifier at full power. The cell solution is centrifuged for one hour at 8000 rpm. The pellet is discarded, and the supernatent is applied to a 37 cm X 6 cm chromatography column containing 500 ml of Whatman-DEAE previously equilibrated with 0.10M Tris pH 7.5. After the protein is applied the column is washed with 500 ml of equilibration buffer, followed by buffer containing 0.10M NaCl. The column is washed with this salt until the yellow flavin band has been eluted. The ferredoxin is then eluted using buffer containing 0.50 M NaCl. The

protein is diluted two-fold with distilled water and a few milligrams of ribonuclease and deoxyribonuclease are added along with a small amount of $MgCl_2$. After four hours of nuclease treatment at room temperature the protein is dialyzed against 0.050 M Tris pH 7.5 overnight using Spectrophor 3500 M.W. cutoff dialysis tubing. After dialysis, the protein is applied to a second column containing 250 ml of Sephacel-DEAE equilibrated with 0.10M Tris buffer pH 7.5. After the protein is applied the column is washed with buffer containing 0.145 M NaCl. By this method the rubredoxin can be effectively separated from the ferredoxin (it elutes right before the ferredoxin). The ferredoxin fractions are diluted two fold with distilled water and concentrated by applying the protein to a 35 cm X 2.8 cm column containing 65 ml of Whatman-DEAE pre-equilibrated with 0.10M Tris pH 7.5. The ferredoxin is first washed with buffer containing no salt followed by 200 ml of buffer containing 0.145 M NaCl . The protein is finally eluted with buffer containing 0.50M NaCl. The concentrated protein is diluted to about 125 ml (ca. 1 mg protein /ml) , and the solution is then made 60% saturated in neutralized ammonium sulfate. The solution is then centrifuged at $4^{o}C$ for 15 minutes at 10,000 rpm , the pellet is discarded and the solution is saturated in neutralized ammonium sulfate. The protein is stored anaerobically overnight at $4^{o}C$. The precipitated protein is centrifuged at $4^{o}C$ for 15 minutes at 10,000 rpm , the

pellet is dissolved in Tris buffer (ca. 7-10 mg protein/ml) and applied to a 103 cm X 5 cm Sephacel G-75 column equilibrated with 0.10 M Tris /0.10 M NaCl pH 7.4. The eluted protein is fractionated and fractions with optical ratios, A_{390}/A_{280}, of greater than 0.795 are pooled and stored anaerobically in neutralized saturated ammonium sulfate at 0°C. For Clostridium acidi-urici those ratios higher than 0.775 are pooled. Generally, 2000 grams of Clostridium pasteurianum cells yield between 160-180 mg of ferredoxin. For Clostridium acidi-urici 100 grams of cells gave about 50 mg of ferredoxin.

E. Isolation of rubredoxin from Clostridium pasteurianum and Clostridium acidi-urici

The impure rubredoxin isolated during the separation of ferredoxin is purified by first concentrating the protein using amicon ultrafiltration containing a 5000 M.W. cutoff membrane. The protein is concentrated to about 3-4 ml, and then it is applied to a 103 cm X 5 cm Sephacel G-75 column equilibrated with 0.10 M Tris / .10 M NaCl pH 7.4. The protein is fractionated and fractions with optical ratios, A_{280}/A_{490}, less than 2.6 are pooled and dialyzed against .010 M Tris using 3500 molecular weight cutoff tubing. The rubredoxin was stored as a lyophilized powder at 0°C. Typically, 2000 g of Clostridium pasteurianum cells gave about 50 mg of

rubredoxin, whereas an average yield of 3 mg of rubredoxin was obtained from 100 g of Clostridium acidi-urici cells.

F. Partial purification of hydrogenase protein from Clostridium pasteurianum

For hydrogenase isolation, 300 grams of freshly harvested actively growing cells were dissolved in 300 ml of buffer containing 0.10 M Tris/ .005 M $Na_2S_2O_4$ pH 8.5 that had been thoroughly deaired by boiling the water and bubbling it generously for about 15 minutes using either argon or nitrogen gas. One gram of chicken egg white lysozyme was added to the cell suspension. The pH of the solution was adjusted to 8.0 and the cell suspension poured into 300 ml centrifuge bottles, closed under an argon or nitrogen atmosphere and incubated at room temperature with occasional stirring for two hours. The cell debris was then spun down for one hour at 9000 rpm. After centrifuging, the containers were put into a 60°C water bath for 15-20 minutes and the tubes were centrifuged again for 20 minutes. The yellowish-green supernatent was applied anaerobically to a 37 cm X 5.6 cm column containing 150 ml of Pharmacia Q-Sepharose fast flow DEAE that was previously equilibrated with 0.10 M Tris/.003 M $Na_2S_2O_4$ pH 7.5 buffer. The greenish pass-thru contains the unidirectional hydrogenase. The bidirectional hydrogenase was isolated by first washing the column with 150 ml buffer containing 3 mM dithionite.

This was followed by washing with 0.10 M NaCl until the brown band begins to move down one half the length of the DEAE, after which the salt was changed to 0.250 M. The first brown band eluting contains the hydrogenase. Hydrogenase activity was detected using a methyl viologen/hydrogen gas coupled reduction assay. The hydrogenase proteins were collected anaerobically using a collecting system diagrammed in Figure XIII. The bidirectional hydrogenase can be concentrated by diluting the protein two-fold with oxygen free water and then applied to a second small DEAE column followed by quick elution with 0.50 M NaCl.

G. Preparation of apoferredoxin

Apoferredoxin was prepared using a procedure originally described by Rabinowitz (41) , but modified slighty. Native ferredoxin was dissolved in 0.10 M Tris pH 7.4 (2 mg protein/ml buffer) and made 12% w/v in trichloroacetic acid. The solution was allowed to incubate in an ice bath for about 60 minutes after which the denatured protein was centrifuged for 15 minutes at 10,000 rpm. The supernatant was discarded and the protein pellet dissolved in 1% w/v $NaHCO_3$ to make the final concentration about 4 mg of protein/ml . The solution was made 10% in trichoroacetic acid and the treatment was repeated twice more. After the third spin the pellet is

Figure XIII. Diagram of anaerobic set-up used for the application, purification and collection of hydrogenase protein from Clostridium pasteurianum

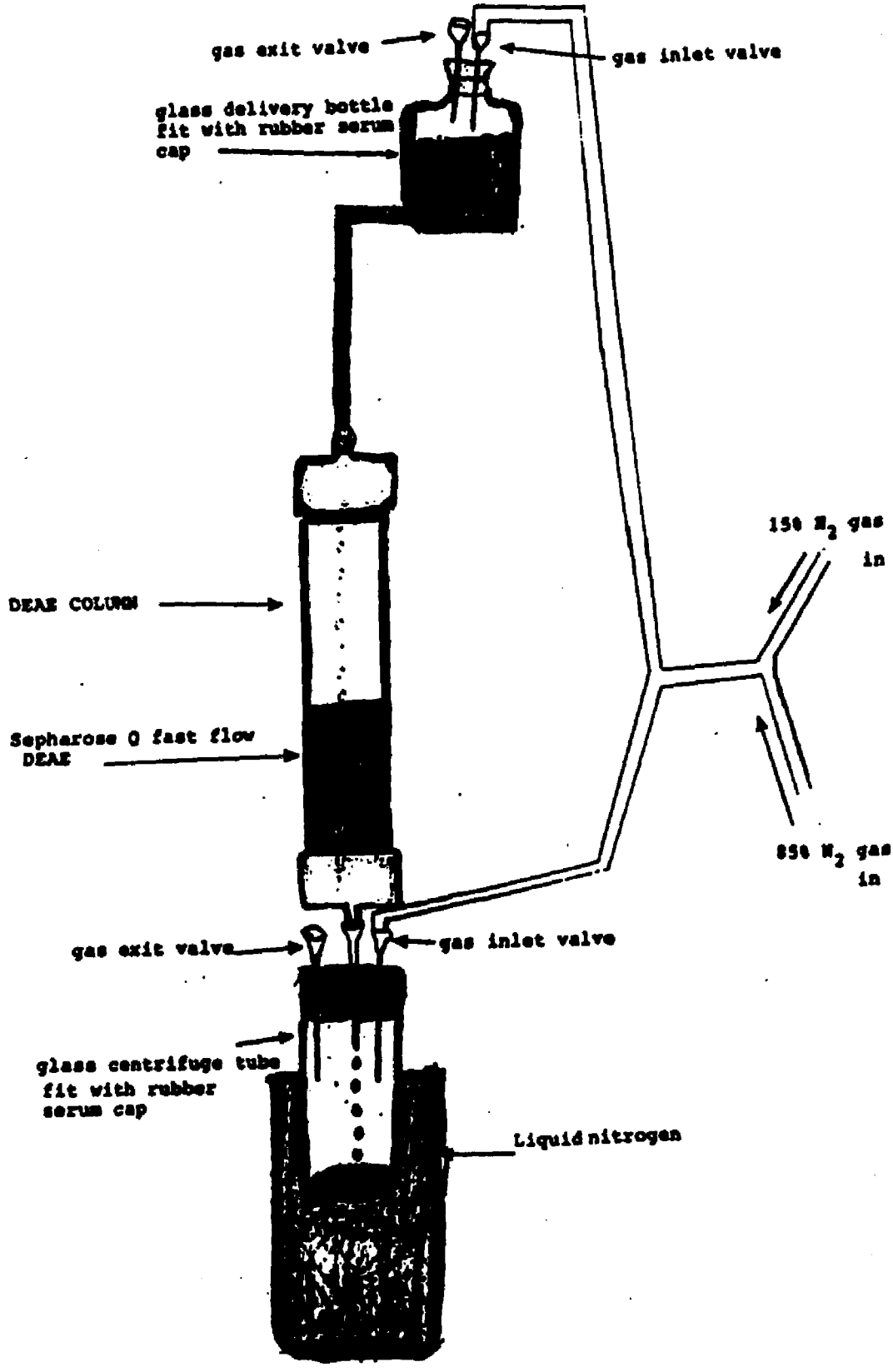
gas exit valve
gas inlet valve
glass delivery bottle fit with rubber serum cap
DEAE COLUMN
Sepharose 0 fast flow DEAE
15% N_2 gas in
85% N_2 gas in
gas exit valve
gas inlet valve
glass centrifuge tube fit with rubber serum cap
Liquid nitrogen

dissolved in a minimum amount of 5% w/v $NaHCO_3$, and dialyzed against several exchanges of distilled water using 3500 M.W. cutoff dialysis tubing. The dialyzed protein was lyophilized and stored in a dessicator at 0^oC.

H. Reconstitution of apoferredoxin

The reconstitution of apoferredoxin was accomplished using the procedure also described by Rabinowitz (41). Typically, 16 mg of apoferredoxin was dissolved in 4 ml of 0.25 M Tris/ 0.14 M mercaptoethanol/ 8 M urea pH 8.3 . The solution was allowed to incubate for 4 hours under anaerobic conditions. Then 800 ul of 0.10 M Na_2S was added followed immediately by the addition of 36 ml of 0.10 M Tris/0.070 M mercaptoethanol pH 7.4 . Finally, 800 ul of 0.10 M $Fe(NH_4)_2(SO_4)_2$ was added. The blackish brown solution was then applied to a small Whatman-DEAE column equilibrated with 0.10 M Tris pH 7.4 . The reconstituted protein was eluted using buffer containing 0.35 M NaCl. For reconstitution of methylated apoferredoxin, prior to application to DEAE, the protein was dialyzed against 0.050 M Tris pH 7.4. The yields of reconstituted protein varied between 15%-45% . Yields were greatest when the reconstitution procedure was done in an anaerobic glove box. Yields were also improved when HPLC grade water was used in preparing the solutions for reconstitution.

I. Reductive methylation of *Clostridium pasteurianum* ferredoxin

Reductive methylation of clostridial-type ferredoxin was accomplished using the procedure of Jentoft and Dearborn (48). For reductive methylation of apoferredoxin or native oxidized ferredoxin the following procedure was used. Apoferredoxin was dissolved in 0.10M HEPES buffer pH 8.3 for a final concentration of 2 mg protein/ml . For native oxidized ferredoxin, the protein was applied to a small Whatman-DEAE column equilibrated with 0.10M HEPES buffer pH 8.3 and then generously washed with 0.10M HEPES buffer pH 8.3 until complete buffer exchange has occurred. The protein was rapidly eluted with 0.10M HEPES buffer containing 0.40M-0.50M NaCl pH 8.3 and then diluted to a final concentration of 2 mg/ml using 0.10M HEPES pH 8.3. A 20-30 fold molar excess of ^{13}C-labeled formaldehyde (99% atom) was added to the protein and incubated for one hour at room temperature. A 90-fold molar excess of solid sodium cyanoborohydride was then added over three one hour intervals. After the final addition the flask was sealed with parafilm and allowed to incubate about 15 hours at room temperature. For oxidized ferredoxin , the flask was thoroughly deaerated with nitrogen or argon to minimize denaturation due to oxygen exposure. The protein was separated from the other reagents either through dialysis or by purification on DEAE.

Reductive methylation of reduced ferredoxin was accomplished by first gently bubbling the oxidized ferredoxin with prepurified hydrogen gas. About 100 ul of partially purified hydrogenase was added anaerobically to the solution and incubated under hydrogen gas in a sealed flask fitted with a rubber septum cap for about one hour. Then a 50-fold molar excess of enriched formaldehyde was added to the protein solution. After a one hour incubation a 90-fold molar excess of solid sodium cyanoborohydride was added through the septum cap by dissolving the solid in a small volume of the protein solution. After a 15 hour incubation at room temperature under hydrogen gas the procedure was repeated twice more. The methylated ferredoxin was then separated from hydrogenase and other reagents using DEAE chromatography.

^{14}C-labeling of apoferredoxin was typically achieved using radioactive formaldehyde with a specific activity of 20000 cpm/umole CH_2O, whereas for oxidized ferredoxin the specific activity was 40000 cpm/umole of CH_2O.

J. Cytochrome C - ferredoxin reductase assay

The ferredoxin/ferredoxin reductase-cytochrome C biological activity coupled assay was performed using the procedures described by Lode (25).

K. Determination of midpoint reduction potential

Midpoint reduction measurements of ferredoxin were

performed using a procedure described by Magliozzo (27). A solution of ferredoxin in 0.10 M Tris/0.10 M NaCl at the desired pH is gently bubbled with prepurified hydrogen gas in a 3 ml cuvette sealed with a serum cap. The hydrogen gas is scrubbed by first bubbling it through a pyrogallol solution (15% w/w in 50% NaOH) and then through deaired distilled water to prevent contamination from the pyrogallol. After bubbling, the optical absorbance at 425 nm is recorded (A_{ox}) and about 6 ul of defrosted partially purified bidirectional hydrogenase is added anaerobically to the cuvette. The decrease at 425 nm is followed until no more change is observed and recorded (A_{red}). The protein was then reoxidized by gently bubbling the solution with a pasteur pipette or with prepurified nitrogen gas which contains enough oxygen to reoxidize the ferredoxin. The gas is bubbled through distilled water before entering the protein solution as not to concentrate the ferredoxin during bubbling. The reoxidation of ferredoxin is followed by monitoring the A_{425} absorbance until 97.5%-98% of the original absorbance is attained. The pH of this solution was then carefully measured using a Radiometer 26 pH meter. Trials where A_{ox} was less than 97% of the initial absorbance were discarded. The ratio of oxidized to reduced ferredoxin is determined in the following way: The ratio of extinction coefficients at 425 nm for the reduced to oxidized ferredoxin for Clostridium pasteurianum is 0.435 (26). Therefore ,

$$\frac{\text{[reduced ferredoxin]}}{\text{[oxidized ferredoxin]}} = \frac{A_{red} - 0.435(A_{ox})}{A_{ox} - A_{red}}$$

The midpoint reduction potential of the ferredoxin was determined through use of the Nernst equation where n = 1. The solution potential (E_{soln}) in mV is determined at one atmosphere which gives E_{soln} = - nF/RT X (pH) , which is approximately equal to -59.16 (pH) at 25°C.

L. Preparation of anaerobic glove box

A glove box is prepared by the following procedure. The glove box is initially purged by using a slow flow of prepurified grade nitrogen or argon gas for about 24 hours. The box is then purged using a recirculating system . A mixture of nitrogen and hydrogen (5:1 v/v) is delivered through a gas port directly into the glove box. This gas is then recirculated using a small diaphragm pump. The gas is passed through an activated oxygen scrubbing catalyst (BASF R3-11) and then through a dewar immersed in liquid nitrogen to remove any water vapor from the gas. The gas is then recirculated back into the box. All solutions going into the box were thoroughly deaired by first boiling the water for at least 15 minutes, followed by bubbling with nitrogen or argon gas passed through pyrogallol and a water trap for at least one hour. Samples were passed into the glove box through a transfer

chamber. The chamber is alternately flushed with nitrogen/hydrogen gas mix and vacuumed with a mechanical pump.

M. Direct detection of reduction linked proton binding

Direct detection of reduction linked proton binding in Clostridium pasteurianum was carried out using an experiment described by McIntosh (27). Initially, Clostridium pasteurianum was made 0.530 mM in 1mM Tris·HCl/500mM NaCl at the desired pH. The protein was concentrated to 500 ul using Amicon ultrafiltration and the volume brought up to 3 ml with 1mM tris buffer. The concentration procedure was repeated at least six times to ensure complete exchange with buffer. The protein solution was then stored anaerobically in a small sealed flask. Electrolytically reduced methyl viologen (0.200M in buffer) was transferred anaerobically to a separate sealed flask as well. These solutions were brought into an anaerobically prepared glove box as earlier described. For actual proton binding experiments the following procedure was used: 800 ul of 0.53 mM ferredoxin in buffer was aliquoted into a small test tube and the pH of the solution was measured. The pH of the methyl viologen solution was adjusted to that of the protein using HCl or NaOH and 100 ul was added to the ferredoxin. The pH was monitored until no more change was observed and was recorded. For experiments involving hydrogenase reductions

of ferredoxin, the protein mixture was back titrated with 0.010 M NaOH. The number of micromoles of hydrogen bound was determined from the observed pH differences upon reduction of the protein and for the buffer alone.

N. Alpha-^{2}H-Cystine preparation

Alpha-^{2}H-DL-cystine was made using a modified procedure from Wood and Devigneaud (49). A schematized diagram for the synthesis is illustrated in Figure XIV.

Preparation of alpha-^{2}H-S-benzyl-DL-cysteine

50 g of S-benzyl-L-cysteine was placed inside a scrupulously dry 2L round bottom flask fitted with a drying tube containing KOH pellets. 750 ml of acetic anhydride were added to the flask followed immediately by 120 ml of 99.8 atom % D_2O. The flask was then fitted with a 100 cm reflux condenser attached to a drying tube. The reaction mixture was gently heated , using a heating mantle, until all the amino acid dissolves. Gentle heating and great caution was essential since overheating leads to explosive boiling. The yellow solution containing the dissolved amino acid was cooled down to room temperature using a 25^{o}C water bath and an additional 50 ml of D_2O was added to hydrolyze any unreacted acetic anhydride. The solvent was removed using rotary evaporation at 60^{o}C and the cake-like white residue was

Figure XIV. Schematized diagram for the synthesis of alpha-^{2}H-DL-cystine

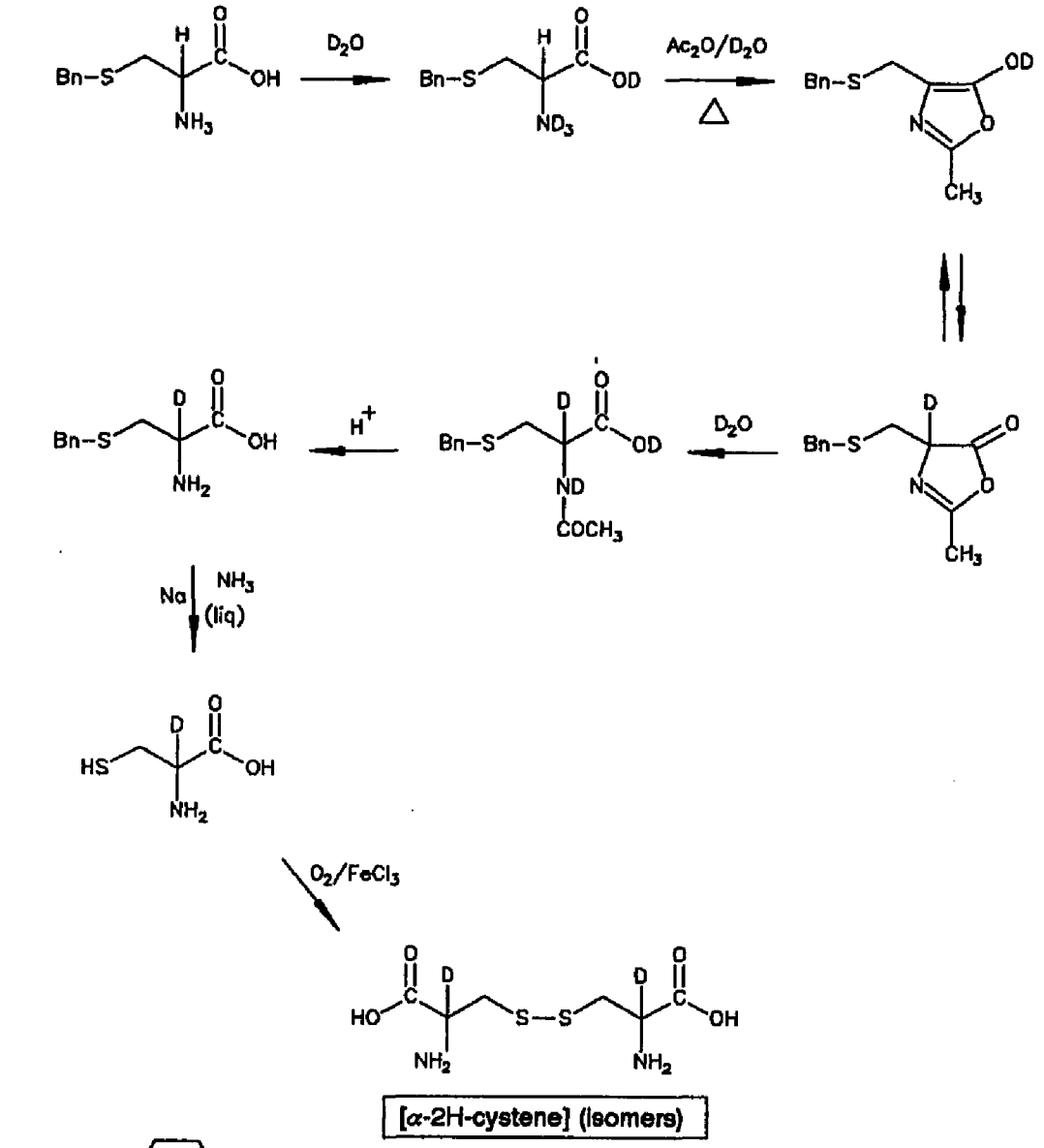

[α-2H-cystene] (isomers)

Bn= CH_2 

taken up in 400 ml of 6N HCl. This mixture was refluxed gently for 16 hours and then cooled to room temperature. Upon cooling, a coffee brown precipitate forms. The pH of the solution layer was raised to 6 using concentrated NH_4OH and left overnight at 4^oC. The precipitate is collected by vacuum filtration, washed with water and then cold ethanol. The ethanol wash continued until the precipitate becomes a creamish light brown color. The precipitate is finally dried with anhydrous ethyl ether and stored in vacuo over anhydrous $CaCl_2$ overnight at room temperature. A typical yield for this step was 85%.

The dried precipitate from the prior step was recrystallized by adding 49 g of it to 450 ml of 3N HCl with gentle heating. The solution was boiled with 1 g Norite for about 5 minutes and then filtered through Whatman #2 filter paper using vacuum filtration. This step was repeated until the filtrate was nearly colorless. The clear solution was cooled to room temperature , and small portions of concentrated NH_4OH were added until significant precipitation was observed. The precipitate was stored overnight at 4^oC for complete precipitation. The white crystals were collected with vacuum filtration, washed with ice water, 10% cold ethanol and finally diethyl ether. The crystals were dried in vacuo overnight over $CaCl_2$. Upon drying, colorless fluffy white crystals of alpha-^{2}H-S-benzyl-DL-cysteine appear. The yield for this step was approximately 80%.

Debenzylation of alpha-^{2}H-S-benzyl-DL-cysteine

The debenzylation was accomplished by first dissolving about 5 g of the alpha-^{2}H-S-benzyl-DL-cysteine from the above step in 700 ml of liquid ammonia condensed from gaseous ammonia at -78.6^{o}C in a round bottom flask. Strips of fresh sodium, first cleaned by immersion in ethyl alcohol, were added to the ammonia until its dark blue color persists. The reaction mixture was stirred in order to facilitate the dissolving of the amino acid. Additional 5 gram portions were added and the sodium treatment repeated until almost all of the reactant has been added. After the addition of the last portion, enough sodium was added to maintain a constant blue color which was maintained for about 5 minutes. Finally, enough amino acid was added to turn the solution colorless. The solvent was removed by evaporation at room temperature. The white residue was taken up in 250 ml of ice/water mixture , transferred to a 500 ml separatory funnel , and then extracted with three 200 ml portions of diethyl ether. The yellow aqueous phase containing the ^{2}H-cysteine was heat treated at 60^{o}C in order to remove any dissolved ether. The solution was then allowed to cool to room temperature and the pH of the solution was adjusted to 10.5 using HCl or NaOH. Two drops of 10% w/w ferric chloride in water were added and the purple solution was gently bubbled with air for 48 hours after which the color

turned yellow. The pH was readjusted to 7.0 and the solution was allowed to precipitate overnight at 4°C. The precipitate is filtered, washed with water and dissolved in a minimum amount of 1N HCl. The solution was treated with Norite as described and the clear solution had added to it small amounts of concentrated NH_4OH until an intense white precipitate is formed. The precipitate was left overnight at 4°C, filtered, washed first with distilled water followed by 10% v/v ethanol in water. The crystals were finally dried with diethyl ether. The white crystals of alpha-^{2}H-DL-cystine were stored <u>in vacuo</u> over $CaCl_2$. The yield from this step varied between 50%-70%. The ^{1}H-NMR spectrum of this material showed about an 85% decrease in the intensity of the resonance corresponding to the alpha-cysteinyl hydrogen (Figure XV). Higher labeling was observed (93%) if the S-benzyl-L-cysteine was pre-exchanged with 99.8 atom % D_2O. This was done by adding small amounts of clean sodium metal to a D_2O solution of S-benzyl-l-cysteine until the amino acid dissolves. Although this method led to a higher isotopic label, nearly 50% of the starting material was lost.

O. Potassium ferricyanide oxidation of ferredoxin

Potassium ferricyanide oxidation of ferredoxin was based on the procedure described by Johnson (28). Native ferredoxin was dissolved in 0.050 M K_2HPO_4 pH 7.4 (3 mg protein/ ml buffer) and cooled for 1 hour at 0°C. In a

Figure XV. 300 MHz ^{1}H-NMR of normal and alpha-^{2}H-labelled cystine

Top - normal DL-cystine

Bottom - alpha-^{2}H-DL-cystine

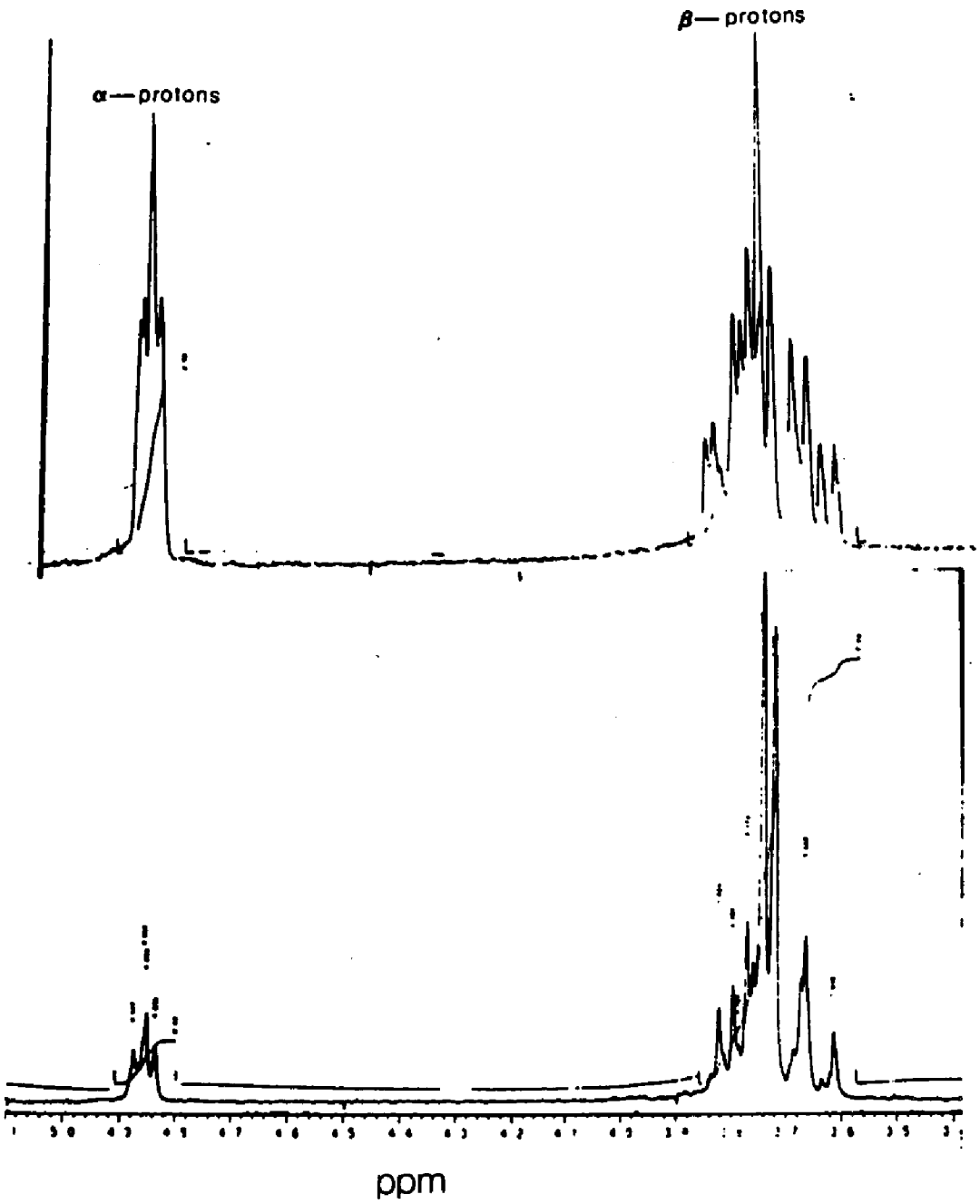
β— protons
α— protons
ppm

separate test tube 100 mg $K_3Fe(CN)_6$ was dissolved in 1 ml 0.050 M K_2HPO_4 pH 7.4 and also cooled. For CP ferredoxin a 15 fold molar excess of potassium ferricyanide was added, whereas a 7 fold excess was used with CAU. The proteins are incubated in an ice water bath under nitrogen gas, 15 hours for CP and 13.5 hours for CAU , respectively. The brown color changes to an amber red color after oxidation. For partial purification of the ferricyanide treated ferredoxin, the protein was first applied to a Whatman-DEAE column equilibrated with 0.050 M K_2HPO_4 pH 7.4, washed with buffer and then eluted with buffer containing 0.500 M NaCl. The eluted protein was then desalted and concentrated using an Amicon ultrafiltration unit fitted with an Amicon YM 5 membrane. For further purification of ferricyanide treated ferredoxin, the protein was applied to a 103 cm X 2.5 cm Sephacel G-75 column equilibrated with anaerobically prepared 0.050 M phosphate pH 7.4 . This column was run anaerobically to prevent denaturation during the approximate 18 hour run. For molecular weight determinations, marker proteins included hemoglobin (64000), myoglobin (16000), and cytochrome C (12500) were used. The different molecular weight fractions are pooled separately and applied to Whatman-DEAE columns equilibrated with 0.050 M phosphate PH 7.4. Each column is washed with buffer containing no salt, followed by 0.10 M, 0.20 M and finally 0.35 M NaCl, respectively.

P. Preparation of NMR samples

Samples for ^{1}H-NMR spectroscopy were prepared in the following way: Ferredoxin, precipitated in saturated ammonium sulfate, was dissolved in 0.050 M KD_2PO_4 (99.9 atom %) buffer (adjusted to the desired pD using KOD or DCl). The protein solution was concentrated to 0.30 ml using an Amicon ultrafiltration cell containing a YM 5 membrane. The volume was brought up to 3 ml and concentrated again. This procedure was repeated seven to eight times. The protein was concentrated to a final volume of about 400-500 ul. Samples were then loaded into 5mm Wilmad cylindrical NMR tubes (cat. no. 527-PP), along with 10-25 ul of DSS (sodium 2,2-dimethy-2-silapentane-5-sulfonate), used as an internal reference. ^{13}C-NMR samples are prepared by dissolving the ferredoxin in 0.050 M potassium phosphate/100mM NaCl for a final concentration of between 1mM-2mM. All samples contained approximately 33% D_2O to provide a lock signal. ^{13}C-methanol was used as an internal reference standard for spectra (49.405 ppm relative to TMS). 10mm Wilmad NMR tubes (cat. no. 513-3PP) were used for all carbon spectra. pH measurements were taken on a Radiometer 26 pH meter. For measurements directly inside the NMR tube a 3mm X 180mm Ingold combination glass electrode was used. Unless specified the pH values are reported as uncorrected pH meter readings.

Q. Preparation of EPR samples

Reduced samples of ferredoxin (2-3 mg/ml buffer) in standard 3 mm Wilmad EPR tubes were prepared by addition of solid sodium dithionite followed by gentle vortexing. The top of the tube was flushed with a slow stream of argon or nitrogen and the tube sealed with a small rubber septum. The samples were immediately frozen and stored in liquid nitrogen.

Q. Instrumentation

NMR spectra were obtained using a JOEL GX-400 FT spectrometer. ^{1}H-NMR was performed at 400 MHz with a sweep width of 40000 Hz. For protein spectra , a pulse delay of 0.100 sec was used. Typically, 32 K spectra were processed using a broadening factor of 3-6 Hz. Similar conditions were used for ^{2}H-NMR except that a frequency of 80 MHz was used. For ^{13}C-NMR 100 MHz was used. The sweep width was 25000 Hz with a 0.10 sec pulse delay. A standard proton decoupler was used for proton-decoupled ^{13}C-NMR.

EPR spectra were recorded using a Varian X-band V-4500 spectrometer fitted with a Heli-Trans liquid helium transfer system. Low temperature EPR spectra were taken at 12-15^{o}K using a frequency of approximately 9.4 GHz. The modulation amplitude was usually 2 G and power was set to 5 mW.

Circular dichroism spectra were obtained using a Jobin Yvon Mark V dichrograph. Spectra were taken in 3 ml

CD quartz glass cuvettes. Spectra were acquired between 600-250 nm with a scan rate of 2 nm/sec.

UV-visible spectra were recorded on a Varian Cary 219 UV-visible spectrometer. Spectra were taken in either 1 ml or 3 ml quartz glass cuvettes. Most UV-visible spectra were measured between 600-250 nm with a scan rate of 2 nm/sec. The period was between 0.5-1.0 and the slit width was 1-2 nm.

Scintillation counting was done on a Beckman LS 6800 scintillation counter. Typically, cpm determinations were made after a 20 minute accumulation period.

I. An examination of the origin of the pH dependent midpoint reduction potential in Clostridium pasteurianum 2(4Fe-4S) ferredoxin

Various literature articles have reported the existence of a pH dependent midpoint reduction potential (E_{mdpt}) in several iron-sulfur proteins. Some of these pH dependencies are presented in Table III. Despite their varied polypeptide compostion, for all ferredoxins reported, except HIPIP ferredoxin, the E_{mdpt} becomes more negative as the pH is raised. This observation suggests that the pH dependency arises independent of the polypeptide, and therefore, it is generally believed that the pH dependence must be a property of the Fe-S center. The proton binding behavior of iron-sulfur proteins is of interest for a number of reasons. Many enzymes which catalyze reactions involving protons are iron-sulfur proteins including nitrogenases, most hydrogenases and several oxidases. In addition, NADH dehydrogenase , a mitchondrial protein complex involved in energy transduction during oxidative phosphorylation , contains a number of iron-sulfur centers.

Reduction-linked hydrogen ion binding has often been examined by observation of proton dissociation equilibria (pKs) which depend on the protein oxidation state. If a proton binding site (e.g. an amine or a carboxylic acid) has an oxidation-state dependent pK, then the extent of

Table III. PH dependencies of the midpoint reduction potentials for several iron-sulfur proteins

TABLE III

Fe-S Cluster	Source	Estimated Em at pH 7.0	pH dependence	
2Fe-2S	Spinach	-428 mV	-4mV/pH unit	(37)
	Parsely	-416	-7	(66)
	Ox heart (N-1a) from mitochondria	-380	-60	(54)
4Fe-4S	B. polymxya I	-377	-11	(37)
	C. vinosum	-482 (pH 8)	-11	(37)
	C. vinosum HIPIP	+350	0	(38)
	C. tartarvorum	-424	-3	(37)
	P. aerogenes	-427	-7	(37)
	C. acidi-urici	-434	-2	(37)
	C. pasteurianum	-403	-12	(37)
		-391	-13	(27)
		-410	0	(55)
	Ox heart (N-2) from mitochondria	-20	-60	(54)

protonation can change with a change in the protein oxidation state. Consider , for example, a site with a pK of 7 in the oxidized protein and 10 in the reduced protein. At pHs in the 7-10 range, reduction of the protein will lead to a significant increase in the extent of protonation of the site (the pK_{ox} is lower than the pH while pK_{red} is higher), resulting in reduction-linked hydrogen ion binding.

Magliozzo et al. have shown that the pH dependent E_{mdpt} (27) of CP 8Fe Fd does not arise from a pH dependent protein conformation change. Rather, it was proposed that the pH dependence arose from oxidation-reduction equilibria involving hydrogen ion binding. The authors reported that oxidized 2(4Fe-4S) CP ferredoxin had a hydrogen binding site with a pKa of about 7.4 and a pKa of greater than 9 in the reduced form (27) . Sykes et al. (50) has also reported a pKa of around 7.4 in oxidized CP ferredoxin using kinetic spectrotitrimetric measurements of a redox mediator . Similar results were observed in synthetic Fe-S model compounds as well. For example, Job et al. (51) have reported a pKa of 7.4 for a water soluble 4Fe-4S model compound , and Tanaka et al. (52) have reported oxidation-state dependent pKa values of less than 4 and 9.0 for a lipid soluble 4Fe-4S model compound in the oxidized and reduced forms, respectively. Furthermore, it was reported by McIntosh et al. (27) , that proton binding in CP ferredoxin is reduction-linked by direct observation

of pH changes on reduction or reoxidation .

Oxidation-state dependent proton binding presents the possibility of cotransport of electrons and protons in protein complexes and in membrane systems. It has been shown that a 4Fe-4S model compound can indeed cotransport electrons and protons (53). Reduction-linked hydrogen ion binding is also indicated by the negative 60 mv/pH unit dependence of the E_{mdpt} reported for a 4Fe-4S model compound in aqueous micellar solution below pH 9 (52). The possible significance of this to proton translocation in mitochondrial oxidative phosphoryation is underscored by the -60mV/pH unit dependencies of the E_{mdpt} observed for the iron-sulfur centers N-1 and N-2a in NADH dehydrogenase (54).

Although there is substantial evidence for reduction-linked proton binding in CP 2(4Fe-4S) ferredoxin, there are reports that contradict the data supporting a pH dependent E_{mdpt} in CP ferredoxin. Most notably, a recent article by Prince et al. (55), has shown rather convincingly using EPR and potentiometry that there is no pH dependent E_{mdpt} in CP 8Fe ferredoxin . It is also unclear as to the particular sites in the protein molecule which might be involved in oxidation-state dependent proton binding. The model compound work implicates the $Fe_4S_4S_4^{cys}$ centers themselves, but the possiblity of peptide sites in addition to the iron-sulfur centers remains . Since the pH dependence of the E_{mdpt} is

exhibited above 7 , only peptide sites with pKa near or above 7 are relevent. If iron-bound cysteines are considered iron-sulfur cluster sites, the remaining potential sites are Tyr-2 , Lys-3 and the N-terminal alanine. The protein contains no histidine, arginine or free cysteine, and glutamic or aspartic acids are unlikely to have a pK that high.

Presented in this section are experiments which explore the possibility of amine site (Lys^3 or the N-terminal alanine) participation in the oxidation-state dependent proton binding behavior in CP 8 Fe ferredoxin. Additionally, experiments will be presented which reexamine some of the procedures used in the original determinations of the pH dependent midpoint reduction potential in CP ferredoxin.

To examine the possibility of amine participation in oxidation-state dependent proton binding , ^{13}C-labelled formaldehyde was used to reductively methylate the amine groups (Figure XVI) and the pKa values of the modified amines were determined using ^{13}C-NMR (48). Oxidation-state dependent proton binding will be determined by comparing the pKa of the modified amines in their oxidized and reduced forms. Reductive methylation has been used to modify a large number of proteins, including lysozyme (56), ribonuclease A (57,58) , serum albumin (59), alpha-lactalbumin (60), and concanavalin B (61-63). Because the methyl groups are small, only small changes in physical

Figure XVI. Reaction scheme for the reductive methylation of Clostridium pasteurianum 8Fe ferredoxin

Reaction Scheme for Reductive Methylation

$$CH_2O + H_2N{-}R \longrightarrow H_2C{=}N{-}R + H_2O$$

$$H_2C{=}N{-}R + NaCNBH_3 \longrightarrow CH_3{-}NH{-}R$$

$$CH_3{-}NH{-}R + CH_2O \xrightarrow[\text{fast}]{NaCNBH_3} (CH_3)_2{-}N{-}R + H_2O$$

and chemical properties are found after methylation, and only slight alteration in the amine pKa values are observed.

RESULTS AND DISCUSSION

A. Titrations of methylated amines in CP 8Fe Fd

Reaction of CP 8Fe Fd with ^{13}C-formaldehyde in the presence of sodium cyanoborohydride leads to methylation of the amines . Reaction with formaldehyde preferentially leads to dimethylation, since reaction with a second equivalent of formaldehyde proceeds more rapidly than the first (48). The proton decoupled ^{13}C-NMR spectrum of the modified apoferredoxin is presented in Figure XVII. In the decoupled spectrum of the methylated apoferredoxin, the two peaks shown between 40 and 45 ppm correspond to amino-methyl resonances. The two downfield peaks around 60 ppm arise from natural abundance signals from the buffer. The proton coupled ^{13}C-NMR spectrum of methylated apoferredoxin , Figure XVIII, show quartets with an average coupling constant of approximately 142 Hz , indicative of methyl groups, and consistent with previous results (58). The resonances near 42 ppm and 44 ppm, respectively, are characteristic of unperturbed dimethylated N-terminal and dimethylated lysine resonances (56-63). Therefore the peak near 44 ppm is assigned to the N,N'-dimethyl Lys^3 resonance whereas the peak near

Figure XVII. Proton noise decoupled ^{13}C-NMR spectrum of tetramethylated Clostridium pasteurianum 8Fe ferredoxin

Conditions: 30 mg apoprotein/ml in 0.10M tris buffer, 100% D_2O, temperature, 20^{o}, 1000 accumulations, 65536 points, pulse delay, 0.400 sec, acquisition time, 1.634 sec, spectral width, 40000 Hz . Spectrum is referenced to ^{13}C-CH_3OH (49.405 ppm).

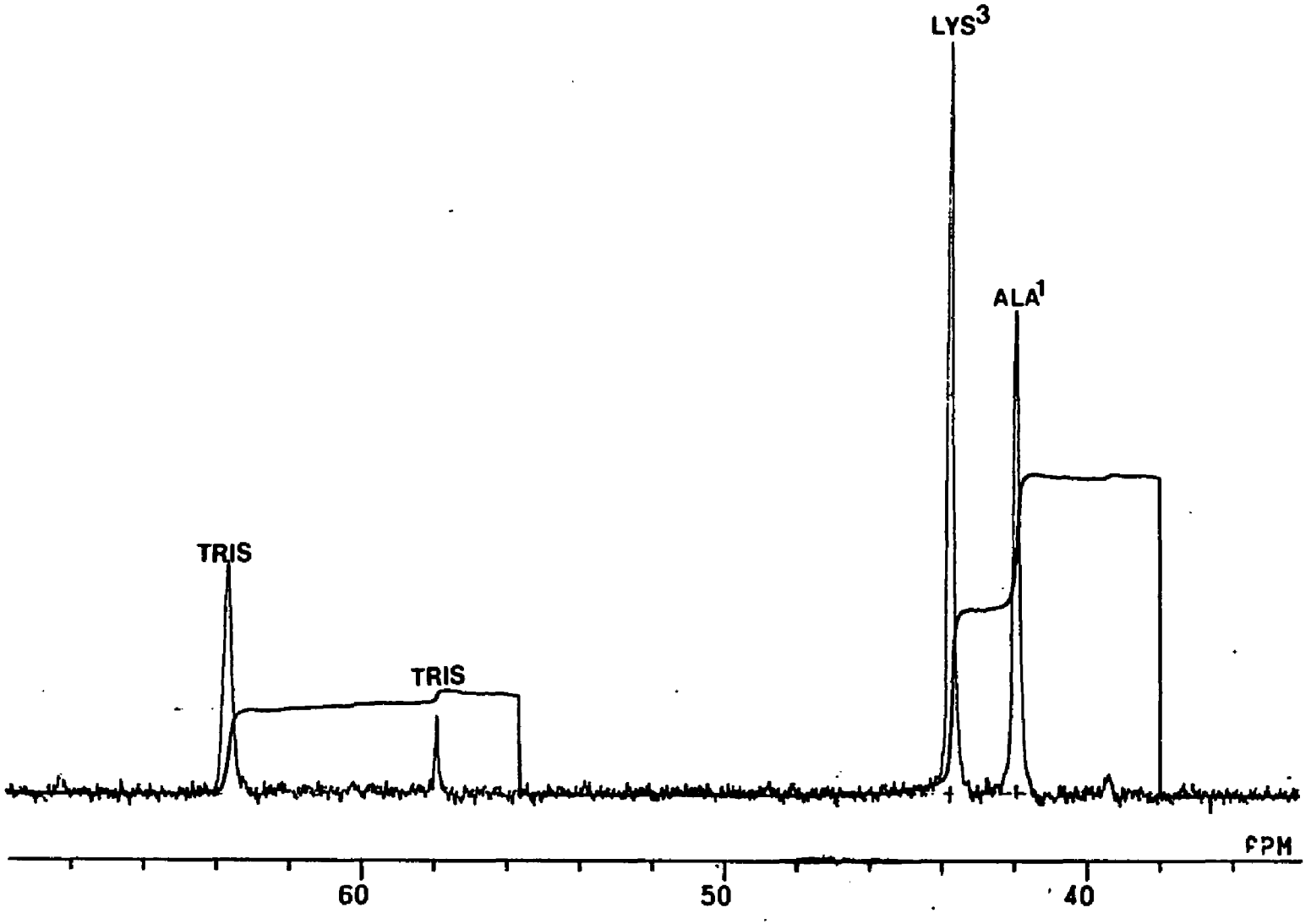
LYS3
ALA1
TRIS
TRIS
PPM
60
50
40

Figure XVIII. Proton coupled ^{13}C-NMR spectrum of tetramethylated Clostridium pasteurianum 8Fe ferredoxin

Conditions: same as Figure XVII except 2500 accumulations

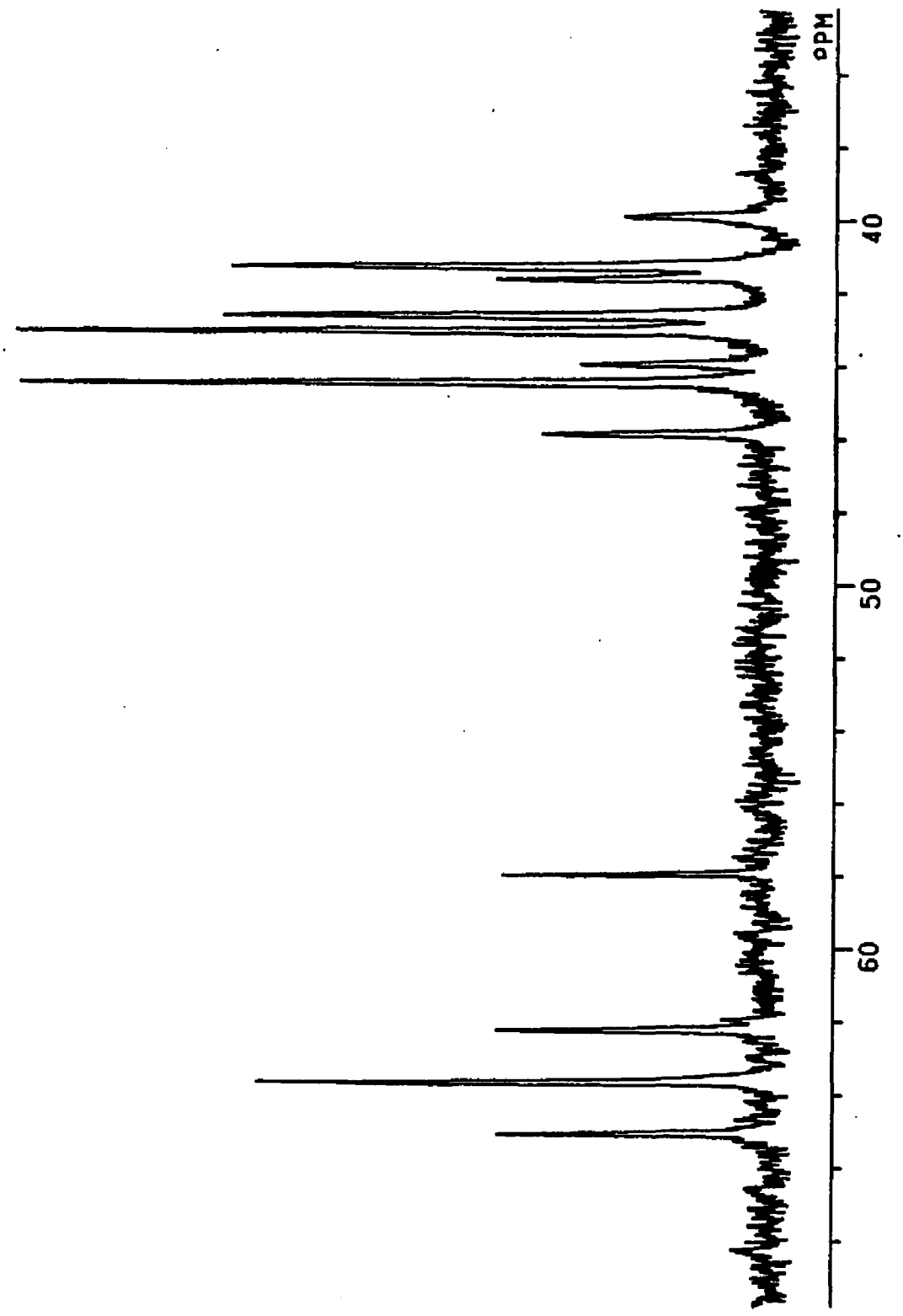
PPM
40
50
60

41.3 ppm is N,N'-dimethyl Ala^1. The corresponding monomethyl resonances are expected between 31 and 34 ppm, and no evidence of any monomethyl derivative is observed when formaldehyde is used in excess. When the reaction is monitored using ^{14}C-formaldehyde followed by scintillation counting, evidence of extensive modification is also found (Table VIII).

Modification reactions were typically performed using either Fd_{apo} or hydrogenase reduced native Fd . It is interesting to note that approximately an eight-fold lower extent of methylation was observed using short incubation times when oxidized rather than reduced native Fd was used. This was true for a wide range of ionic strength and pH conditions. This observation is consistent with the difficulty Hong and Rabinowitz observed for reaction of the N-terminus of CAU Fd in a range of modifying reactions (64). It seems unlikely that limited accessibility is the cause of the poor reactivity of the native Fd , as the protein is very small. Indeed the x-ray structure of the extensively homologous Fd from PA indicates that both residues should be solvent exposed (65,67). Even fairly strong ion-pair interactions do not appear to profoundly limit reactivity, as demonstrated by modification of the ion paired Lys^{13} in lysozyme (56). Even in the apoprotein the N-terminal does not react completely, as shown by the relative intensities of the lysine and alanine peaks in the decoupled carbon NMR

spectrum of the apoprotein (Figure XVII). This differential intensity seen in Figure XVII is not a result of varying Nuclear Overhauser enhancements, as nearly the same ratio of the intensities is seen in the coupled spectum. Because the pK of the N-terminal alanine is lower than that of lysine, it was expected (56) that it should preferentially react with formaldehyde. The reason for the diminished N-terminal reactivity is not well understood, nor is the general lack of reactivity exhibited by the oxidized form of the protein.

To assess the effects of methylation on the structure of the protein, a variety of spectroscopic techniques were used. The UV-visible spectrum of oxidized native and modified reconstituted ferredoxin were essentially identical (Figure XIX), as was the circular dichroism spectrum of oxidized samples of native and modified material (Figure XX) , and the EPR spectra of the reduced proteins were also identical (Figure XXI). However, small differences were observed in the ^{1}H-NMR spectra of native and reconstituted modified ferredoxin (Figure XXII). The resonances downfield of 11 ppm arise from protons on cysteinyl beta-carbons (34) and are very sensitive to small changes in the environment about the iron-sulfur centers. The two sharper resonances arise from alpha cysteinyl protons (34). As can be seen, the general features of the spectra are similar, but there are small (0.01 to 0.20 ppm) shifts in some of the downfield

Figure XIX . UV-visible absorption spectrum of oxidized and modified reconstituted Clostridium pasteurianum 8 Fe ferredoxin

Conditions: 0.18 mg/ml in 0.10M tris buffer / 0.25M NaCl, pH 7.4, temperature , 27°

Native ferredoxin - Top (offset) spectrum
Modifed ferredoxin - bottom spectrum

Note: Both spectra taken at same concentration, however, the spectrum of native ferredoxin is offset to higher absorbances

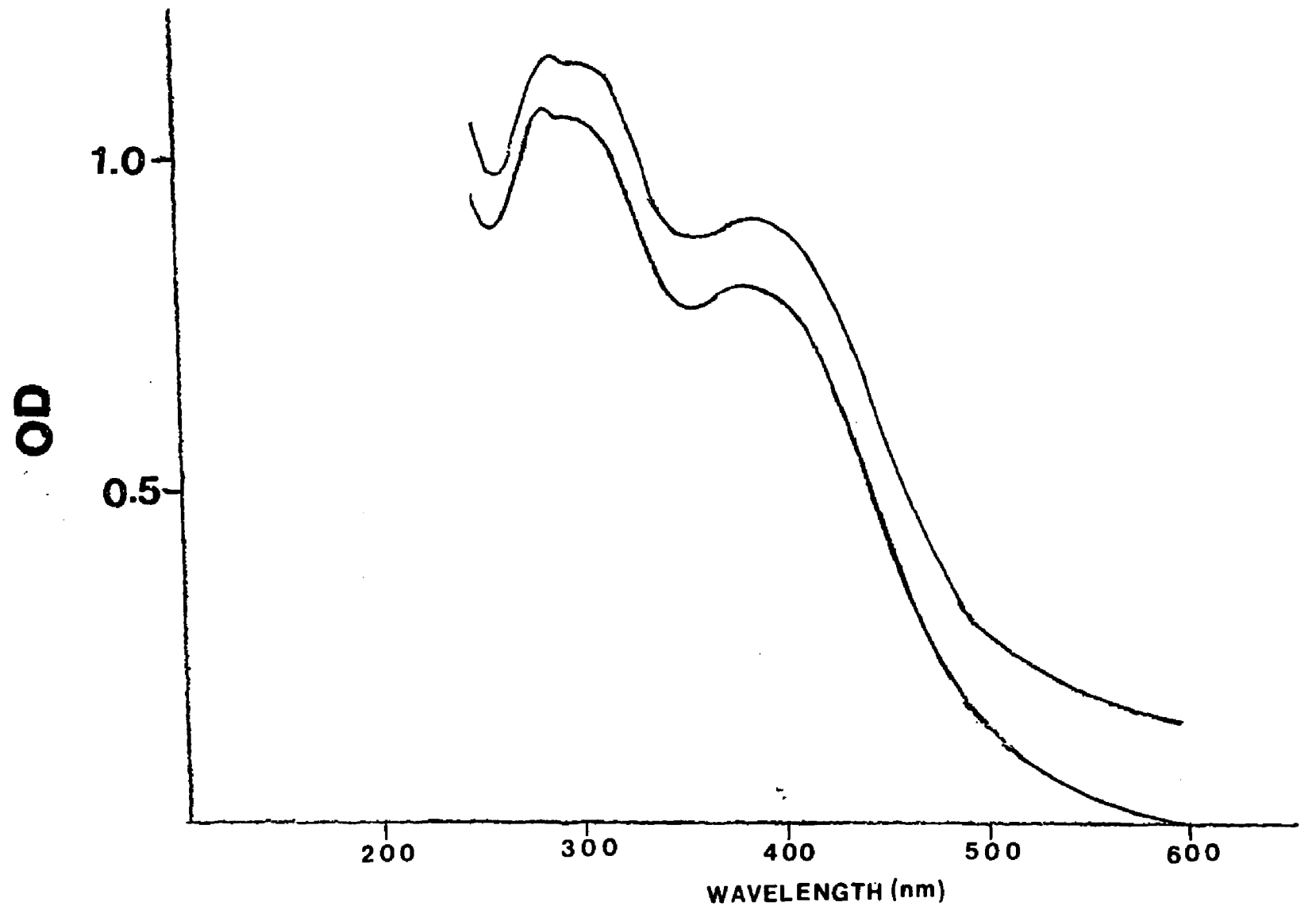
OD
1.0
0.5
200
300
400
500
600
WAVELENGTH (nm)

Figure XX. Circular dichroism spectrum of oxidized and modified reconstituted *Clostridium pasteurianum* 8Fe ferredoxin

Conditions: 3 mg/ml in 50 mM K_2HPO_4 / 0.10M NaCl, pH 7.36

MF - modified ferredoxin

NF - native ferredoxin

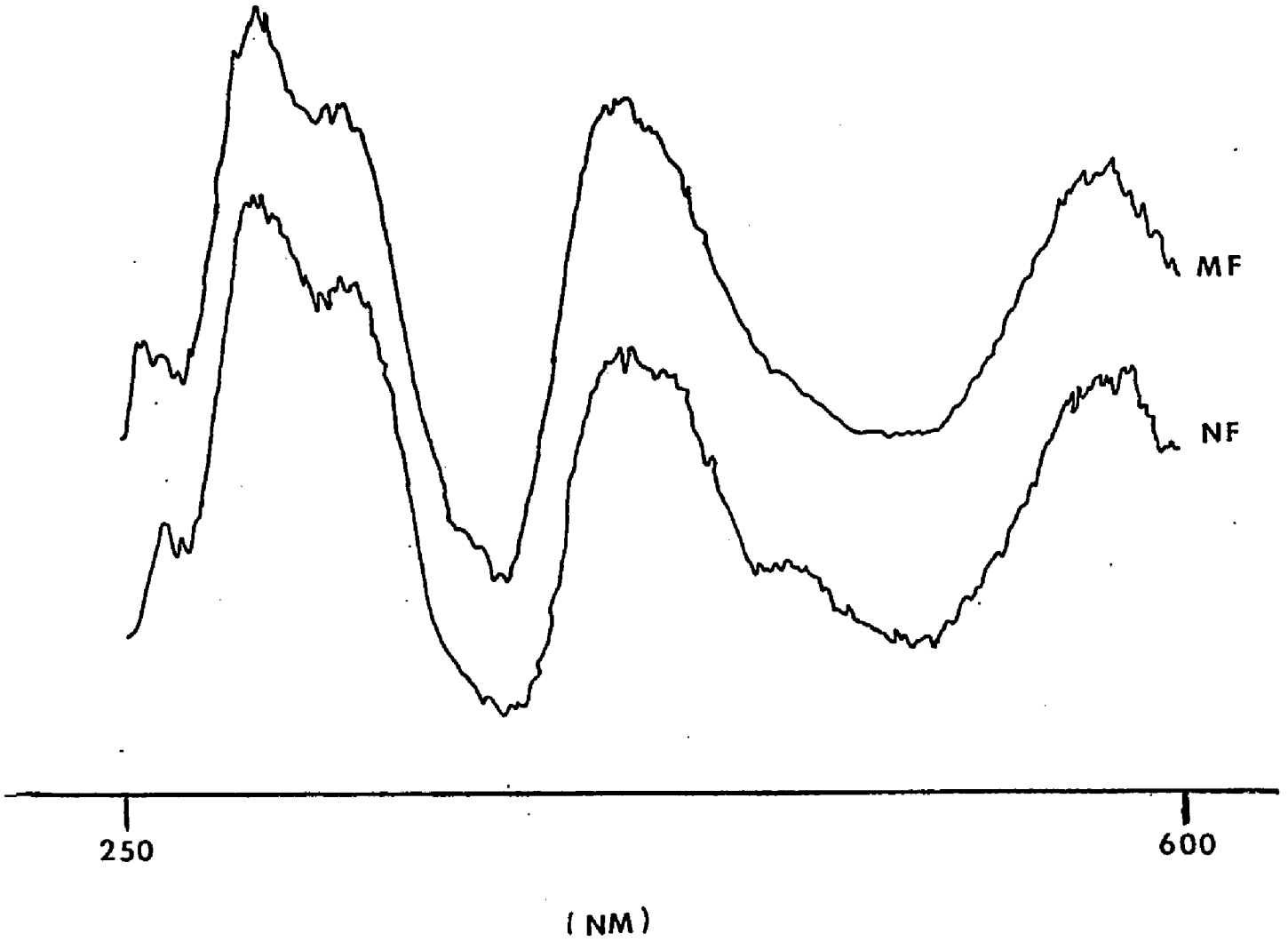
MF
NF
250
600
(NM)

Figure XXI. EPR spectrum of dithionite reduced native and modified reconstituted Clostridium pasteurianum 8Fe ferredoxin

Conditions: 3 mg/ml in 0.20M tris buffer/ 0.10M NaCl, pH 8.3, temperature, 15°K

MF - modified reconstituted ferredoxin

NF - native ferredoxin

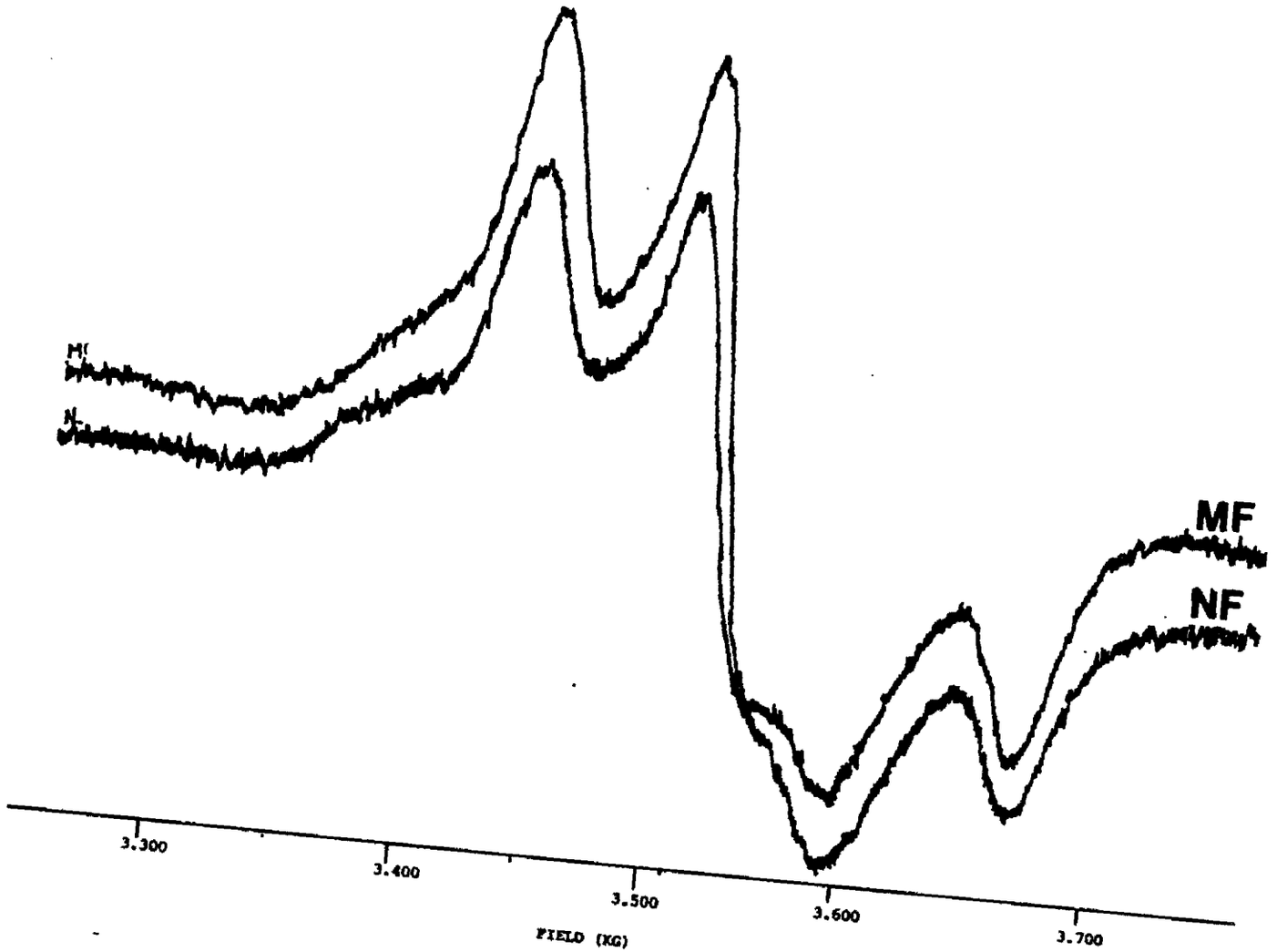
MF
NF
3.300
3.400
3.500
3.600
3.700
FIELD (KG)

Figure XXII. ^{1}H-NMR spectra of the downfield region of native and modified Clostridium pasteurianum 8Fe ferredoxin

Conditions: Native 6 mg/ml, modified, 3mg/ml. For both spectra, 25 mM K_2DPO_4 buffer/ 0.50M NaCl in 99.9% D_2O , pH 7.6 , 2000 accumulations, pulse repeat time, 2.3 seconds, temperature , 21^{o}C

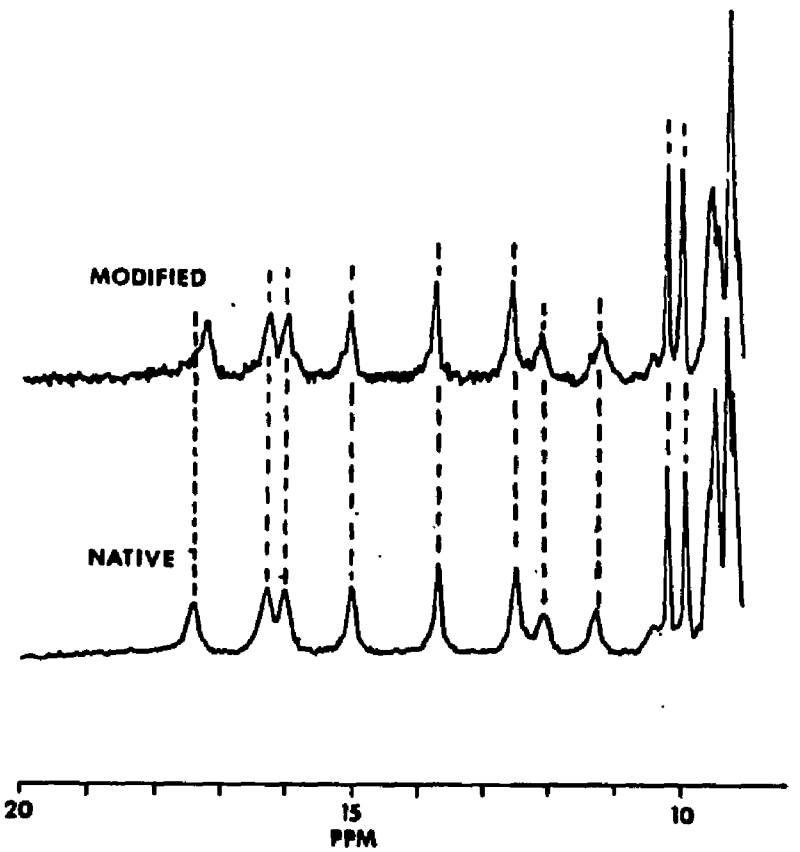
MODIFIED
NATIVE
20
15
10
PPM

resonances. These small shifts are likely to indicate only minor changes in conformation around the 2(4Fe-4S) centers as a result of methylation.

The midpoint reduction potential of hydrogenase reduced native and methylated Fd was determined optically as a function of pH in 0.10M K_2HPO_4/0.10 M NaCl (Figure XXIII). Although by this method both proteins exhibit a pH dependent E_{mdpt} , in the pH range 6.7 - 9.2, there is no significant difference in the E_{mdpt} between native and modified reconstituted Fd. The theoretical curve used to fit the data was calculated from a model of two equivalent oxidation-state dependent proton binding sites, as described previously (27). The values of the three parameters used for the fit shown in Figure XXIII are pK_{ox} = 7.3 , pK_{red} = 8.9 and E_m , the midpoint reduction potential, equals -394 mV for the fully protonated form of the protein. In the pH range observed the calculated reduction potentials are relatively insensitive to increases in pK_{red}, and so 8.9 should be viewed as a lower limit to pK_{red}. The values obtained for pK_{ox} and pK_{red} compare well with the values of pK_{ox} = 7.4 (27,50) and pK_{red} = 8.9 reported earlier (27) for this protein. Although the previously reported value of E_m = -371 mV for this protein is more positive than found here, the previous measurements were conducted in a buffer of considerably higher ionic strength. A similar ionic strength dependence of E_m in this protein has been

Figure XXIII. The pH dependence of the apparent midpoint reduction potential , E_m , and native and modified Clostridium pasteurianum 8Fe ferredoxin

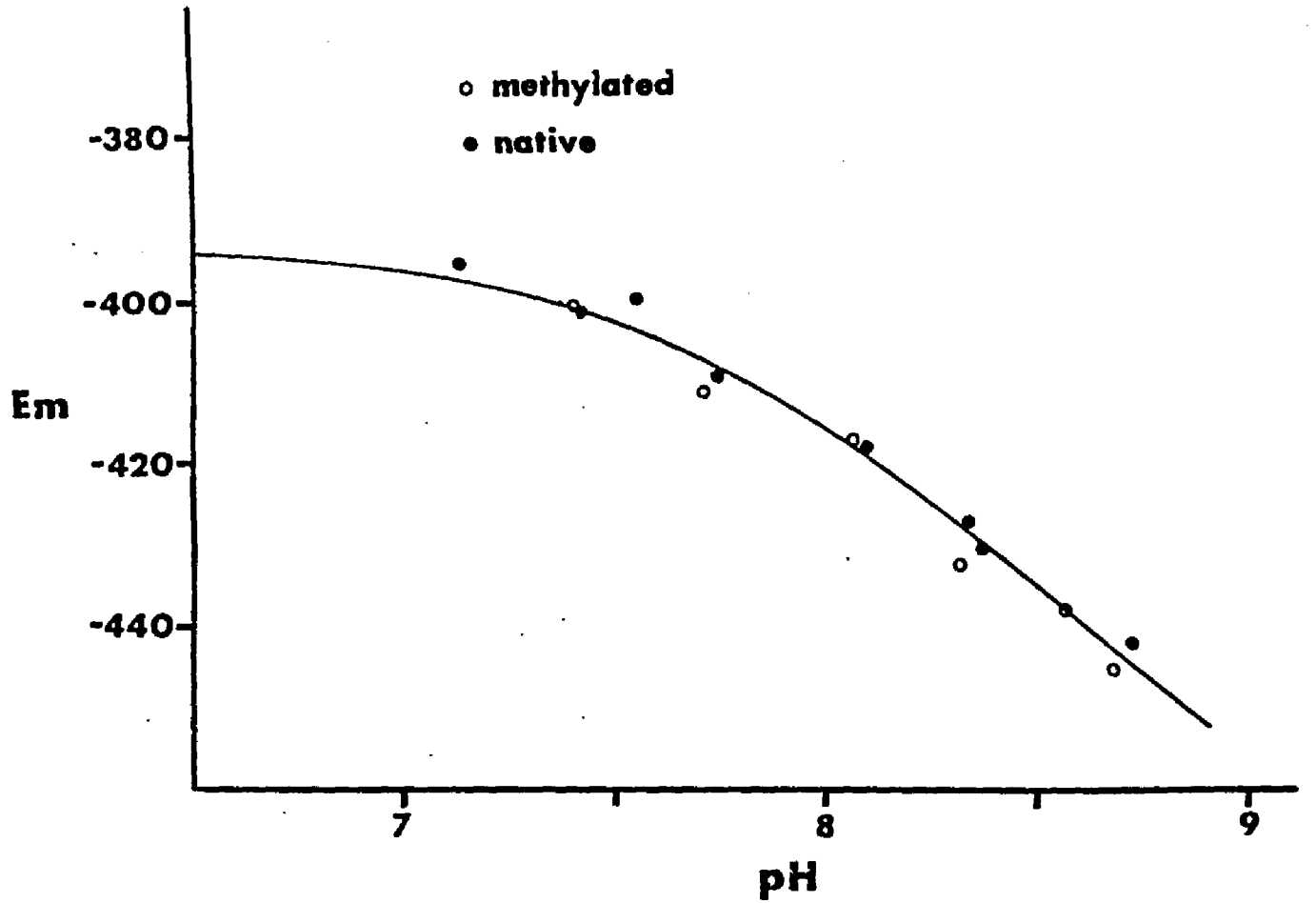
o methylated
• native
-380
-400
-420
-440
Em
7
8
9
pH

previously reported (27).

As judged by a ferredoxin-dependent cytochrome C reduction assay, there may be an appropriate reduction in biological activity of the dimethylated Fd relative to native Fd. However, this difference is within the experimental error of the assay. In contrast, as measured by optical absorbance at 390 nm, under aerobic or anaerobic conditions the dimethylated Fd was appreciably less stable than native unmodified Fd. In aerobic solution at pH 7.9 the half-life of the modified reconstituted Fd was decreased by 50% . Sensitivity of the stability of CAU Fd to modification of the N-terminal amine has previously been reported (64).

The titration results for dimethylated Lys^3 and the N-terminal alanine are seen in Figures XXIV, XXV and XXVI. The titration curves were fit assuming independent titration sites. For the simulated titration curves of reduced Fd the situation was more complex. A hydrogenase/hydrogen gas reduction system was used, and consequently the solution potential was approximately equal to (-60mV) X (pH). Thus, the fraction of reduced ferredoxin varied as a function of pH, from approximately 55% reduced at pH 6.8 to about 90% reduced at pH 8.0. Assuming a fast exchange condition between the oxidized and reduced forms of the protein, the observed chemical shift represents weighted averages of oxidized and reduced peak positions. The curve in Figure XXVI was simulated by

Figure XXIV. ^{13}C-NMR titration curves for modified Clostridium pasteurianum apoferredoxin

Conditions: 0.30 mM protein in 0.050M K_2HPO_4 / 100 mM NaCl , 33% D_2O , pulse repeat time, 2.04 seconds

The solid lines are drawn using the Henderson-Hasselbach equation with pK values as shown

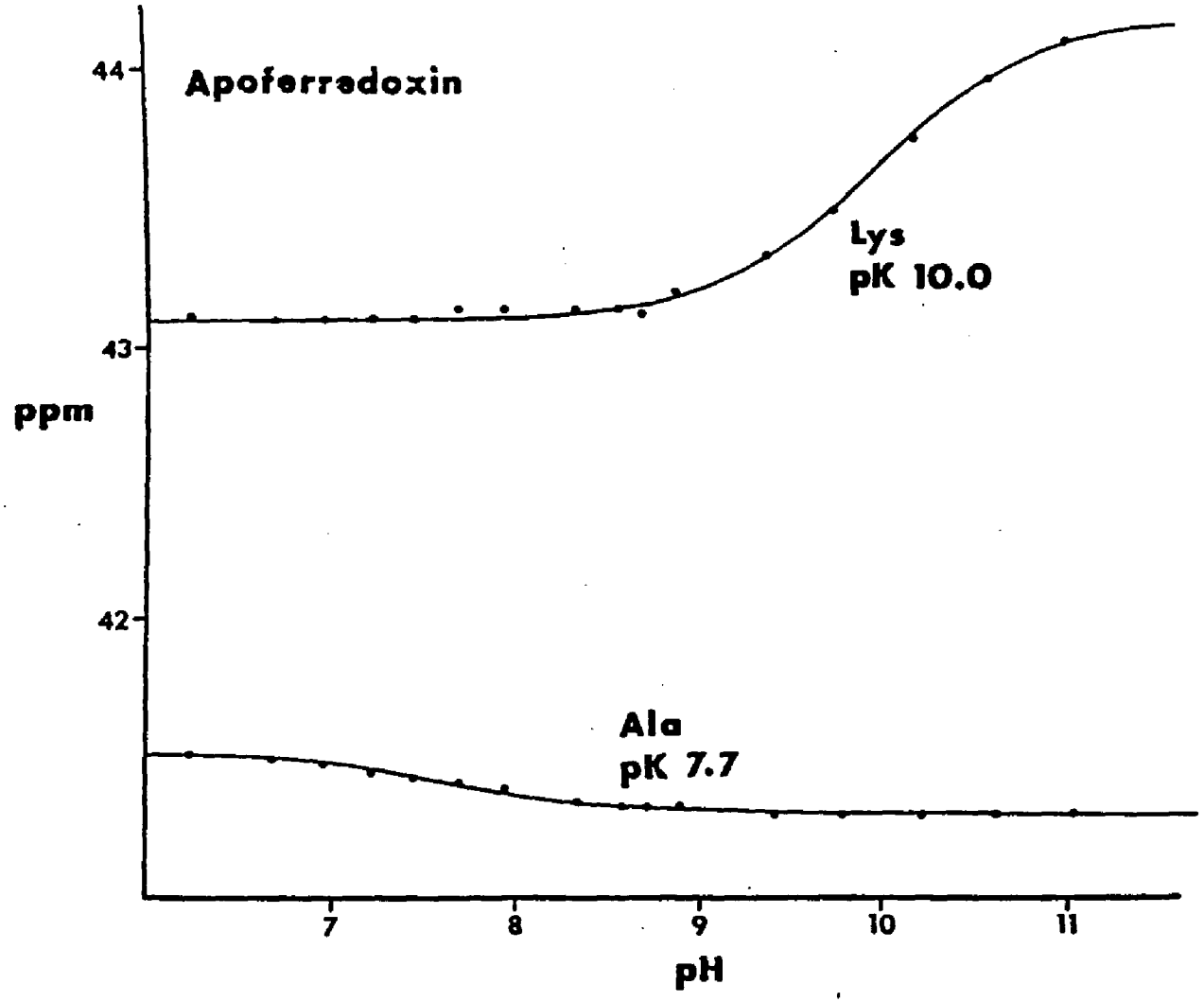
Apoferredoxin
Lys
pK 10.0
Ala
pK 7.7
ppm
44
43
42
7
8
9
10
11
pH

Figure XXV. ^{13}C-NMR titration curves for modified oxidized Clostridium pasteurianum ferredoxin

Conditions: 0.09 mM protein in 0.050M K_2HPO_4 / 100 mM NaCl , 33% D_2O , pulse repeat time, 0.504 seconds

The solid lines are drawn using the Henderson-Hasselbach equation with pK values as shown

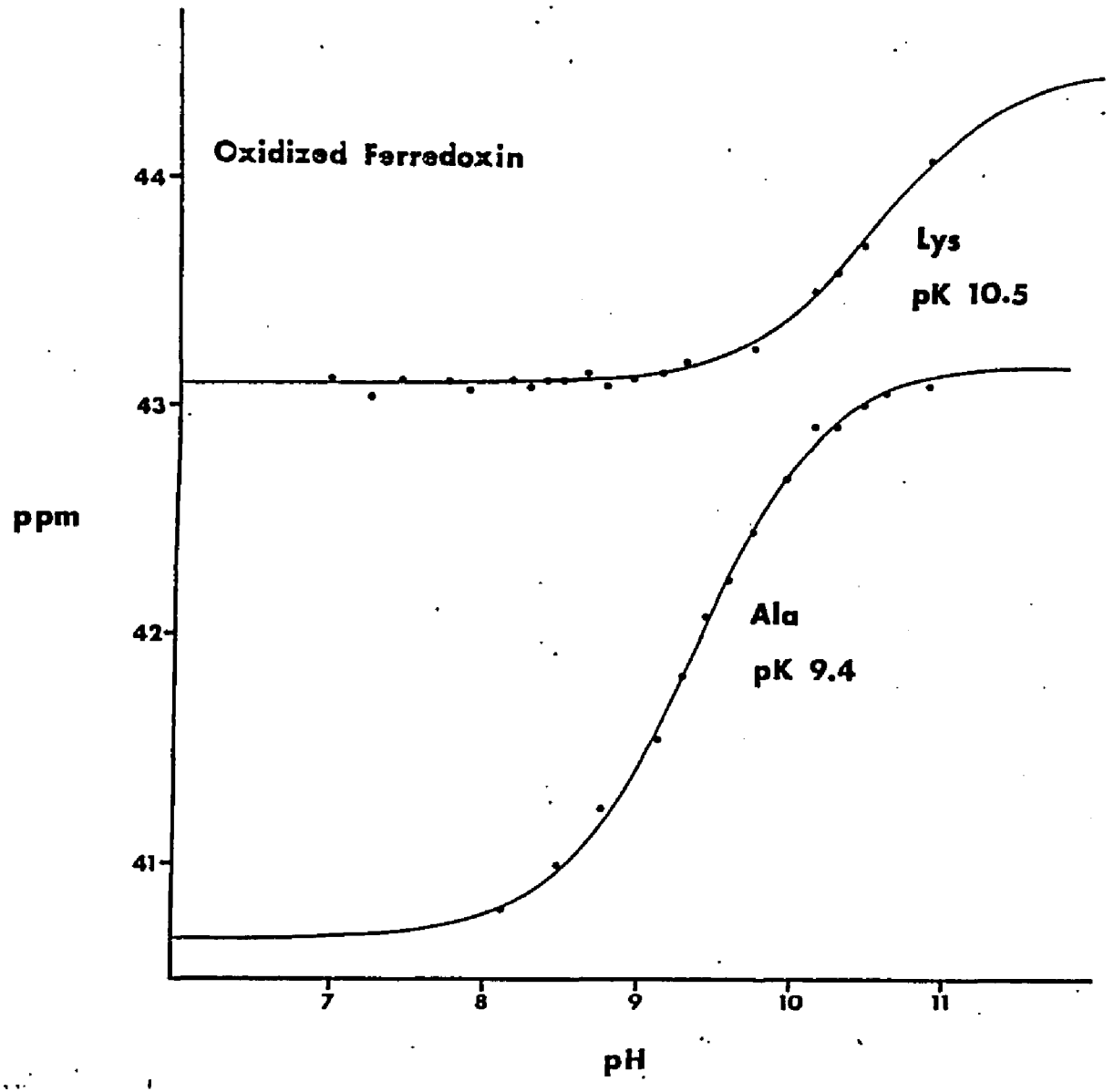
Oxidized Ferredoxin
Lys
pK 10.5
Ala
pK 9.4
ppm
44
43
42
41
7
8
9
10
11
pH

Figure XXVI. ^{13}C-NMR titration curves for modified reduced Clostridium pasteurianum 8Fe ferredoxin

Conditions: 0.40 mM protein in 0.050 M K_2PO_4 / 100 mM NaCl buffer, 33% D_2O

The solid line for the lysine titration was drawn using the Henderson-Hasslebach equation. The solid line for the alanine titration was drawn as described in text.

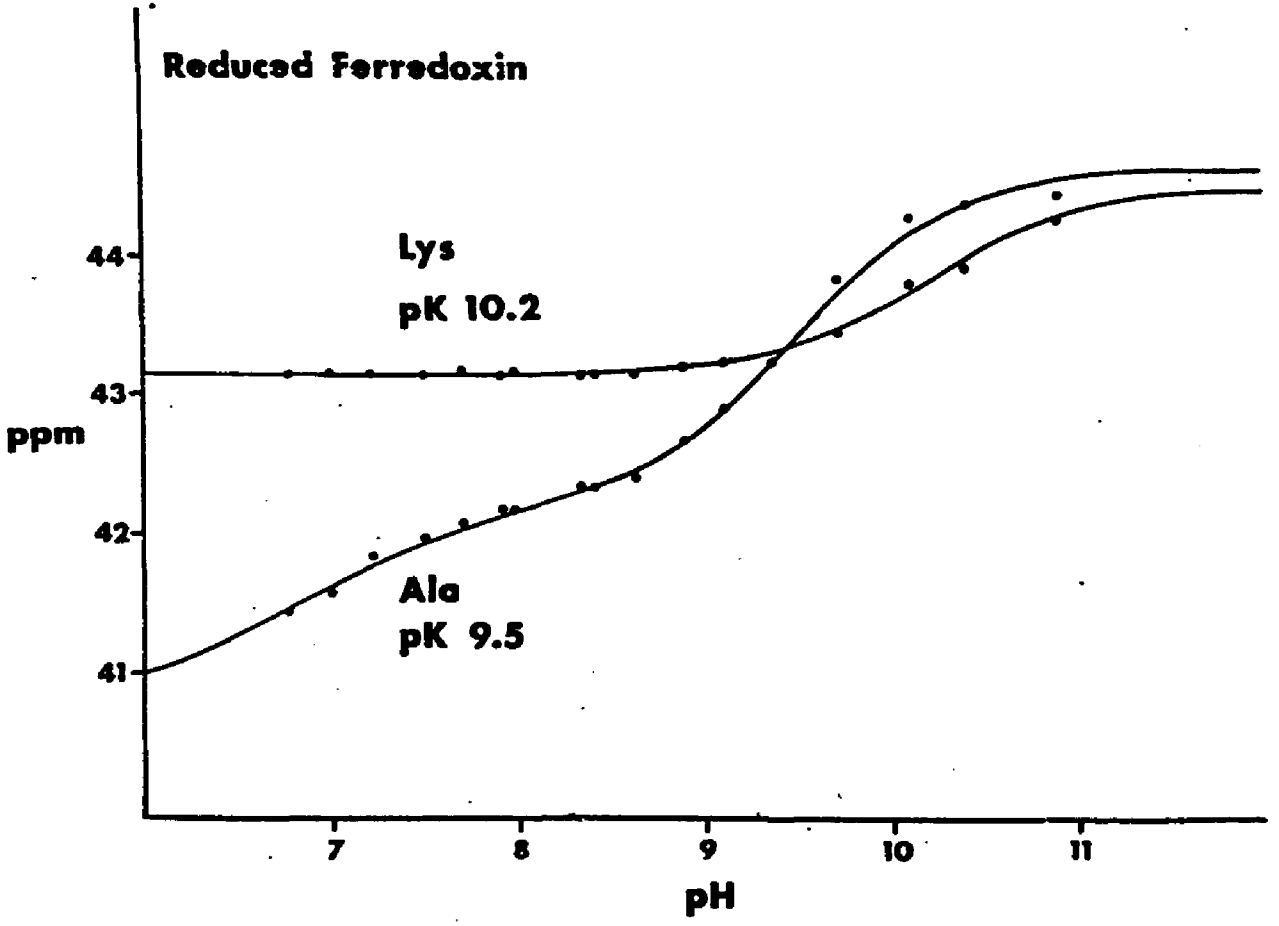
Reduced Ferredoxin
Lys
pK 10.2
Ala
pK 9.5
ppm
44
43
42
41
7
8
9
10
11
pH

computation of the fraction of reduced protein using values of E_m measured in 33% D_2O, followed by calculation of the reduction weighted avarages for the chemical shift. For a given pH, the chemical shifts for the oxidized protein were obtained from Figure XXV, and the chemical shifts for the reduced proteins were simulated in the normal way using the pK and the chemical shift extremes as variables. As can be seen in Figure XXVI, the titration appears biphasic. The section at low pH reflects the pH dependent mixture of oxidized and reduced protein , and the section at higher pH , where the protein is essentially completely reduced , arises from actual titration of the reduced proteins.

The titration behavior of the dimethylated lysine is in good agreement with what has been observed in other methylated proteins (56-63). These resonances are expected to occur near 43 ppm in the protonated amine and exhibit approximately 1 ppm downfield chemical shift with increasing pH, with a pK slightly above 10 (48,56,60). The pK values found for the dimethylated Fd_{apo} , Fd_{ox} and Fd_{red} dimethylated lysine residue are 10.0 , 10.5 and 10.2, respectively.

The titration of the dimethyl alanine in the apoferredoxin is also in reasonable agreement with what has been observed in other proteins (Table IV) . The chemical shift is approximately 41.5 and 41.3 ppm in the protonated and unprotonated states, respectively, with a

Table IV. ^{13}C-NMR titration parameters for N-terminal dimethyl alanyl resonances of ferredoxin, lactalbumin and concanavalin A

TABLE IV

^{13}C-NMR TITRATION PARAMETERS FOR N-TERMINAL DIMETHYL ALANYL RESONANCES

protein	pK	chemical shift (ppm) low pH	chemical shift (ppm) high pH	range (ppm)	reference
Oxidized native ferredoxin	9.4	40.7*	43.2	2.5	this work
Reduced native ferredoxin	9.5	42.2	44.6	2.4	this work
Apoferredoxin	7.7	41.5	41.3	-0.2	this work
Apo lactalbumin	7.4	41.98	41.55	-0.43	60
Native lactalbumin	8.33	42.25	41.54	-0.71	60
Concanavilin A	7.9	41.8	41.4	-0.4	61

*Value estimated from fitting of ^{13}C-NMR titration curve.

pKa of about 7.7 (Figure XXIV). For comparison, the N-terminal dimethyl alanine in apolactalbumin exhibits a pKa of 7.4 with chemical shifts of 41.6 and 42.0 ppm at high and low pH, respectively. The N-terminal dimethyl alanine in concanavalin A exhibits a pK of 7.9 with approximate chemical shifts of 41.8 and 41.4 ppm at low and high pH. In contrast, the pK seen for the dimethyl alanine in modified oxidized native Fd is 9.4, an increase of 1.7 pK units from the apoprotein (Figure XXV). Finally, in the reduced form of the protein (Figure XXVI) , the ^{13}C-NMR titration curve yields a similar pK (9.5) and chemical shift range (+2.5 ppm). Since the pKa of both amines remains unchanged in the oxidized and reduced forms it is concluded that the amines have no role in the oxidation-state dependent proton binding proposed to exist in this protein.

B. Reexamination of techniques used for the direct detection of reduction linked proton binding

Evidence for direct detection of proton binding in CP 8Fe Fd upon reduction was reported by McIntosh et al. (27). In this experiment CP Fd was reduced with excess methyl viologen and changes in pH were recorded before and after reduction. By this method it was shown that the pH became more alkaline when Fd underwent reduction, and this effect was attributed to proton binding to the reduced protein. Similarly , upon reoxidation with

potassium ferricyanide the pH became more acidic, indicating that protons were released back into solution when the protein undergoes oxidation. The authors concluded that CP 8Fe Fd showed reduction-linked proton binding, thus, supporting the view that this protein has a pH dependent E_{mdpt}. Since these results were in contradiction to the results obtained by Prince et al. (55) and the titration experiments using methylated Fd , however, it became necessary to reexamine the experiments of McIntosh et al. by repeating the experiments more carefully.

Several precautions were implemented to assure the reliablity of results when repeating these experiments. First, all experiments were performed in an anaerobic glove box prepared as described earlier. Additionally, more controls were included to minimize the uncertainty in the actual experimental results. When the experiment involving direct detection of reduction-linked proton binding in CP 8Fe Fd is performed inside an anaerobically prepared glove box, the results are quite different from those reported (Table V). These results , in contrast , show that there is no proton binding when CP Fd undergoes reduction. Although there is a small rise in the pH after reduction, comparable to that seen in buffer only, it could not be large enough to ascribe it to proton binding to Fd. Another experiment was performed to determine whether the possiblity existed that the Fd in

Table V. Detection of reduction-linked proton binding in methyl viologen reduced *Clostridium pasteurianum* 8Fe ferredoxin

Table V

Trial	umole Fd	initial pH	pH after addition of methyl viologen
1	0	7.03	7.08
2	0	7.60	7.63
3	0	8.19	8.22
4	0.42 umol	7.67	7.69
5	0.42 umol	7.70	7.76
6	0.42 umol	8.23	8.29
7	0.42 umol	8.23	8.26

this experiment had not undergone reduction upon treatment with reduced methyl viologen. Although the easiest route for this would be EPR spectroscopy , in practice the signal arising from reduced methyl viologen would dominate the spectrum making interpretation extremely uncertain. Instead, experiments were initiated to assess the reduction process. First, oxidized methyl viologen was reduced using a hydrogenase/hydrogen gas system as described, and the pH was recorded before and after reduction. These results , presented in Table VI , indicate that a pH change is detectable when methyl viologen undergoes reduction. The change in the pH does not arise from the reduced methyl viologen, rather , the drop in the pH is due to oxidation of H_2 gas into protons by hydrogenase protein. The electrons released are then used to reduce the methyl viologen. Because methyl viologen is a one electron acceptor it was expected that one proton would be released per reduction event. When the solution is back titrated to the original starting pH using hydroxide and the control values subtracted it was found that the number of protons released was only 75% of the theoretical with respect to the methyl viologen . However, using the Nernst equation using a hydrogenase determined solution potential of pH X (59.16 mV) and a midpoint reduction potential of about -463 mV for methyl viologen the actual amount of reduced methyl viologen is actually 93% of the total methyl viologen. As a result,

Table VI. Detection of reduction-linked proton binding in hydrogenase reduced methyl viologen

Trial	umoles oxidized methyl viologen present	pH before hydrogenase addition	pH after hydrogenase addition	# umoles OH^- required for titration
1	0 umoles	8.97	8.46	0.7 umoles
2	0 umoles	9.01	8.46	0.9 umoles
3	0 umoles	9.04	8.47	0.8 umoles
4	4.5 umoles	8.96	7.85	4.2 umoles*
5	4.5 umoles	9.00	7.94	4.2 umoles*
6	4.5 umoles	9.02	7.98	4.3 umoles*

* - represent values uncorrected versus control

the actual number of proton equivalents released is closer to 85% of the theoretical. These results indicate that this technique is satisfactory for the detection of pH changes during oxidation/reduction , and that reliable quantitation can be achieved with regards to the number of protons being exchanged in the redox process.

To confirm the results obtained in the first experiment, a hydrogenase/hydrogen gas system was used to reduce oxidized CP 8Fe Fd (Table VII). Since Fd is a molecule which contains two redox centers, each involved with a single electron reduction, it was expected that two protons would be released by hydrogenase per reduced Fd molecule. As is seen in Table VII, the number of protons released by hydrogenase is closely stoichiometric with the predicted theoretical outcome (80-85% of theoretical). The variations seen in the actual results compared with the expected outcome might arise from uncertainty in the measurements or from an increase in the midpoint reduction potential of ferredoxin at higher concentrations making the protein harder to reduce. The results, however, confirm the results from experiment 1 , and indicate that there is no reduction-linked proton binding in CP 8Fe Fd. These results, taken together, indicate that the original determination of reduction-linked proton binding was in error and that the conclusions presented were inaccurate. The source of error in the original experiments probably arose from two complicated side reactions that occur when

Table VII. Detection of reduction-linked proton binding in hydrogenase reduced *C. pasteurianum* 8Fe ferredoxin

TABLE VII

Trial	umoles of oxidized ferredoxin	pH before hydrogenase addition	pH after hydrogenase addition	# moles OH^- required for titration
1	0.751 umoles	9.01	8.59*	0.85 umoles
2	1.15 umoles	9.00	8.71*	0.51 umoles
3	1.97 umoles	8.92	8.76*	0.55 umoles
4	0.751 umoles	9.01	8.27	2.10 umoles**
5	1.15 umoles	8.97	8.11	2.45 umoles**
6	1.97 umoles	8.93	8.09	4.00 umoles**

* - hydrogenase addition in absence of H_2 gas

** - represent values uncorrected versus control

Fd is reduced with methyl viologen or reoxidized with potassium ferricyanide. For the reduction of ferredoxin with methyl viologen , the first side reaction arises from the oxidation of reduced methyl viologen by oxygen in the air (even at low concentrations in a glove box) to produce hydroxide ions, which has the effect of raising the pH. Because the buffer is only 1 mM and the methyl viologen is nearly 50 mM , even small increases in the oxidation of reduced methyl viologen by oxygen can have measurable effects on the pH. The second side reaction , associated with the reoxidation of reduced CP Fd using potassium ferricyanide, arises from denaturation of the protein. Treatment of Fd with ferricyanide results in the degradation of the iron-sulfur center, and consequently the protein undergoes denaturation. When holoferredoxin denatures at low buffer concentrations the pH becomes more acidic (data not shown). Therefore, the results observed by McIntosh upon reoxidation of reduced protein most likely arose from the effects of protein denaturation, rather than the proported proton release suggested.

C. Reexamination of techniques used in determination of E_{mdpt} of CP 8Fe Fd using hydrogenase reduction and UV-visible spectroscopy

Various methods are available for the determination of the E_{mdpt} of CP 8Fe Fd . By far, however, the method of choice has been UV-visible spectroscopy. This is possible

because the spectra of the oxidized and reduced forms of the protein are significantly different. The largest differences seen in extinction coefficients between the two states is at 425 nm (26), and the difference at this wavelength between the oxidized and reduced forms of the protein has been used in determination of the pH dependent E_{mdpt} in this protein. The protein is reduced using a hydrogenase/hydrogen gas system. To determine the reproducibility of this experiment, it was performed as described by Magliozzo et al. (27), except that the ionic strength was reduced from 0.50 M to 0.10M NaCl and the buffer was 0.10M Tris . The results obtained in this experiment are shown in Figure XXIII. The E_{mdpt} shows the same type of behavior as was reported previously (27,37). The protein shows a negative pH dependence on E_{mdpt} (-16mV/pH unit between pH 7-8 and -30mV/pH unit between 8-9). These results, consistent with others, indicate the reproducibility of this technique in determining E_{mdpt}. It is not altogether clear as to why a pH dependent midpoint reduction potential is obtained using UV-visible absorption spectroscopy , whereas no such pH dependence is observed when analyzed using EPR or polarimetry. The lack of any detectable proton binding to the ferredoxin protein upon reduction is also consistent with the absence of a pH dependent E_{mdpt}. It is possible that the UV-visible absorption spectroscopy technique for the determination of E_{mdpt} is not reliable for determining the E_{mdpt} directly.

Stombaugh et al. has discussed in some length (37) the inherent uncertainties associated with this technique, most notably , the question of denaturation arises. The accuracy of the E_{mdpt} determination is critically dependent on minimizing protein loss, and since no direct method is available for determining the amount of apoprotein in solution this might lead to a larger uncertainty in the data than would otherwise be expected. Similarly, it is possible that the ratio of A_{red}/A_{ox} of 0.435 used in calculating E_{mdpt} is inaccurate , therefore the values calculated for E_{mdpt} would also be in error.

CONCLUSIONS

Although a pH dependent E_{mdpt} is exhibited by CP 8Fe ferredoxin using hydrogenase coupled reduction and analysis by UV-visible spectroscopy, the experiments presented in this section provide evidence against the existence of a pH dependent E_{mdpt} in Clostridium pasteurianum 8Fe Fd. These conclusions are based on several points , including the lack of any involvement of the amines in reduction-linked proton binding and in particular the lack of any detectable proton binding in the protein when it undergoes reduction. These results are therefore in agreement with the results of Prince and Adams (55), and indicate that there is no pH dependency to the E_{mdpt} of this protein. It is not altogether clear , however, as to why CP 8Fe ferredoxin exhibits a pH

dependent E_{mdpt} using UV-visible spectroscopy. If there is no pH dependent E_{mdpt} in CP 8Fe ferredoxin then it brings into question the validity of oxidation-state dependent proton binding in other clostridial-type ferredoxins as well. If similar results are observed for other ferredoxins indicating the absence of a pH dependent E_{mdpt}, then it appears that hydrogen ion binding is not a general feature of ferredoxins and iron-sulfur proteins. Rather, it is more likely that proton binding is characteristic of only specialized iron-sulfur proteins and model iron-sulfur compounds.

II. Studies on the stability of methylated Clostridium pasteurianum 2(4Fe-4S) ferredoxin

Reductive methylation has been extensively used to characterize the pKa values of methylated amines in various modified proteins, including CP 8Fe ferredoxin. Unlike other methylated proteins, however, the ^{13}C-NMR titration curves obtained for the N-terminal alanine of CP Fd_{ox} and Fd_{red} are quite distinctive. In addition to the unusually high pK values obtained, the chemical shifts and linewidths observed are indicative of a unique chemical environment about the N-terminal amine. Indeed, the x-ray crystallographic structure of the homologous 8Fe Fd from PA shows (65) that the N-terminal is ion paired with a carboxylate group from a nearby Asp^{37} . Consequently, reductive methylation offers a unique opportunity to test for structural homology between CP and PA 8Fe Fd. Specifically, Gerkin (60) has been able to detect the presence of an ion pair in the dimethylated N-terminal amine in alpha-lactalbumin protein through examination of the pKa and linewidth changes in the modified protein . Similar experiments with methylated CP Fd will be presented here to test for the existence of such an N-terminal ion pair. Experiments will also be presented which examine the effects of methylation on the stability of CP 8Fe Fd.

Results and discussion

A. Evidence for N-terminal ion-pair in CP 8Fe Fd

The ^{13}C-NMR titration behavior of the dimethylated Lys^3 in Fd_{apo}, Fd_{ox} and Fd_{red} (Figures XXIV, XXV and XXVI) are in good agreement with what has been observed in other proteins (56-63). These resonances are expected to occur near 43 ppm in the protonated amine and exhibit an approximate 1 ppm downfield shift with increasing pH , with a pK slightly above 10 (48,56,60). The pK values of Lys^3 found for the apo, oxidized and reduced methylated ferredoxins are 10.0, 10.5 and 10.2 , respectively.

The titration of the dimethyl N-terminal alanine in the apoferredoxin is also in reasonable agreement with what has been observed in other proteins (Table IV). The chemical shift is approximately 41.5 and 41.3 ppm in the protonated and unprotonated states, respectively, with a pK of 7.7 (Figure XXIV). In contrast, the pK seen for the dimethyl alanine in oxidized native ferredoxin is 9.4, an increase of 1.7 units from the apoprotein. An increase of 0.90 units is seen in the N-terminal pK of reductively methylated native alpha-lactalbumin relative to apoprotein, and this difference is attributed to the formation of an ion pair in the native protein (60). The 1.7 unit increase in pK seen in oxidized ferredoxin represents a difference in ion pair energy between the apo

and native protein of only 2.3 Kcal/mole. As cited earlier, an ion pair has been reported in the x-ray structure of the homologous clostridial-type ferredoxin from PA (65,67).

An additional contrast is the chemical shift range exhibited by the N-terminal alanine resonance through the titration. While apolactalbumin and concanavalin A exhibit chemical shift differences (high pH - low pH) of about -0.40 ppm , the chemical shift range exhibited by oxidized ferredoxin is an unexpectedly large +2.5 ppm (Table IV). It is the unprotonated form that exhibits an unusual chemical shift. The chemical shift difference probably does not arise solely from a ring current effect of the nearby Tyr^2, as tyrosine ring current shifts are typically not that large. In reduced ferredoxin the ^{13}C-NMR titration of the dimethyl alanine resonance yields a similar pK of 9.5, thus, it appears the ion pair remains in the reduced form of the protein.

For the oxidized protein, the dimethyl alanyl resonance rapidly broadens rapidly as the pH is lowered from pH 9.0 and then disappears as the pH is lowered to slightly below 8.0 (Figure XXVII). The linewidth of this resonance is temperature dependent, narrowing as the temperature is raised (Figure XXVIII). Analogous behavior has been seen in other systems. For example, below pH 6.5 the N-terminal dimethyl lysine resonance in ^{13}C-methylated lysozyme (57) broadens extensively. In ^{13}C-methylated

Figure XXVII. pH dependence of the ^{13}C-NMR dimethyl N-terminal alanine resonance in reductively methylated Clostridium pasteurianum 8Fe ferredoxin

Conditions: 0.50 mM oxidized protein in 0.10 M tris/0.50 M NaCl , 25°C , pulse repeat time 0.500 seconds , 5000 scans (pH as indicated)

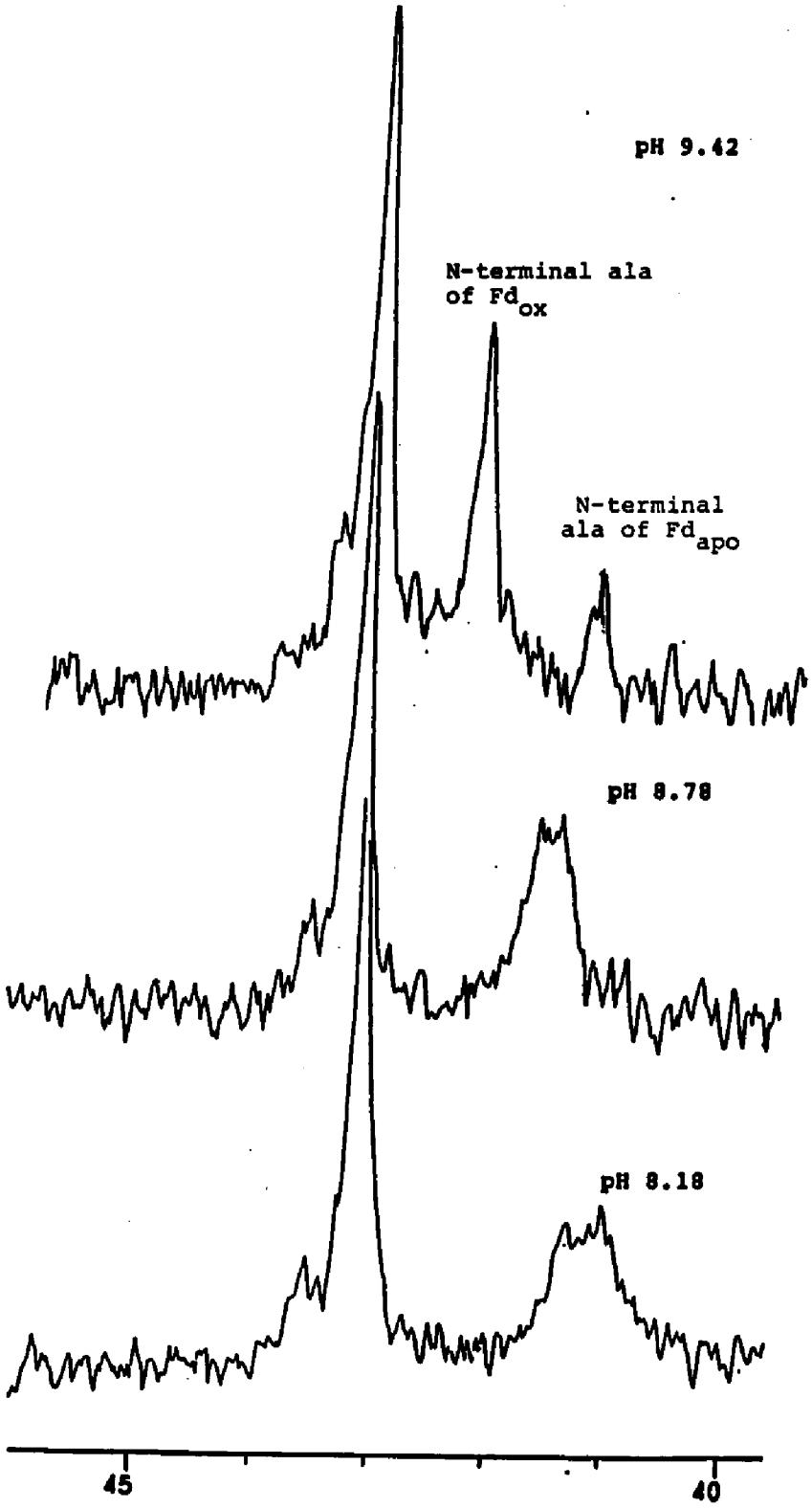
pH 9.42
N-terminal ala of Fd_{ox}
N-terminal ala of Fd_{apo}
pH 8.78
pH 8.18
45
40

Figure XXVIII. Temperature dependence of the ^{13}C-NMR dimethyl N-terminal alanine resonance in reductively methylated Clostridium pasteurianum 8Fe ferredoxin

Conditions: same conditions as Figure XXV except 3500 scans at 8°C and 2500 scans at 25°C

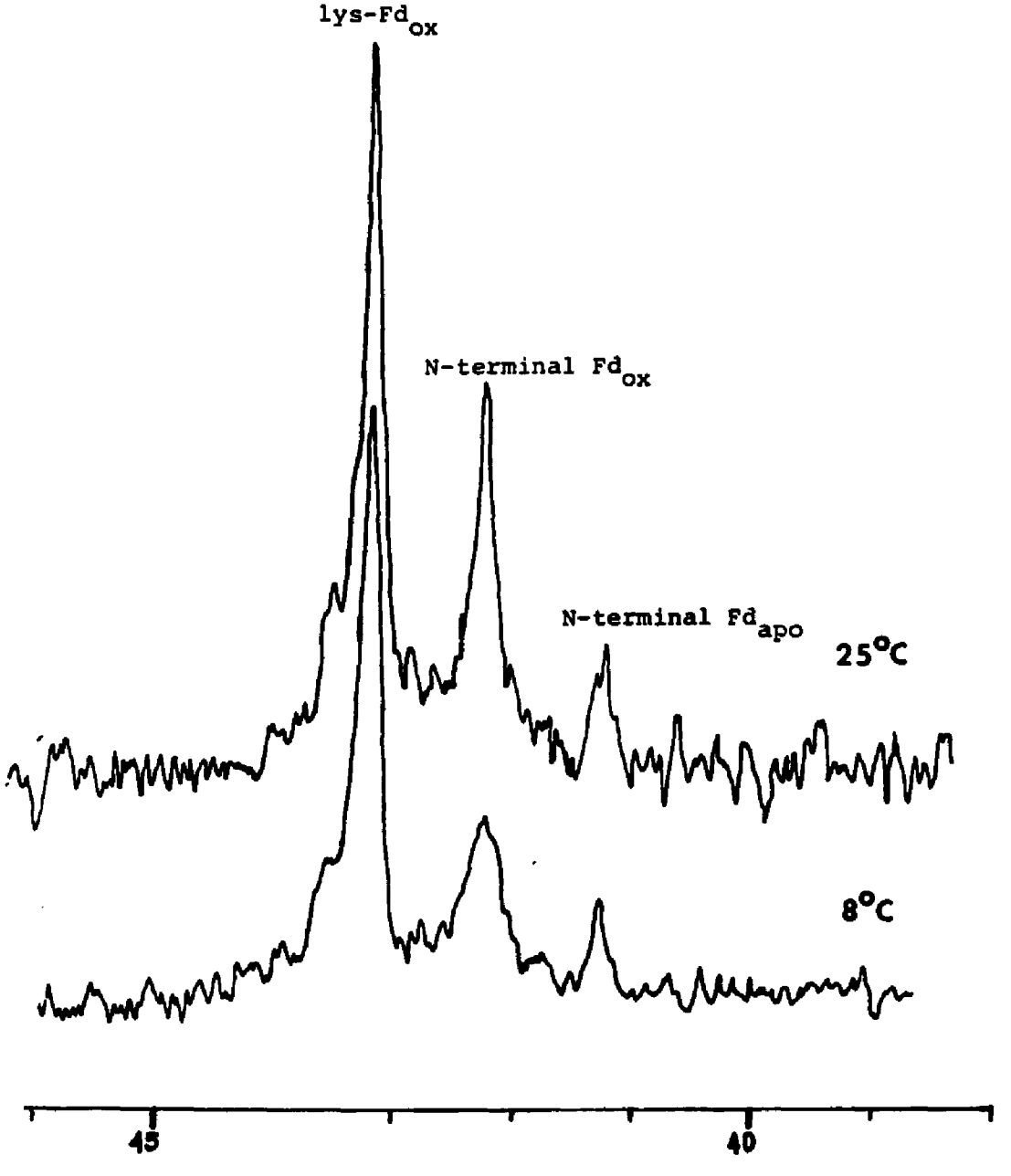
lys-Fd$_{ox}$
N-terminal Fd$_{ox}$
N-terminal Fd$_{apo}$
25°C
8°C
45
40

concanavalin A (61,62) broadening has also been observed for some resonances at low pH. In both cases the broadening was attributed (56,62) to chemical shift inequivalence of the diastereomers. That is, if the two methyl groups bound to the dimethylated amine are in different chemical enviroments as a result of immobilization of the amine, as might be the case if the amine is tied up in an ion pair, then the carbon atoms of the methyl groups will behave like inequivalent diastereomers. The methyl groups, however , can interchange by rotation about the alpha carbon-nitrogen bond, but if this exchange is slow on the NMR time scale it will result in a broadening of the NMR carbon resonances. If on the other hand the exchange rate is rapid then a narrow resonance will appear at a chemical shift position that is intermediate between the two diastereotopic chemical shift positions. Since nitrogen inversion must by necessity proceed through the unprotonated amine, it is the proton exchange rate which gives rise to the observed pH dependence (62). The broadening observed in concanavalin A and lysozyme occurs at lower pH values than seen with ferredoxin.

In the modified ferredoxin, the alanine resonance in the spectrum of the oxidized protein is broad below pH 8 and narrows as the pH is raised. The pK for the dimethyl alanine is 9.4. Only one peak is seen, and so the proton exchange rate and the rate of interchange of diastereomers

or rotation about the amine-carbon bond must be fast on the NMR time scale. The broadening observed as the pH is lowered would arise from a pH dependent slowing of either nitrogen inversion or amine bond rotation. Since the onset of broadening occurs at a pH below the pK of the amine, the broadening is not directly a consequence of the formation of the ion pair. In theory a conformation change which occurs near pH 8 could hinder either the amine bond rotation or the rate of nitrogen inversion, but there is no evidence to support the possibility of such a pH dependent protein conformation (27). Thus, it appears more likely that the dependence of the rate of nitrogen inversion on the proton exchange rate is the origin of the observed broadening, as has been proposed for other systems (56,62).

It is interesting to note that although the ion pair of the dimethyl N-terminal alanyl amine persists in the reduced form of the protein, the line broadening which occurs as the pH is lowered is much less extensive (data not shown).

In general, dimethyl amino groups are expected to be nearly the same or only slightly less basic than the analogous unmethylated amine (48). However, the methyl groups on the dimethylated N-terminal alanine may weaken the ion-pair , as suggested by the marked lowering of stability of the modified protein. As a result, the pK of this amine in the native protein may be somewhat higher

than 9.4.

B. Additional evidence for the existence of a unique chemical enviroment around the N-terminal amine in CP 8Fe

Additional evidence for the existence of a unique N-terminal environment is suggested by the proteins resistance to modification of the N-terminal amine. When the protein is methylated in its oxidized form an approximate eight-fold lower extent of labeling is observed compared to methylation of apoferredoxin or hydrogenase reduced ferredoxin. This was true for a range of ionic strength and pH conditions (Table VIII). This observation is consistent with the difficulty Hong et al. (64) observed for reaction of the N-terminus of oxidized native CAU 8Fe Fd in a range of modifying reactions. It is unlikely that limited accessibilty is the cause of the poor reactivity of the native ferredoxin, as the protein is very small. Indeed, the X-ray structure of PA Fd indicates that both residues should be solvent exposed (65,67). Even ion-pair interactions in the ion-paired Lys^{13} in lysozyme do not appear to profoundly limit reactivity (56). The reason for the general lack of reactivity exhibited by the oxidized form of the protein is not well understood.

Even in the apoprotein the N-terminal does not react completely, as shown by the relative intensities of the lysine and alanine peaks in the decoupled carbon NMR

Table VIII. ^{14}C-radioactive labelling of reductively methylated Clostridium pasteurianum oxidized ferredoxin under various ionic strength , pH and denaturing conditions

Table VIII.

Exp	incubation	pH	[NaCl]	[denaturant]	CH_3/mole	Fd
1	18 hrs	6.8	0.15M	-------	0.34	
2	18 hrs	8.3	-----	-------	0.70	
3	18 hrs	8.0	0.15M	-------	0.73	
4	36 hrs	8.0	0.15M	-------	0.84	
5	18 hrs	9.8	0.15M	-------	1.10	
6	36 hrs	9.8	0.15M	-------	2.30	
7	3* hrs	9.3	0.15M	50% DMSO	1.57	
8	5* hrs	9.3	0.15M	50% DMSO	1.84	
9	2* hrs	9.3	0.15M	70% DMSO	0.78	

* -- short incubation periods due to significant protein denaturation

spectrum of the apoprotein (Figure XVII). Because the pK of the N-terminal alanine is lower than that of lysine, it was expected that it should preferentially react with formaldehyde. The diminished reactivity of the N-terminal alanine in apoferredoxin might arise from accessibility problems, as suggested by experiments using Bradford reagent (Bio-Rad assay). In these experiments apoferredoxin is first reacted with Bradford reagent . However, if the apoprotein is reacted with Bradford reagent at higher pH and in the presence of 8M urea and mercaptoethanol the apoferredoxin reacts with Bradford reagent to a greater extent (> 30%). The results seen in the latter experiment is consistent with the idea that the diminished reactivity of apoferredoxin with Bradford reagent might be caused by a lack of accessibility of the apoprotein. Control experiments showed that the Bio-Rad reagent did not react with 8M urea and 0.14M mercaptoethanol in the absence of protein, therefore, urea amd mercaptoethanol presumably reduced disulfides and exposed various parts of the protein that are normally inaccessable to reaction with the reagent. This data also suggests that the apoprotein probably has some secondary structure to it. Therefore, it is possible that the N-terminal amine is partially buried in this unreactive region giving rise to the different carbon NMR intensities seen in the two modified amines.

Reductive methylation on the reduced form of the

protein was the most efficient and yielded large amounts of methylated protein with the lowest loss of protein (20%). It is interesting to note that use of other reductants such as methyl viologen and dithionite to reduce ferredoxin did not result in the same extent of labeling.

C. Stability of methylated ferredoxin

As measured by optical absorbance at 390 nm, under aerobic or anaerobic conditions the methylated ferredoxin was appreciably less stable than native unmodified ferredoxin (Figure XXIX). Under aerobic conditions, the half-life of the modified Fd at pH 7.9 was decreased by nearly 65%. Furthermore, the stability of the native and modified protein is sensitive to the pH as well (Figure XXX). Under anaerobic conditions, the stability of the modified protein is about the same as native unmodified ferredoxin under aerobic conditions . These results suggest that the decreased stability is not solely due to increased exposure of oxygen leading to protein degradation. Instead, it is possible that methylation disrupts some important structural interactions within the protein, presumably the N-terminal amine , directly. Therefore, the N-terminal ion-pair probably is important in maintaining the structural integrity of the protein. Although the ion-pair in the methylated amine contributes only 2.3 kcal/mole of stabilizing energy, this value could

Figure XXIX. Stability of native and reductively methylated oxidized Clostridium pasteurianum ferredoxin under aerobic and anerobic conditions at room temperature at pH 8.3

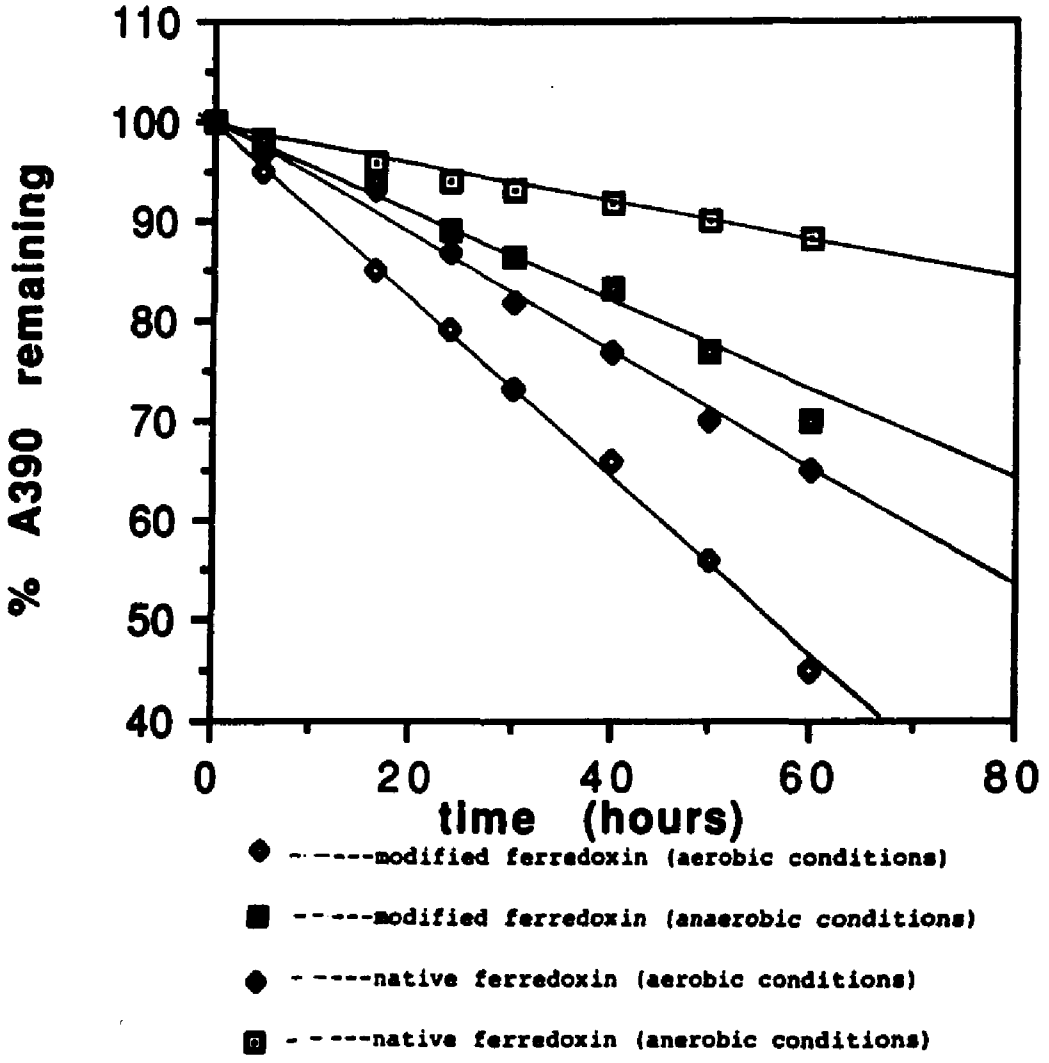
110
100
90
80
70
60
50
40
% A390 remaining
0
20
40
60
80
time (hours)
-----modified ferredoxin (aerobic conditions)
-----modified ferredoxin (anaerobic conditions)
-----native ferredoxin (aerobic conditions)
-----native ferredoxin (anerobic conditions)

Figure XXX. Stability of native Clostridium pasteurianum oxidized ferredoxin at different pH values and a comparison of stability for native and methylated protein at pH 7.93

Conditions: .18 mg/ml in .10M tris/.10M NaCl
temp, 27°C

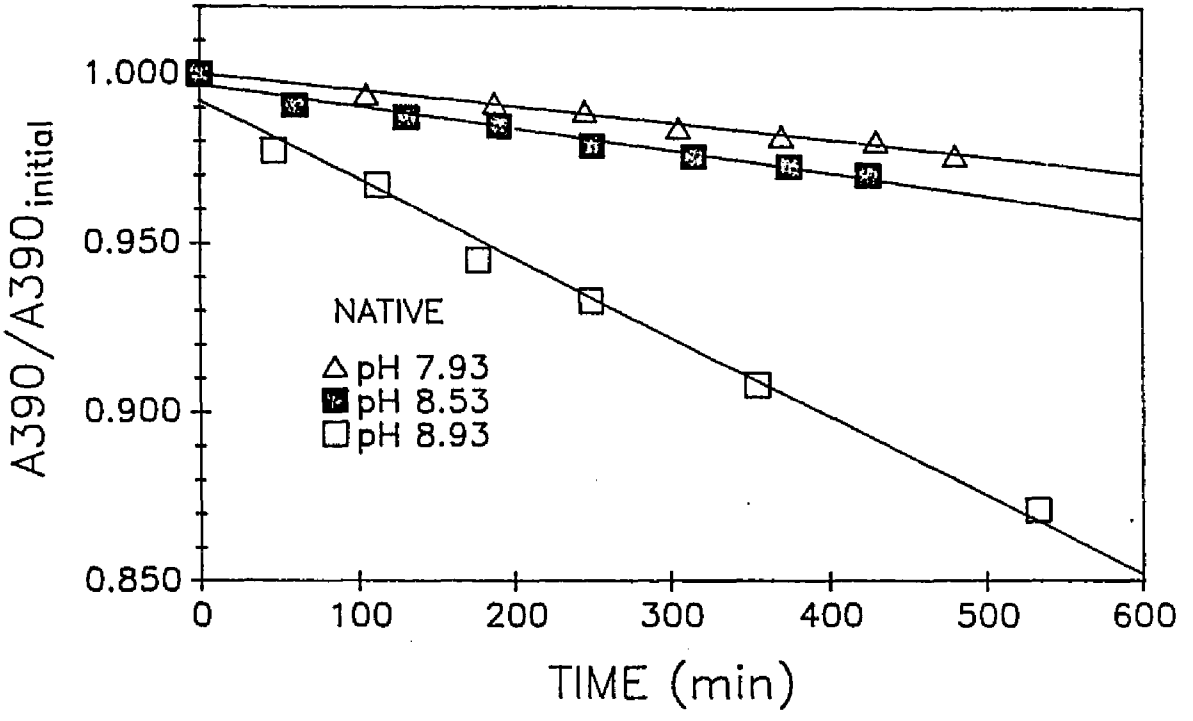
1.000
0.950
0.900
0.850
A390/A390initial
NATIVE
pH 7.93
pH 8.53
pH 8.93
0
100
200
300
400
500
600
TIME (min)

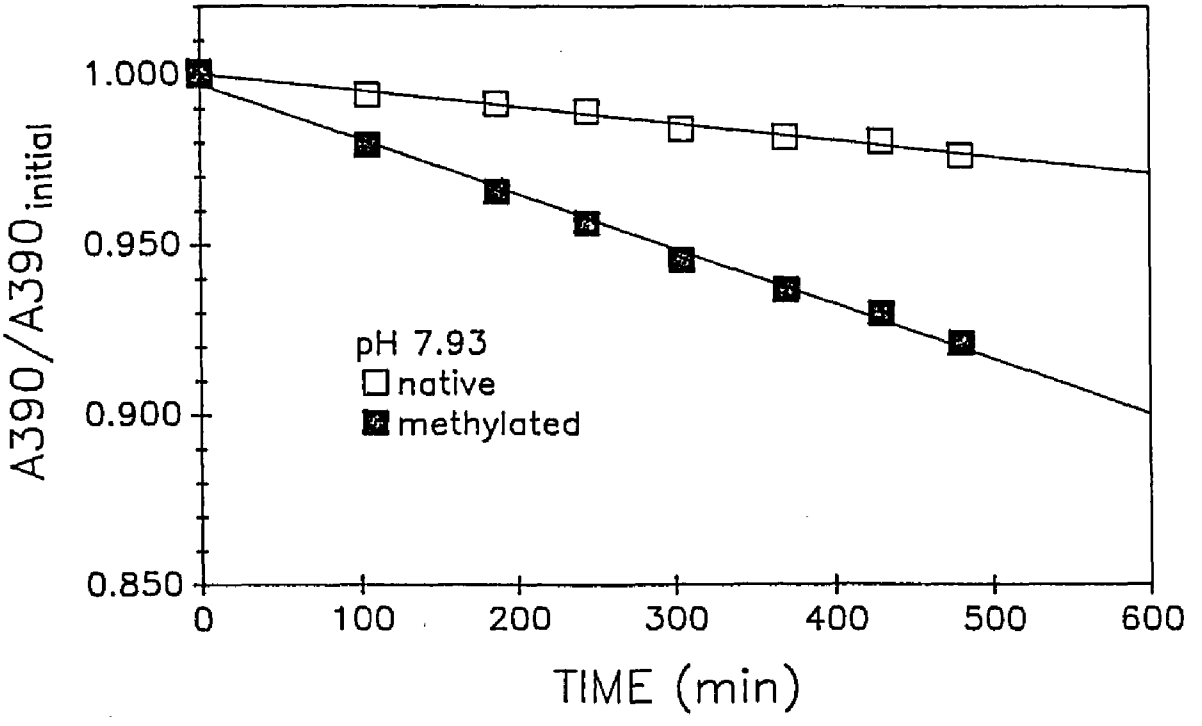
1.000
0.950
0.900
0.850
A390/A390initial
pH 7.93
native
methylated
0
100
200
300
400
500
600
TIME (min)

be significantly higher in the native unmodified protein.

The resolution of the x-ray structure of PA 8Fe Fd is insufficient to characterize the exact chemical environment around the N-terminal, therefore, it is difficult to know exactly what changes occur when the N-terminal amine undergoes methylation. However, computer simulations can be created to help unravel the complex details. Specifically, when the N-terminal amine undergoes methylation hydrogen atoms are replaced by non-polar methyl groups. The methyl groups are incapable of hydrogen bonding to the carboxylate group that originally made up the ion-pair and this results in the weakening of the salt bridge. When parameters are programmed into the computer simulation in order to obtain minimum energy conformations for the unmodified, monomethylated and dimethylated N-terminal amine when it is involved in an ion-pair with a carboxylate side group , conformations such as those shown in Figure XXXI are obtained. In the unmodified amine two hydrogen atoms on the nitrogen are ion-paired with the two carboxylate oxygens. In the dimethylated form , the nitrogen adopts a conformation that puts the two methyl groups away from the carboxylate oxygens and this results in only one hydrogen atom ion-paired with the two carboxylate oxygens. Gas phase calculations indicate that the difference in energies between these two conformations could be as high as 15 Kcal/mole , although significantly lower differences would

Figure XXXI. Postulated ion pair conformations for native unmethylated, monomethylated and dimethylated Clostridium pasteurianum 8Fe ferredoxin

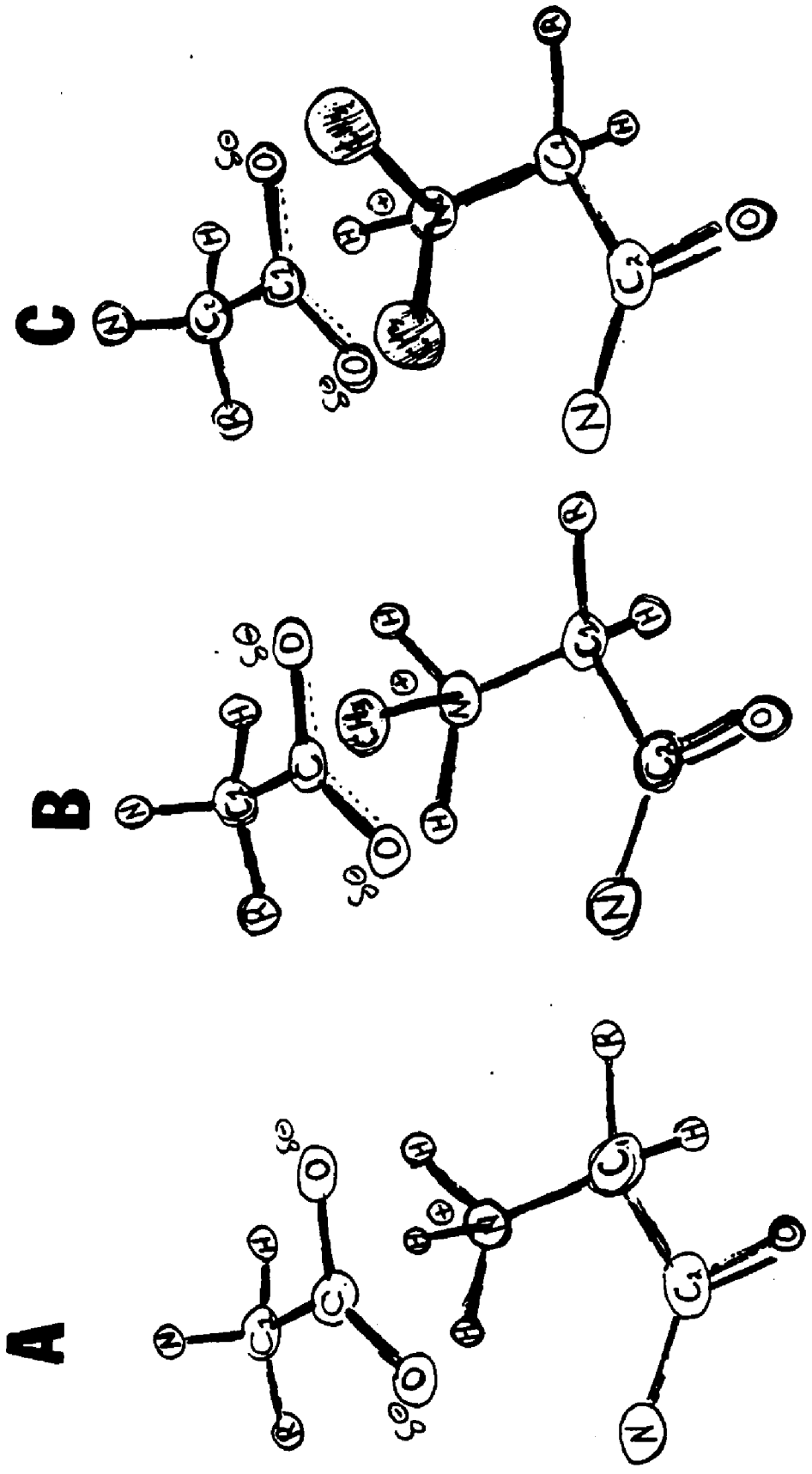
C
B
A

be observed in the liquid phase. A rather interesting result obtained from these computer calculations was the observation that the monomethylated form of the amine would be expected to have almost the same stability as the unmodified protein because two hydrogen atoms would still be available for hydrogen bonding to the carboxylate oxygens. Attempts to obtain a monomethyl derivative in quantitative yields were unsuccessful.

Conclusions

The data presented in this section provides evidence for the existence of an ion pair involving the N-terminal amine in Clostridium pasteurianum 8Fe ferredoxin. The presence of this ion pair is consistent with the x-ray structure of the homologous protein from Peptococcus aerogenes 8Fe ferredoxin. The ion pair persists in both the oxidized and reduced forms. Finally, the ion pair is likely to be important for maintaining the intrinsic stability of the protein.

III. Examination of the optical purity ratio for *Clostridium pasteurianum* 2(4Fe-4S) ferredoxin ; Evaluating the quantitative meaning for A_{390}/A_{280}

Clostridial-type ferredoxins have very characteristic UV-visible absorption spectra. The absorption properties arise from the chromaphoric iron-sulfur center present in the peptide. In particular, the strong electronic absorption band near 390 nm , having an extinction coefficient of about 31,000 , is believed to arise from Fe--->S charge transfer bands in the protein (1). The strong absorption band around 280 nm is thought to arise from contributions from both the iron-sulfur center and also from the presence of aromatic side groups in the peptide. When the protein is denatured and the iron-sulfur centers are removed the UV-visible absorption spectrum shows only absorptions in the UV region. These distinctive absorption properties have been used in the past to characterize the purity of ferredoxin samples. Specifically, the ratio of absorbances at 390 and 280 nm (A_{390}/A_{280}) has been used to evaluate the purity of clostridial 8Fe ferredoxins. For example, *Clostridium pasteurianum*, with a ratio of 0.81 is considered pure protein. As the protein denatures the absorbance at 390 nm decreases, and therefore, the ratio becomes smaller as the protein undergoes denaturation. To date, however, no

method of quantitative analysis has been reported to determine the actual percent of apoprotein present in a partially denatured sample of ferredoxin having a particular purity ratio , A_{390}/A_{280} . Fortunately, chemical modification of ferredoxin using reductive methylation offers an easy and reliable method for examining such a problem. The experiments presented in this section examine the use of reductive methylation in the quantitative correlation of the purity ratio A_{390}/A_{280} with the amount of apoprotein present in partially denatured samples of Clostridium pasteurianum 8Fe ferredoxin.

RESULTS AND DISCUSSION

The UV-visible absorption spectrum of native unmodified and reductively methylated oxidized Clostridium pasteurianum 8Fe ferredoxin are shown in Figure XIX. The two spectra are virtually identical, therefore, methylation of the amines does not lead to significant changes in the electronic absorption properties of the protein. It is thus reasonable to assume that changes in the UV-visible spectra of the methylated protein are likely to be identical to the unmodified native protein. Therefore, the following discussions are based on the assumption that the spectroscopic behavior of the methylated protein is identical to native unmodified

ferredoxin. Figure XXXII shows the UV-visible absorption spectra of methylated oxidized ferredoxin under various stages of denaturation (0% , 16% , 27% and 53% , respectively). As the protein undergoes denaturation the broad absorption band centered around 390 nm decreases in intensity, as does the UV absorption at 280 nm. There are also changes in the general lineshape of the spectrum . The changes in the purity ratio A_{390}/A_{280} appear to be sensitive to the degree of denaturation and thus serve as an indicator of protein purity.

Figure XXXIII displays the proton-decoupled ^{13}C-NMR spectrum of partially denatured reductively methylated CP 8Fe ferredoxin. At pH 9.7 the ^{13}C resonance of the N-terminal amine in methylated holoferredoxin has a different chemical shift than the corresponding peak from the apoprotein. The dimethylated apoprotein resonance appears near 41.3 ppm while the holoferredoxin resonance exhibits a chemical shift of approximately 42.0 ppm. Because the area under each peak is representative of the concentration of each individual species present, the differences in both peak positions and peak intensity in the ^{13}C-NMR spectra enable these peaks to be used as a probe to assess the extent of denaturation in a ferredoxin sample. The relative peak areas can be calculated for each resonance and therefore the ratio of apoferredoxin to holoferredoxin can be calculated. Furthermore, by obtaining a UV-visible absorption spectrum immediately

Figure XXXII. UV-visible absorption spectra of reductively methylated oxidized ferredoxin under different extents of denaturation

Conditions: 50 mM potassium phosphate buffer/0.10 M NaCl , pH 7.60 . For curves shown denatured protein content is A = 53% , B = 27% , C = 16% and D = 0%

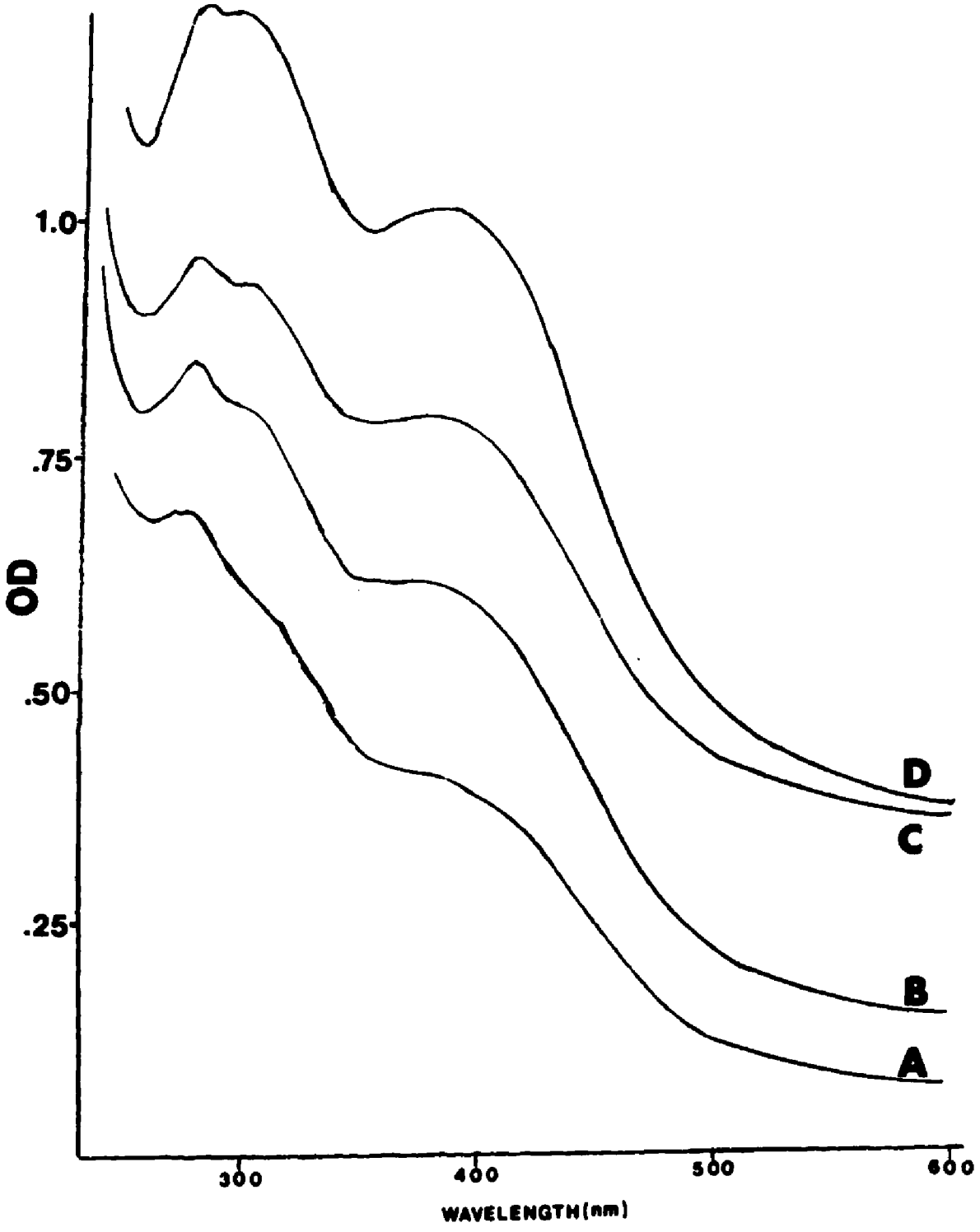
1.0
.75
.50
.25
OD
300
400
500
600
WAVELENGTH(nm)
D
C
B
A

Figure XXXIII. Proton noise decoupled ^{13}C-NMR spectrum of partially denatured reductively methylated oxidized Clostridium pasteurianum ferredoxin

Conditions: 6 mg/ml protein in 50 mM potassium phosphate buffer/0.10 M NaCl, 33% D_2O , pH 9.7 , 1000 scans , pulse repeat time, 0.528 seconds . Chemical shifts were assigned using ^{13}C-NMR as an internal standard with a chemical shift of 49.405 ppm.

Peak near 42 ppm corresponds to dimethylated n-terminal amine in intact holoferredoxin whereas peak near 41 ppm corresponds to N-terminal amine in apoferredoxin.

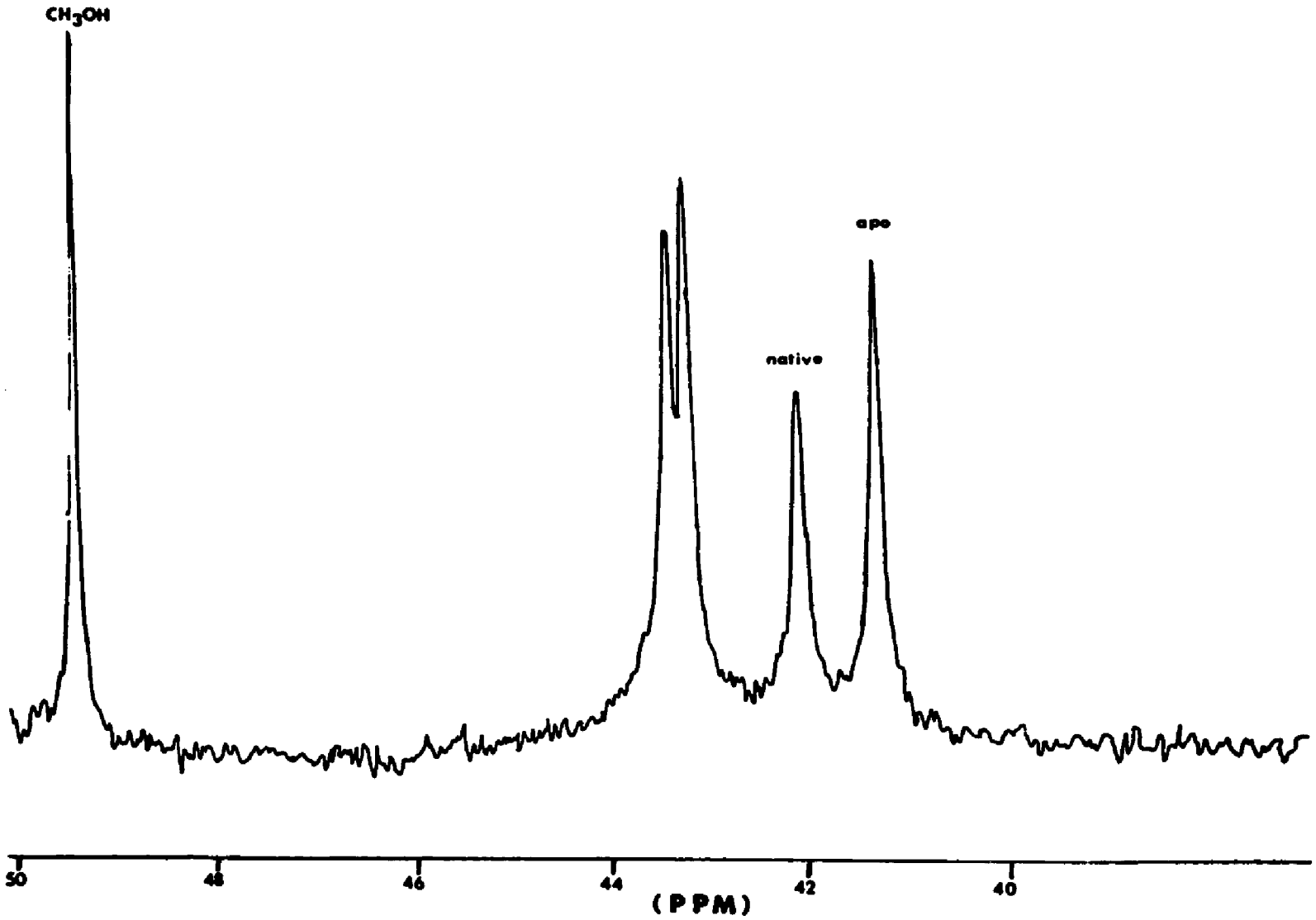
CH3OH
native
apo
50
48
46
44
42
40
(PPM)

after the acquisition of the NMR spectrum, one can correlate the purity ratio, A_{390}/A_{280}, to the extent of denaturation. Thus, it is possible to obtain a reliable quantitative measure of the amount of denatured protein present from the purity ratio. A potential problem faced in the quantitation of the carbon NMR resonances occur because broad-band decoupling is used, leading to Nuclear Overhauser Effects (NOEs). However, only a very small carbon-proton NOE is observed, as would be expected for a paramagnetic protein, and in any case the NOE , if any, is essentially the same in both the native and apoproteins (data not shown). Figure XXXIV displays the proton-decoupled ^{13}C-NMR spectra of three protein samples containing varying amounts of denatured and intact ferredoxin. When the protein mixtures contain mostly holoferredoxin and only small amounts of apoprotein the downfield peak predominates (XXXIV-A) , but as the protein degrades the downfield peak decreases in intensity with a corresponding increase in the upfield peak (XXXIV-B and XXXIV-C). Therefore , it is possible to obtain approximate percentages of holo and apoferredoxin in a partially denatured sample of protein. When the UV-visible spectrum is acquired immediately after obtaining the NMR spectrum it is possible to compose a plot of % apoprotein as a function of the purity ratio, A_{390}/A_{280} (Figure XXXV). In these plots data points are plotted, one in which the buffer was .100 M Tris buffer and the

Figure XXXIV. Proton noise decoupled ^{13}C-NMR spectra of reductively methylated oxidized ferredoxin during various stages of denaturation

Conditions: same as Figure XXXIII

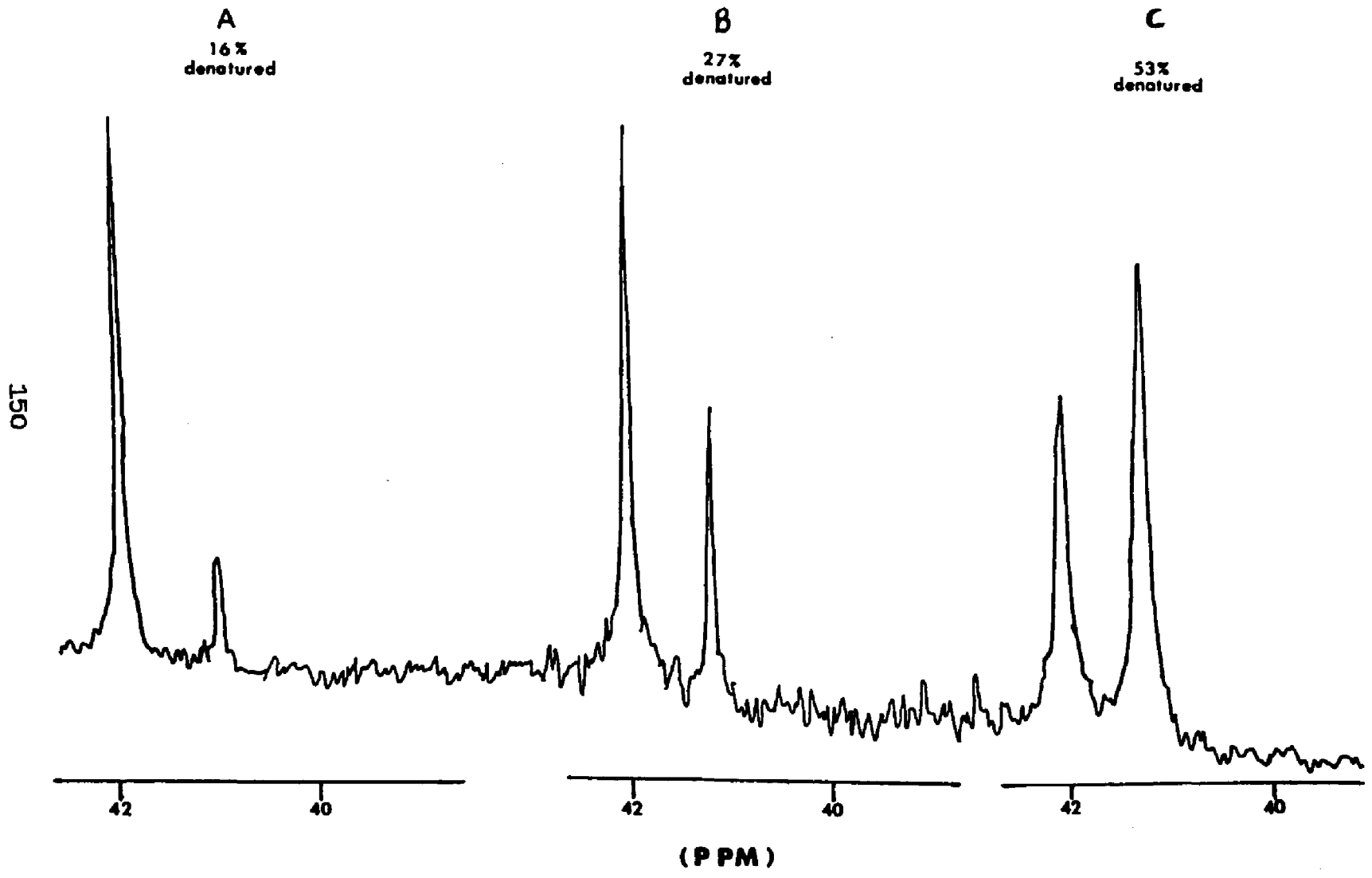
A
16%
denatured
B
27%
denatured
C
53%
denatured
150
42
40
42
40
42
40
(PPM)

Figure XXXV. Plot of % denatured protein as a function of the quality ratio A_{390}/A_{280} determined by NMR and UV-visible absorption spectroscopy and by add-mixture additions of heat denatured ferredoxin

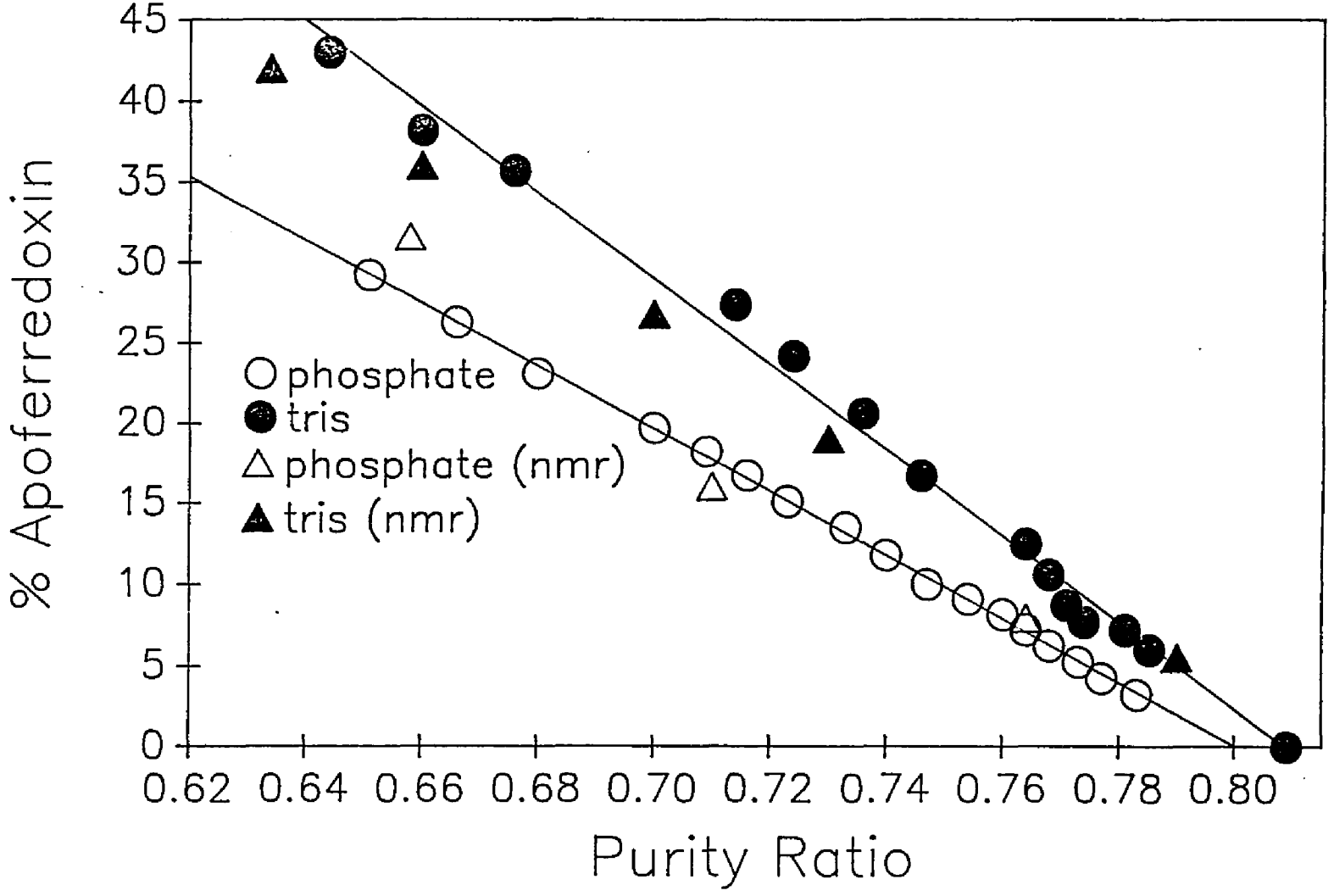
% Apoferredoxin
45
40
35
30
25
20
15
10
5
0
0.62
0.64
0.66
0.68
0.70
0.72
0.74
0.76
0.78
0.80
Purity Ratio
phosphate
tris
phosphate (nmr)
tris (nmr)

other in .050 M potassium phosphate buffer. The results indicate the purity ratios are very similar for the two buffers at a given apoprotein concentration. It appears that there are differences in the % apoprotein content at a given ratio for the two buffers, however, the reasons for these differences are not well understood. The apoprotein content in partially denatured samples of ferredoxin is nearly linear with A_{390}/A_{280} up to about 80% after which a deviation from linearity is observed. Additional data was obtained for protein mixtures containing known amounts of unmodified holoprotein and holoprotein that was heat treated at 100°C for 10-15 minutes. In this experiment purified protein of known concentration that was sufficiently heat treated to denature the protein holoprotein was added to samples containing known amounts of intact purified protein. The curves of % apoprotein versus R for the add-mixture additions of heat denatured protein and native ferredoxin are almost identical to those obtained using NMR spectroscopic analysis (Figure XXXV). The results from these experiments indicate that reliable standard curves for % apoprotein versus A_{390}/A_{280} can be accurately obtained using simple add-mixtures of heat denatured and native ferredoxin. An additional experiment was performed to evaluate the purity ratio when native ferredoxin was added to crude cell extracts obtained from Clostridium pasteurianum cells. Except for some small variations in

the 280 nm absorbance readings it was found that the UV-visible spectra were simple linear combinations of the component spectra (Table IX).

CONCLUSIONS

Experiments presented in this section offer a reliable method for accurately measuring the apoprotein content in a partially denatured sample of ferredoxin . By this method, the amine residues in ferredoxin are first reductively methylated, and ^{13}C-NMR is used to quantitate the relative amounts of apo and holoprotein in partially denatured samples since these resonances are clearly resolved at pH 9.4 or greater. By acquiring the UV-visible absorption spectrum immediately after obtaining the ^{13}C-NMR spectrum it is possible to correlate the optical purity ratio , A_{390}/A_{280} , with the extent of denaturation in samples containing various amounts of apo and holoprotein. Nearly identical curves were obtained for mixtures containing native and heat denatured purified ferredoxin, indicating that accurate standard curves can be obtained using simple add-mixtures. Therefore, ^{13}C-NMR spectroscopy can be used to assess the reliability of other methods in determining the presence of apoprotein in impure ferredoxin samples. Additionally, ^{13}C-NMR spectroscopy also has potential use in ferredoxin denaturation studies involving solvents containing

Table IX. Add-mixtures of crude protein extracts to *Clostridium pasteurianum* 8Fe ferredoxin

TABLE IX

Additions of Native Ferredoxin to Contaminant Protein

	A_{390}	A_{280}	R
NATIVE FERREDOXIN	.8595	1.080	.800
CONTAMINANT FROTEIN	.0600	.6280	.095

(V/V)MIXTURES
ML FERREDOXIN/ML CONTAMINANT FROTEIN

MIXTURE	THEORETICAL A_{390}	ACTUAL A_{390}	THEORTICAL A_{280}	ACTUAL A_{280}	R
1.0/0.0	.8595	.8595	1.080	1.080	.80
0.80/0.20	.7000	.6899	.990	.979	.71
0.73/0.27	.6448	.6312	.956	.921	.67
0.67/0.33	.5920	.5835	.938	.914	.64
0.50/0.50	.4600	.4657	.854	.857	.54
0.38/0.62	.3679	.3700	.802	.798	.46
0.20/0.80	.2199	.2241	.718	.718	.31
0.0/1.0	.0600	.0600	.628	.628	.10

solutes, such as DTNB, that absorb UV-visible light and therefore can alter the reliability of the A_{390}/A_{280} measurement.

IV. Physical, chemical and spectroscopic studies of potassium ferricyanide treated Clostridium acidi-urici and Clostridium pasteurianum 2(4Fe-4S) ferredoxins

Sweeney (42) , originally noted that treatment of Clostridium pasteurianum 2(4Fe-4S) ferredoxin with $K_3Fe(CN)_6$ led to a protein exhibiting a g = 2.01 EPR signal. Although initially thought to be a novel HIPIP-like 4Fe-4S center, upon the advent of the discovery of the 3Fe center, it was subsequently reported by Johnson et al. (28) that the spectroscopic properties of the ferricyanide treated 8Fe ferredoxin from Clostridium pasteurianum were virtually identical to those observed in ferredoxins known to contain 3Fe-4S centers. Consequently, it was thought that ferricyanide oxidation of the 4Fe-4S center in 8Fe ferredoxins led to the formation of an iron-sulfur center virtually identical to those observed in the 3Fe containing ferredoxins. Thomson , et al. (31), has reported spectral similarities in the low temperature MCD spectra of ferricyanide treated CP ferredoxin and 3Fe ferredoxin from D. gigas . Similarly, Johnson , et al. (28), observed analogous spectroscopic behavior using resonance Raman spectroscopy . Stevens , et al. (71) has reported a chemically induced conversion of the 3Fe center of Azatobacter vinelandaii into a 4Fe center in alkaline medium . Ferricyanide conversions of the 4Fe-4S center

into a 3Fe center in several 7Fe ferredoxins has also been proposed by Nagayama, et al. (10,69) , using NMR spectroscopy. Thus, there is abundant evidence to support the view that chemical interconversion of iron-sulfur centers is common to many ferredoxins. Besides being of general interest, interconversion studies have particular application for several reasons . For example, in the study of aconitase , a long known mitochondrial enzyme whose function in the Krebs cycle is to isomerize citrate into isocitrate (12), it has been proposed that the protein is regulated by a interconversion of the inactive 3Fe center form into the active 4Fe form (43,72). In addition, Johnson (31) has reported a detectable EPR signal with a g_{av} value of 2.01 in purified preparations of native CP 8Fe Fd , and that this signal increased in intensity when the protein was exposed to oxygen. This suggests that oxidation of the 4Fe-4S to a 3Fe center occurs spontaneously under normal conditions. The experiments presented in this section characterize in more detail the products formed when Clostridium pasteurianum and Clostridium acidi-urici 8Fe ferredoxin undergoes oxidation in the presence of potassium ferricyanide or oxygen.

RESULTS AND DISCUSSION

Treatment of Clostridium pasteurianum or Clostridium acidi-urici 2(4Fe-4S) ferredoxin with $K_3Fe(CN)_6$ under the

experimental conditions described produced a protein having different spectroscopic properties from the native starting material. Visibly, the dark brown color associated with native 8Fe ferredoxin changes to a light amber red color after ferricyanide oxidation. The UV-visible absorption spectra of the two ferredoxins after ferricyanide treatment is also different from the native starting material (Figures XXXVI and XXXVII). In particular, the A_{max} in the visible region red-shifts from 390 to 400 nm. There is a flattening of the absorption band between 350 and 400 nm, and the absorption band in the UV region narrows some in the region between 270 to 310 nm. UV-visible spectra of this type are typical of 7Fe ferredoxins such as Azatobacter vinelandaii and Psuedonomas putida (Figure XXXVIII) known to contain 3Fe centers. However, spectra of this type are also seen with partially denatured samples of native ferredoxin (Figure XXXIX) and HIPIP ferredoxins as well (16). Consequently, UV-visible spectroscopy does not sufficiently resolve the various species present in the ferricyanide treated ferredoxin solution.

EPR spectroscopy of the ferricyanide treated ferredoxins, however, provides clearer evidence for interconversion of the 4Fe centers into a 3Fe form. The EPR spectrum of ferricyanide treated CAU 8Fe Fd (Figure XL) exhibits an isotropic g = 2.01 signal. Identical EPR spectra were acquired for ferricyanide treated CP 8Fe

Figure XXXVI. Comparison of the UV-visible absorption spectrum of native and potassium ferricyanide treated Clostridium acidi-urici 8Fe ferredoxin

Conditions: 0.15 mg/ml protein in 0.050 M potassium phosphate buffer/ 0.050 M NaCl, pH 7.6 , temperature 27^{o}K.

Top spectrum - native untreated protein
bottom spectrum - ferricyanide treated protein

Note: Top spectrum is offset to higher optical absorbance units for better comparison of spectra .

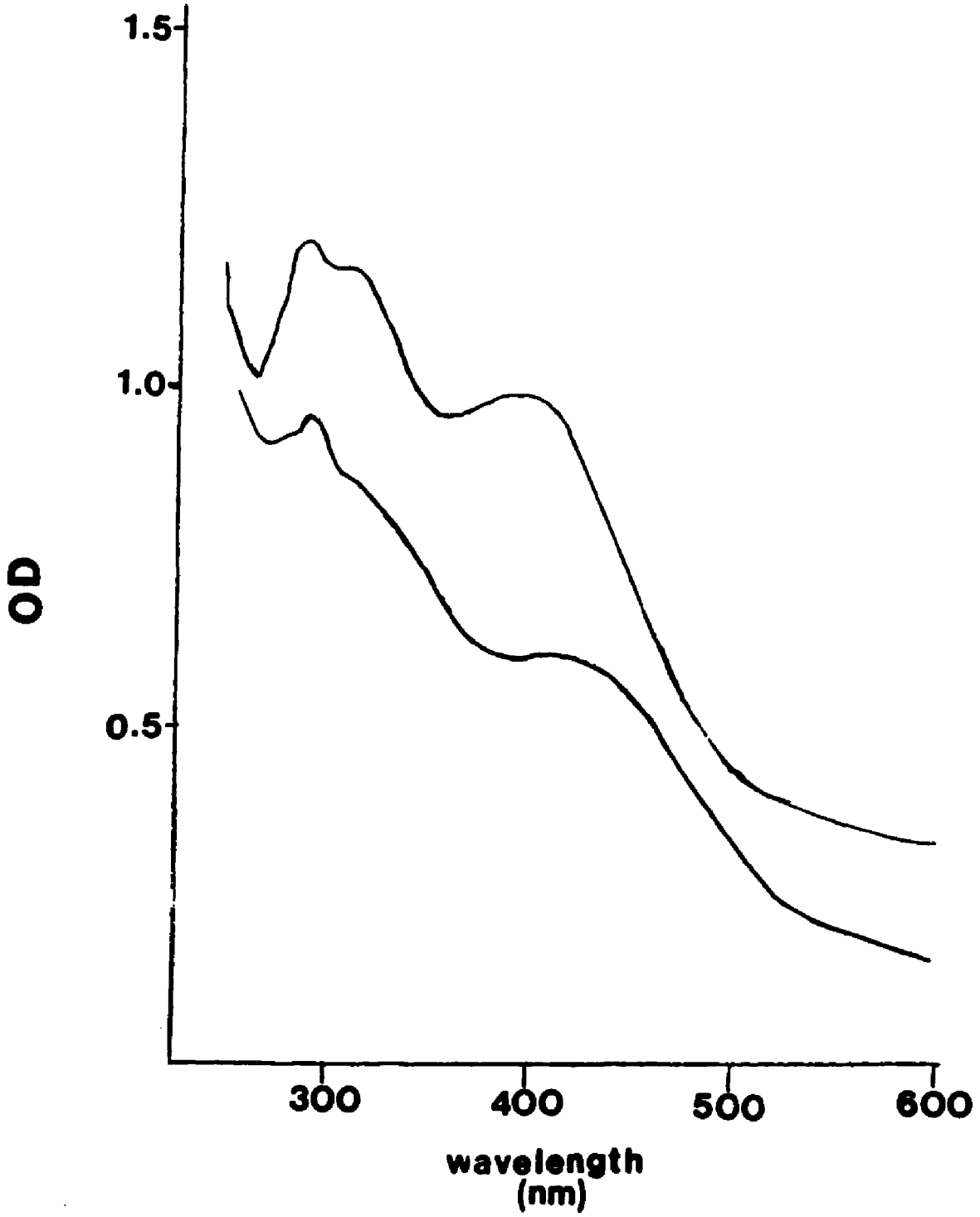
1.5
1.0
0.5
OD
300
400
500
600
wavelength
(nm)

Figure XXXVII. Comparison of the UV-visible absorption spectrum of native and potassium ferricyanide treated Clostridium pasteurianum 8Fe ferredoxin

Conditions: 0.15 mg/ml protein in 0.050 M potassium phosphate buffer/ 0.050 M NaCl, pH 7.6 , temperature 27^{o}K.

Top spectrum - native untreated protein
bottom spectrum - ferricyanide treated protein

Note: Top spectrum is offset to higher optical absorbance units for better comparison of spectra ..

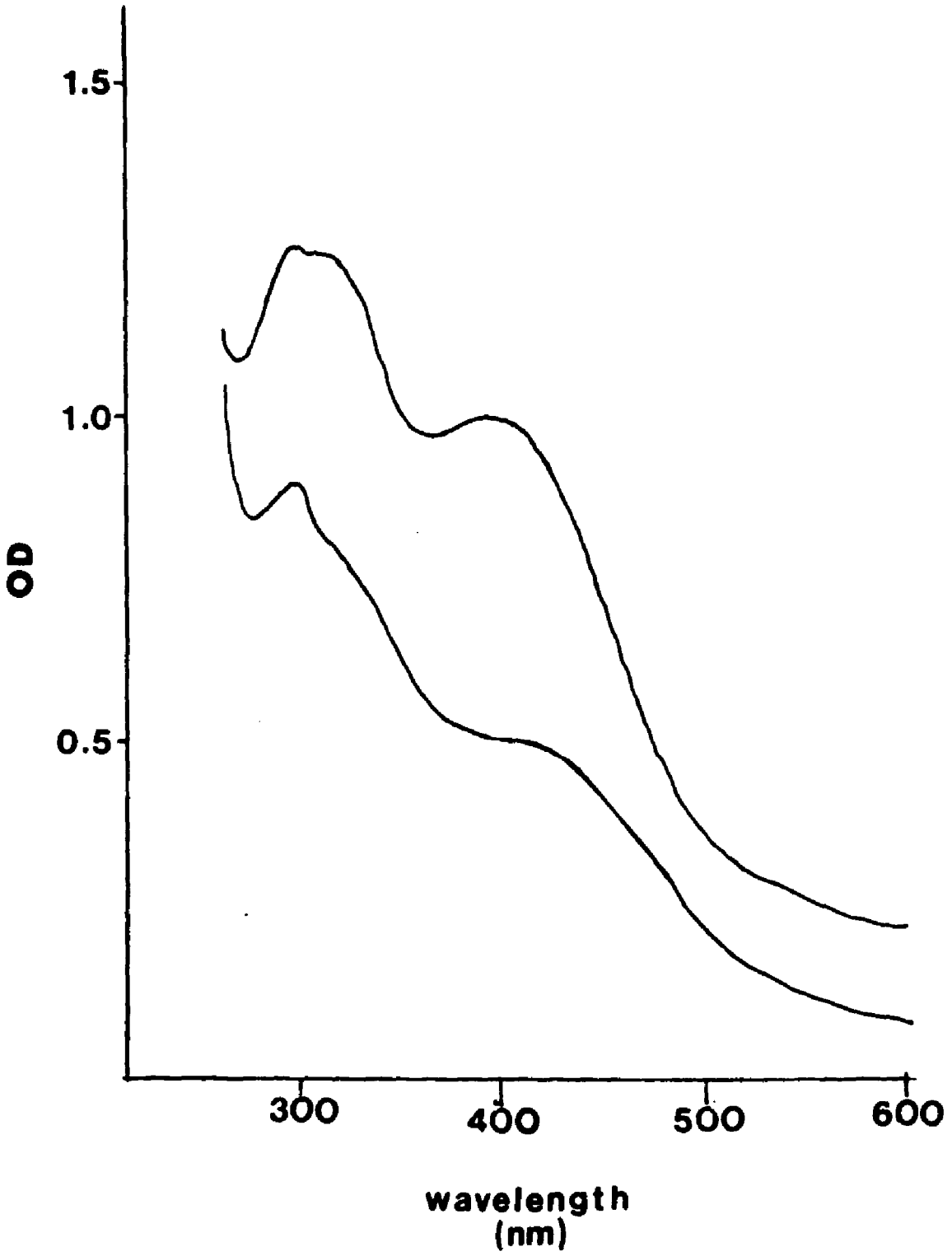
1.5
1.0
0.5
OD
300
400
500
600
wavelength
(nm)

Figure XXXVIII. Comparison of the UV-visible absorption spectrum of native Clostridium pasteurianum 8Fe ferredoxin, potassium ferricyanide treated Clostridium pasteurianum 8Fe ferredoxin and Pseudonomas putida 7Fe ferredoxin

Conditions: 0.15 mg/ml protein in 0.050 M potassium phosphate buffer/ 0.050 M NaCl, pH 7.6 , temperature 27^{o}K.

Top spectrum - native CP protein
middle spectrum - ferricyanide treated CP protein
bottom spectrum - native PP 7Fe protein

Note: Top two spectra are offset to higher optical absorbance units for better comparison of spectra .

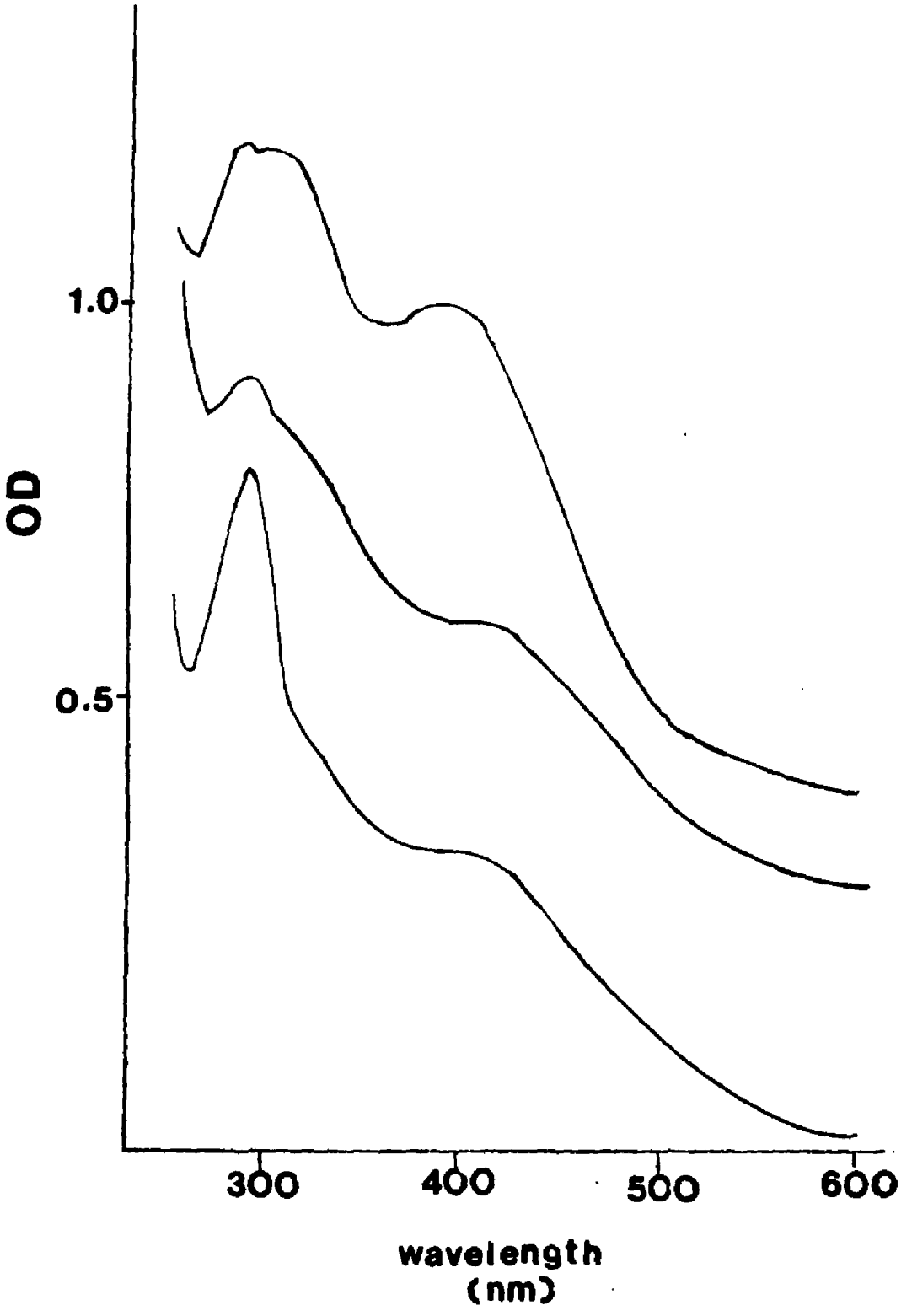
1.0
0.5
OD
300
400
500
600
wavelength
(nm)

Figure XXXIX. Comparison of the UV-visible absorption spectrum of Pseudonomas putida 7Fe ferredoxin, native Clostridium pasteurianum 8Fe ferredoxin, potassium ferricyanide treated Clostridium pasteurianum 8Fe ferredoxin and partially denatured sample of Clostridium pasteurianum 8Fe ferredoxin

Conditions: 0.15 mg/ml protein in 0.050 M potassium phosphate buffer/ 0.050 M NaCl, pH 7.6 , temperature 27^{o}K.

Top spectrum - native PP 7Fe protein (A)

2nd spectrum - native CP 8Fe protein (B)

3rd spectrum - ferricyanide treated CP protein (C)

bottom spectrum - partially denatured CP protein (D)

Note: Top two spectra are offset to higher optical absorbance units for better comparison of spectra .

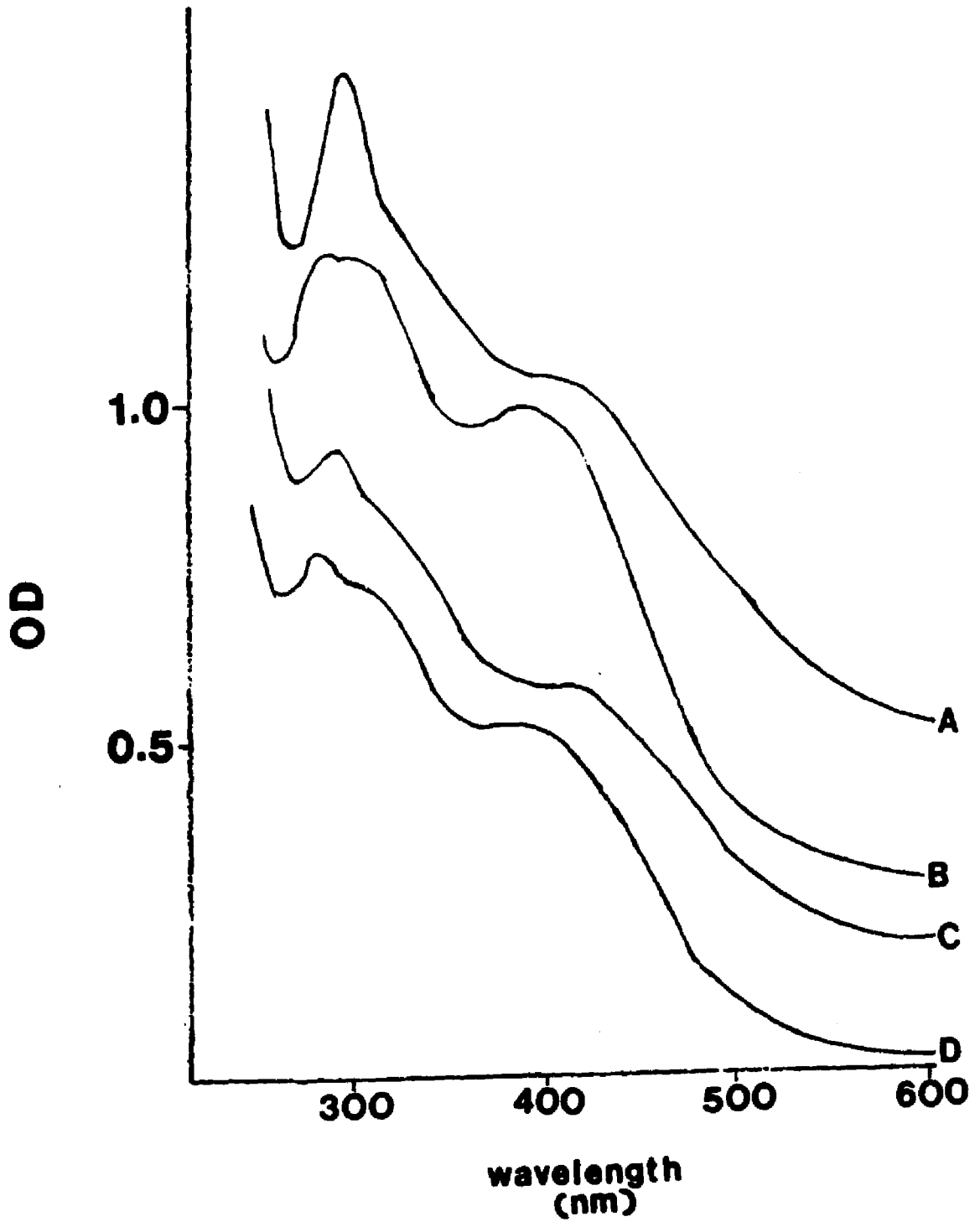
OD
1.0
0.5
300
400
500
600
wavelength
(nm)
A
B
C
D

Figure XL. EPR spectrum of ferricyanide treated *Clostridium acidi-urici* 8Fe ferredoxin

Conditions: 3 mg/ml protein in 0.050 M potassium phosphate buffer/ 0.030 M NaCl, pH 7.5 , temperature , $15^{o}K$

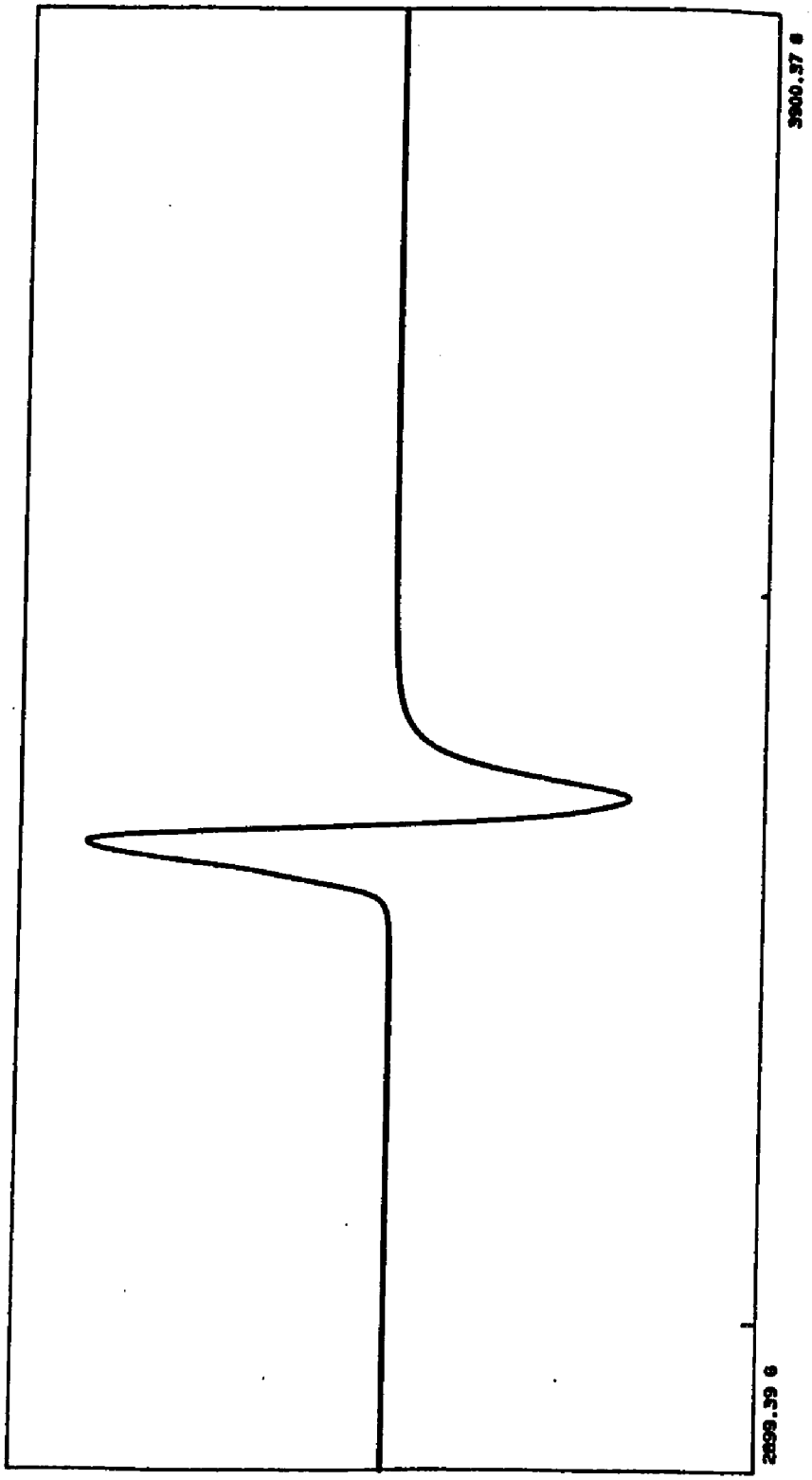
3600.57 0
2599.59 0

Fd , consistent with previous results (28). This signal is characteristic of those found in the 3Fe and 7Fe ferredoxins, and is thought to arise from the 3Fe center in the oxidized form (32). When the EPR spectrum of the ferricyanide treated ferredoxin is taken in the presence of sodium dithionite a signal at g_{av} = 1.94 is observed (Figure XLI) . This signal is typical of a single reduced 4Fe-4S center. Because the protein was reduced in the presence of excess dithionite it is unlikely that this signal arises from incomplete reduction of the 2(4Fe-4S) centers aising from unreacted 8Fe ferredoxin. Rather, the signal is more likely due to the presence of a protein that contains only one 4Fe-4S center. However, it is unclear whether the 4Fe-4S center is a single isolated center or associated with the observed 3Fe centers, as in the 7Fe ferredoxins. Consequently, EPR spectroscopy can detect but cannot distinquish between the presence of 3Fe, 4Fe and 7Fe ferredoxins formed during ferricyanide treatment.

Figure LII displays a time course profile for the conversion of Clostridium acidi-urici 8Fe ferredoxin into a 3Fe form when the protein is treated with a seven-fold molar excess of potassium ferricyanide. Using EPR spectroscopy it is possible to follow over time the evolution of the 3Fe center by monitoring the increase in the g = 2.01 signal. Similarly, a concurrent decrease in the g = 1.94 signal was also observed as the ferricyanide

Figure XLI. EPR spectrum of ferricyanide treated *Clostridium acidi-urici* 8Fe ferredoxin taken in the presence of sodium dithionite

Conditions: same as Figure XL

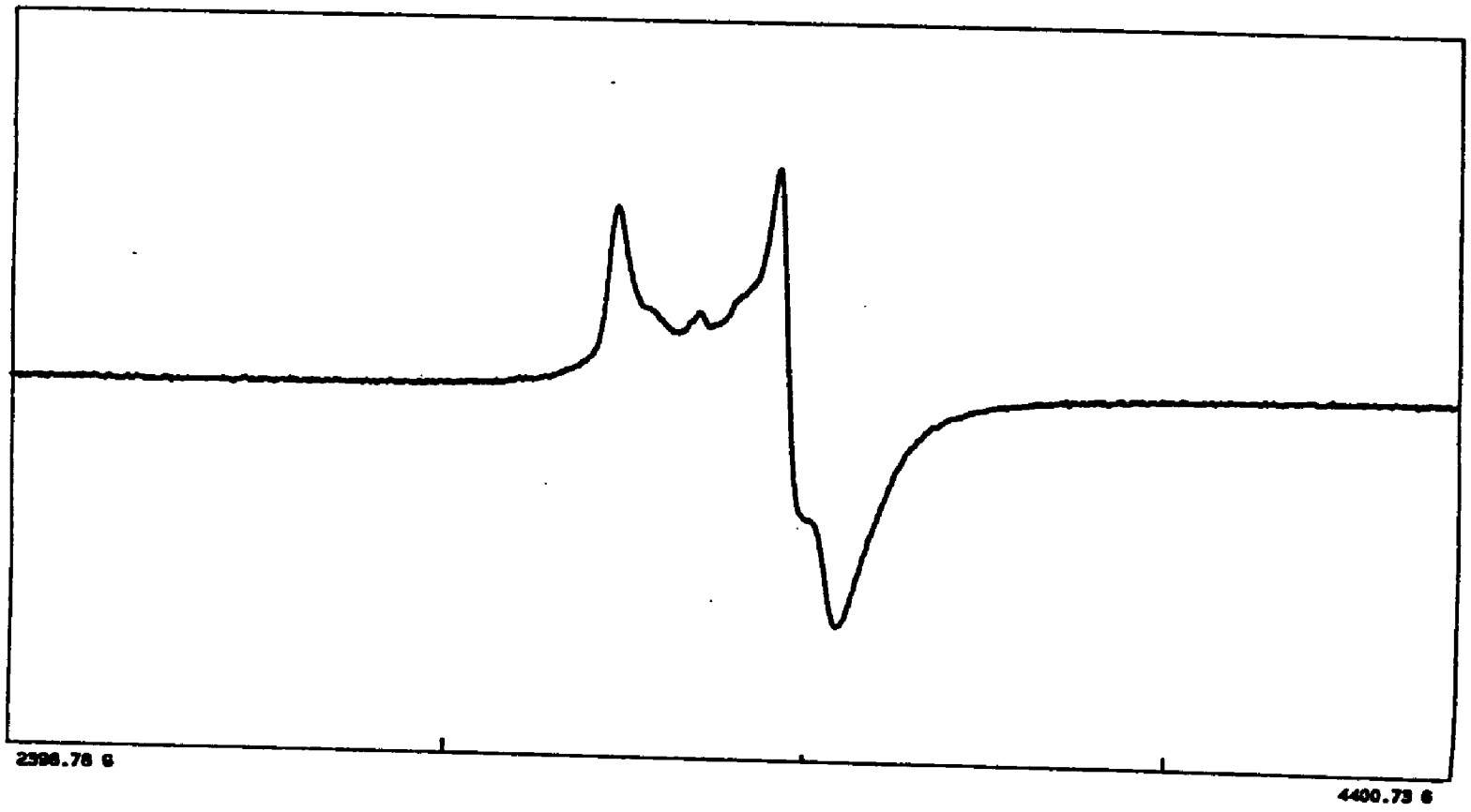
2596.78 G
4400.73 G

Figure XLII. EPR time-course profile for the potassium ferricyanide conversion of Clostridium acidi-urici 8Fe ferredoxin

Conditions: 6 mg/ml protein in 0.050 M potassium phosphate buffer , pH 7.5 , temperature 15^{o}K

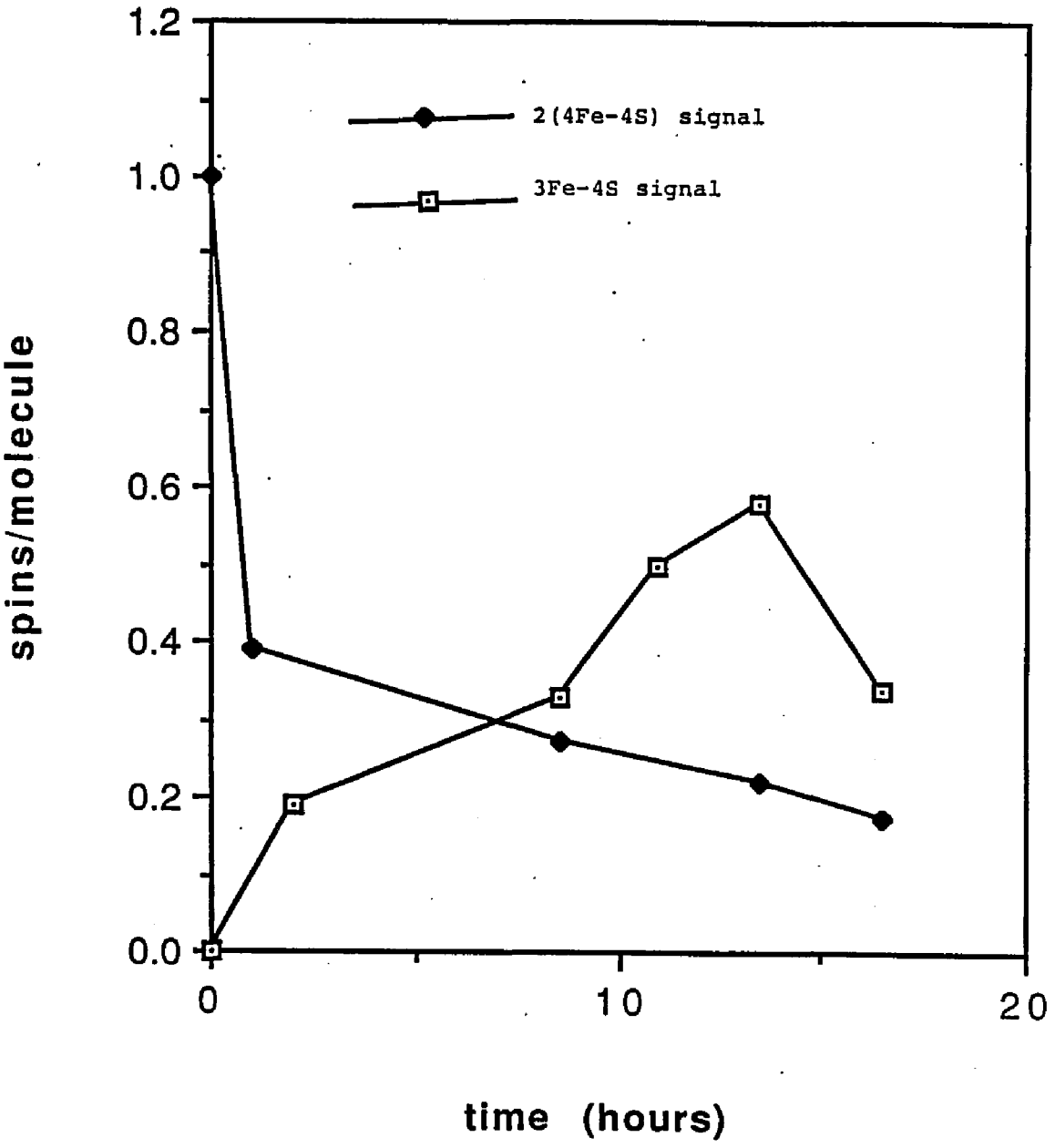
1.2
1.0
0.8
0.6
0.4
0.2
0.0
spins/molecule
2(4Fe-4S) signal
3Fe-4S signal
0
10
20
time (hours)

reaction proceeded. It is seen in this plot that the maximum evolution in the intensity of the 3Fe EPR signal occurs after 13.5 hours, after which a steady decrease is seen probably as a result of protein denaturation. The time course results are consistent with the 15 hour incubation time required for conversion of Clostridium pasteurianum ferredoxin as reported by Johnson et al. (28). Although Johnson originally noted that complete conversion was observed after the incubation period, for Clostridium acidi-urici the 4Fe signal is never completely lost. As discussed earlier, this signal may arise from the presence of a protein containing a single 4Fe-4S center.

The downfield region of the ^{1}H-NMR spectra of the ferricyanide treated ferredoxins are unique (Figures XLIII and XLIV). Additionally, the temperature dependence of the downfield peaks is also unusual (Figure XLV). Although there are differences in the aliphatic and aromatic regions (data not shown) the most notable differences are observed between 10 and 50 ppm. This region shows little resemblance to the spectra seen for known 3Fe and 7Fe ferredoxins. Because the chemical shift and lineshapes of the downfield resonances arise from protons close to the Fe-S centers , these resonances can be used as probes to examine the chemical environment around the Fe-S centers. The unusual NMR spectra indicates the 3Fe center formed as a result of the

Figure XLIII. 400 MHz ^{1}H-NMR spectrum of ferricyanide treated Clostridium acidi-urici 8Fe ferredoxin

Conditions: 4 mg/ml protein in 0.050 M KD_2PO_4/ 0.030 M NaCl , pH_{meter} 7.55 , pulse repeat time, 0.607 seconds , 2500 scans, temperature, 25^{o}K

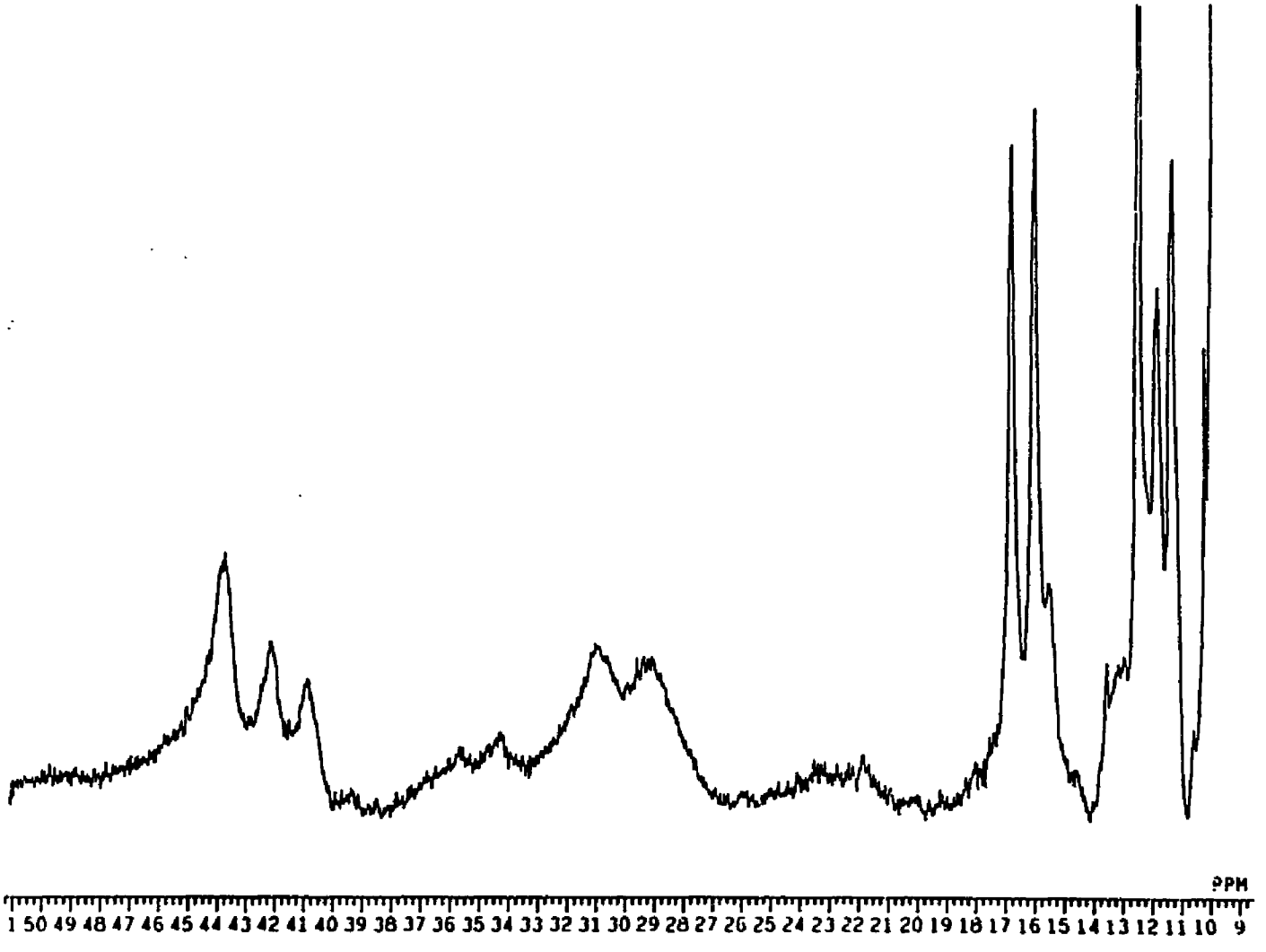
PPM
1 50 49 48 47 46 45 44 43 42 41 40 39 38 37 36 35 34 33 32 31 30 29 28 27 26 25 24 23 22 21 20 19 18 17 16 15 14 13 12 11 10 9

Figure XLIV. 400 MHz ^{1}H-NMR spectrum of ferricyanide treated Clostridium pasteurianum 8Fe ferredoxin

Conditions: 1.5 mg/ml protein in 0.050 M KD_2PO_4/ 0.010 M NaCl , pH_{meter} 7.55 , pulse repeat time, 0.607 seconds , 2000 scans, temperature, $25^{o}K$

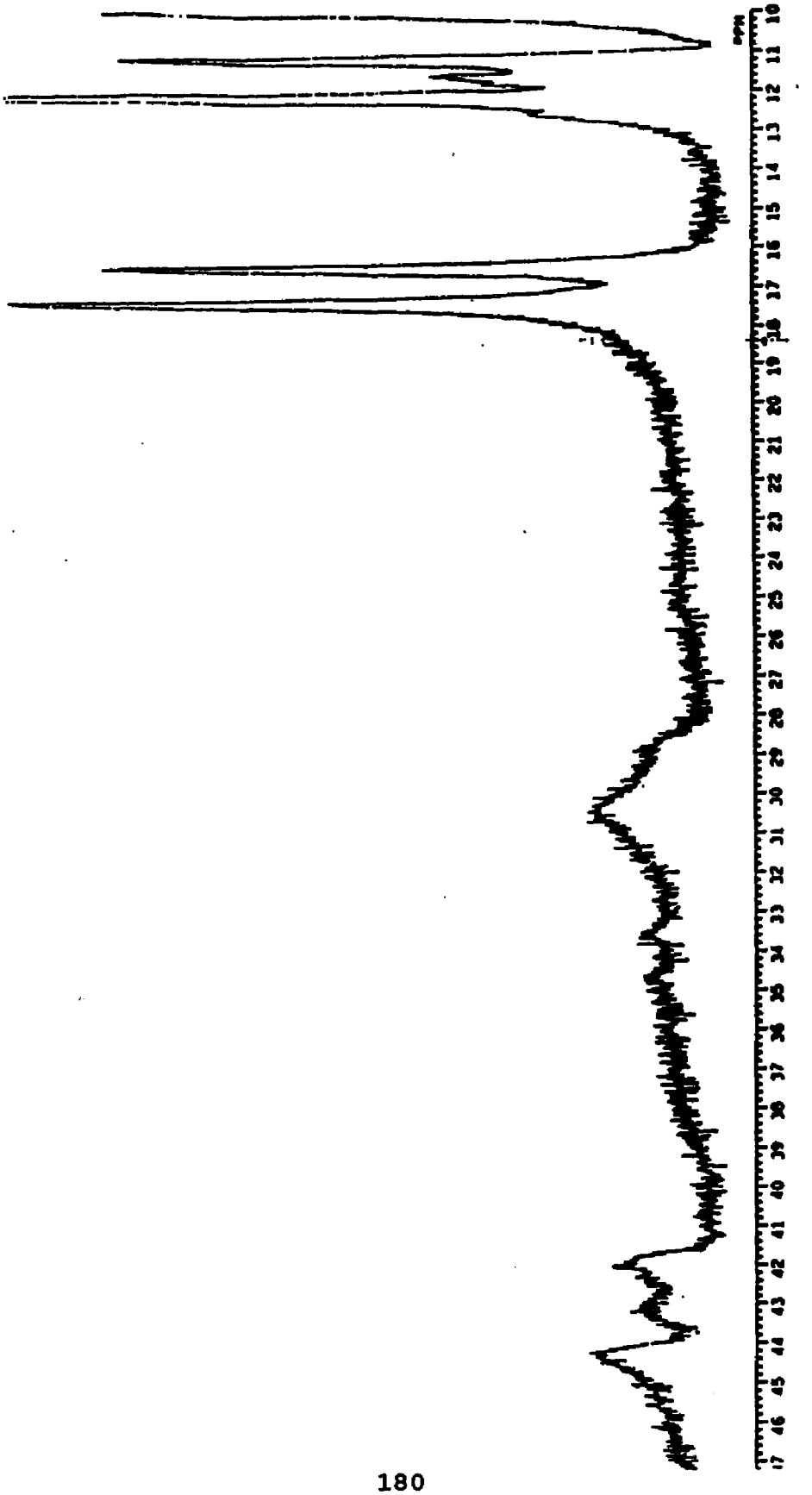
PPM
10
11
12
13
14
15
16
17
18
19
20
21
22
23
24
25
26
27
28
29
30
31
32
33
34
35
36
37
38
39
40
41
42
43
44
45
46
47

Figure XLV. Temperature dependance of the downfield resonances in the ^{1}H-NMR spectrum of ferricyanide treated Clostridium acidi-urici 8Fe ferredoxin

Conditions : same as Figure XLIII

Top spectrum - 37°C

middle spectrum - 25°C

bottom spectrum - 8°C

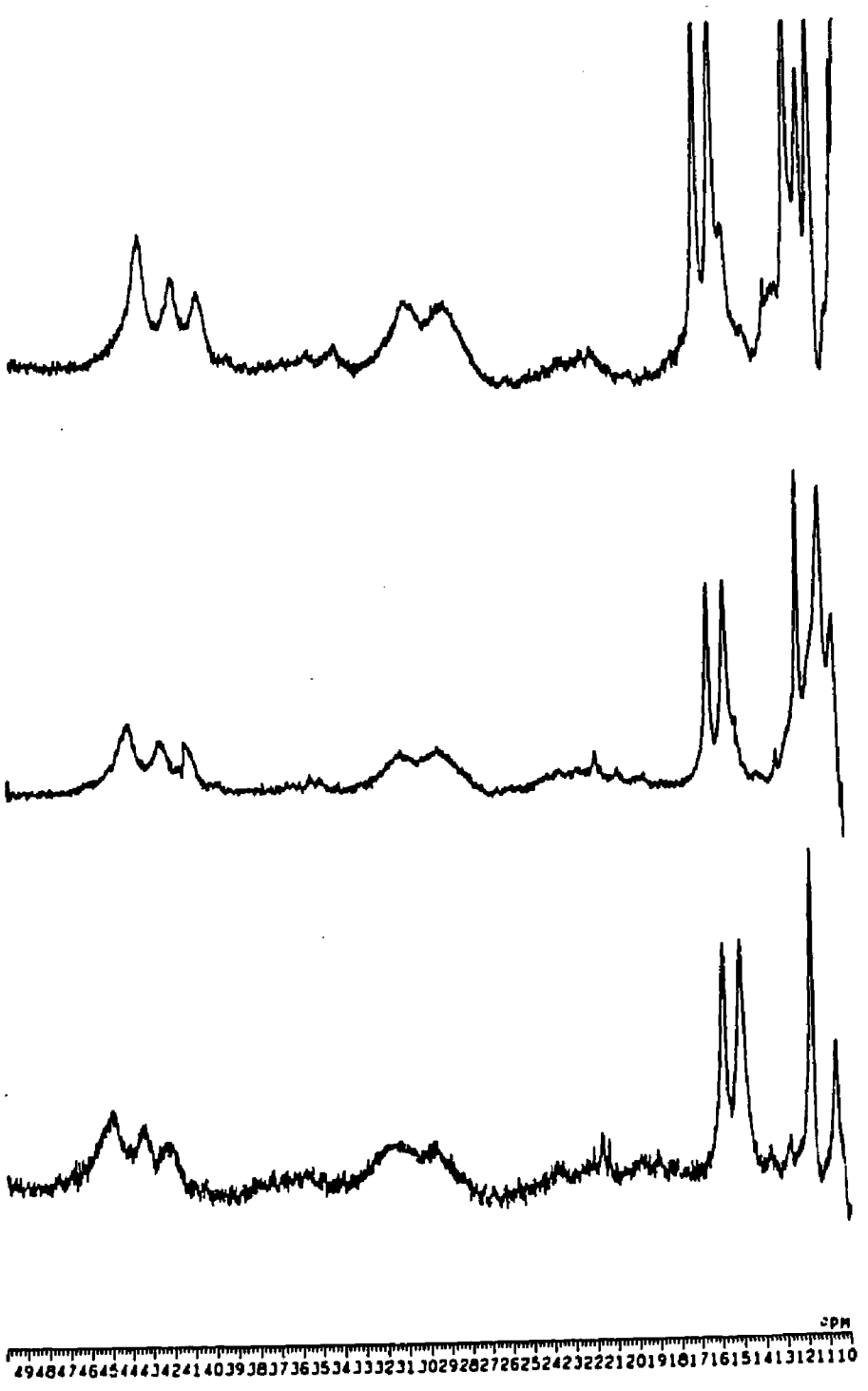
PPM

ferricyanide oxidation is not the same 3Fe center found in 3Fe and 7Fe ferredoxins. Since NMR cannot characterize the actual nature of the 3Fe protein formed upon ferricyanide oxidation it is unclear whether these spectroscopic differences arise from changes in the ligand and chemical enviroment around the normal 3Fe center or from actual changes in the structure of the 3Fe center. The latter case might be ruled out using Mossbauer spectroscopy.

If native 2(4Fe-4S) CP Fd is sufficiently air oxidized , a protein having an identical NMR spectrum to that observed from ferricyanide treatment can be isolated. By this method purified 8Fe ferredoxin is aerobically stored for 2-3 weeks at $4^{o}C$ in 0.10 M Tris buffer at pH 7.5 to allow sufficient time for the native protein to undergo denaturation. The protein is then applied to a Sephacel G-75 chromatography column, and a faint yellow band was usually observed eluting before the 8Fe ferredoxin. When this material is pooled and concentrated a NMR spectrum can be obtained (Figure XLVI). This spectrum is virtually identical to those seen in the ferricyanide treated samples of ferredoxin. These results indicate that the 3Fe conversion products observed after ferricyanide treatment are probably the same as those obtained from air oxidation.

A partial purification of the ferricyanide treated 8Fe Fd was carried out using Whatman-DEAE in an effort to separate unreacted and denatured protein from ferricyanide

Figure XLVI. ^{1}H-NMR spectrum of air oxidized *Clostridium pasteurianum* 3 Fe converted ferredoxin

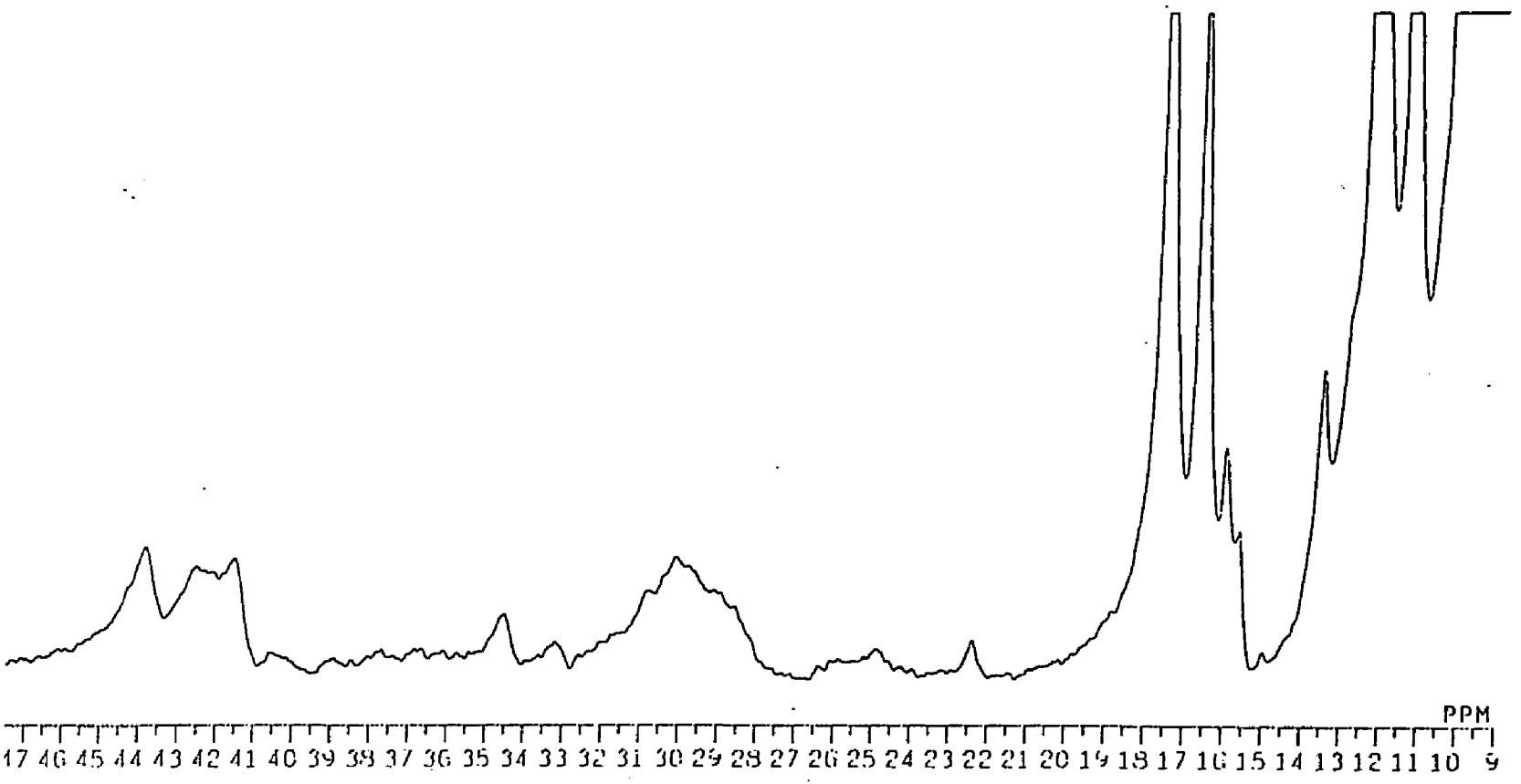
PPM
17 46 45 44 43 42 41 40 39 38 37 36 35 34 33 32 31 30 29 28 27 26 25 24 23 22 21 20 19 18 17 16 15 14 13 12 11 10 9

oxidized Clostridium acidi-urici ferrredoxin. To remove apoprotein and unreacted ferredoxin from the reaction mixture required washing with 0.10M potassium phosphate containing 0.10M NaCl. However, two additional bands, bands II and III, could be eluted by using buffer containing 0.20M NaCl and 0.35M NaCl, respectively. With collaborative assistance from Dr. Micheal K. Johnson at the University of Georgia in Athens, UV-visible, EPR, resonance Raman and MCD spectra were acquired for each of the bands eluted and are shown in Figures XLVII, XLVIII, ILV, L, LI, and LII, respectively. The spectral properties of Band I, eluted with 0.10M NaCl indicate that this band contains predominately unreacted 8Fe ferredoxin. For Band II, eluted with 0.20M NaCl, the data indicates the presence of both 3Fe and 4Fe species, however , there is no evidence for the presence of any 8Fe species. Band III, eluted at high salt, appears to indicate the presence of a pure 3Fe species with some trace 4Fe component. These results indicate that ferricyanide treatment of Clostridium acidi-urici 8Fe ferredoxin can lead to the formation of multiple products having different types of Fe-S centers.

Although Johnson originally reported that ferricyanide treatment of Clostridium pasteurianum led to the apparent formation of a nearly homogeneous 3Fe species (28), a partial purification of ferricyanide treated Clostridium pasteurianum ferredoxin was undertaken. The

Figure XLVII. UV-visible absorption spectra of bands I, II and III for ferricyanide treated *Clostridium acidi-urici* 8Fe ferredoxin

Conditions: 0.070 mg/ml protein in 0.10 M potassium phosphate buffer, pH 7.5

top spectrum - Band I eluted with 0.10M NaCl

middle spectrum - Band II eluted with 0.20M NaCl

bottom spectrum - Band III eluted with 0.35M NaCl

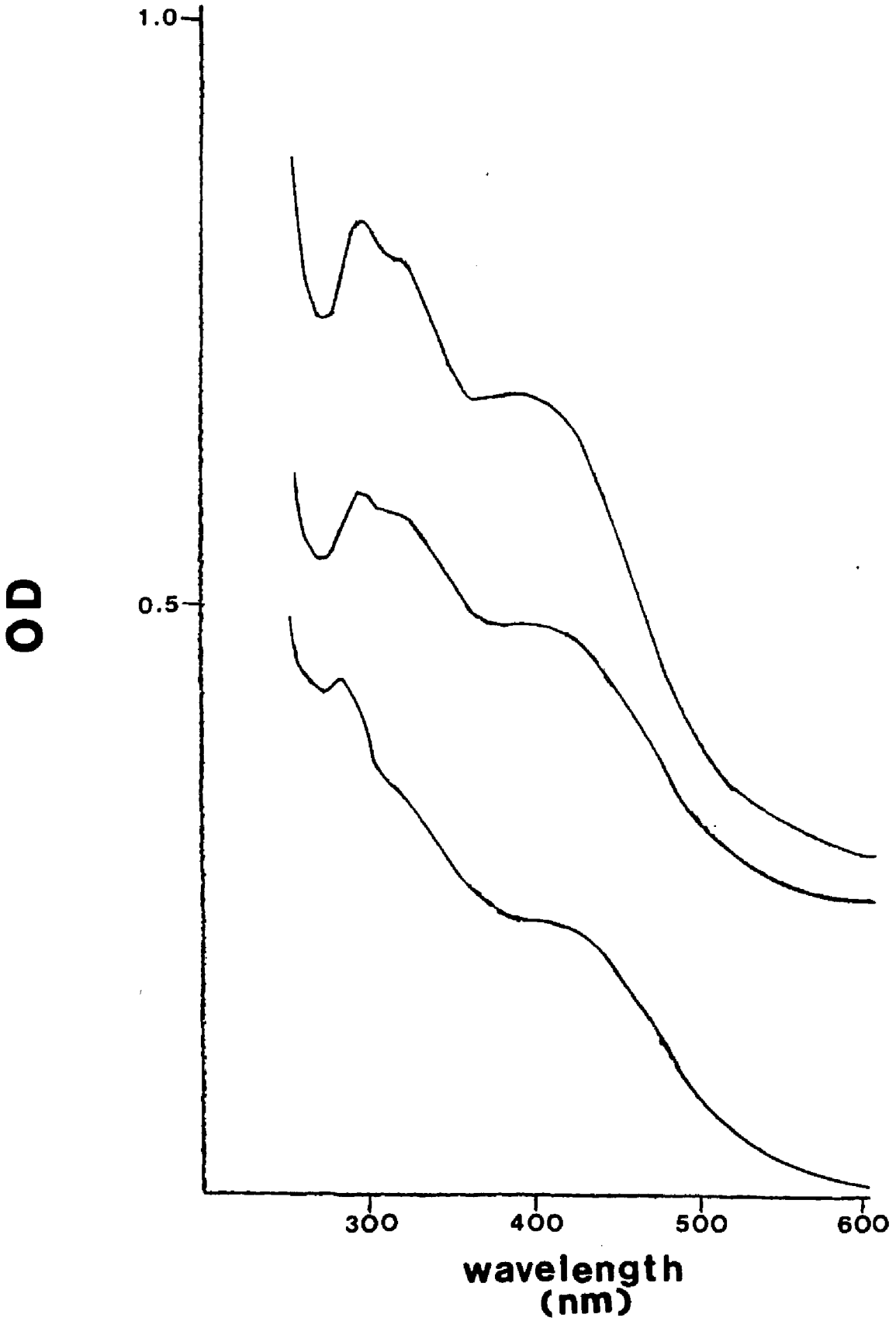
1.0
0.5
OD
300
400
500
600
wavelength
(nm)

Figure XLVIII. EPR spectrum of bands I, II and III for ferricyanide treated Clostridium acidi-urici

Conditions: ca. 2-3 mg/ml protein in 0.10 M potassium phosphate buffer , pH 7.5, temperature, $15^{o}K$.

top spectrum - band I eluted with 0.10M NaCl
middle spectrum - band II eluted with 0.20M NaCl
bottom spectrum - band III eluted with 0.35M NaCl

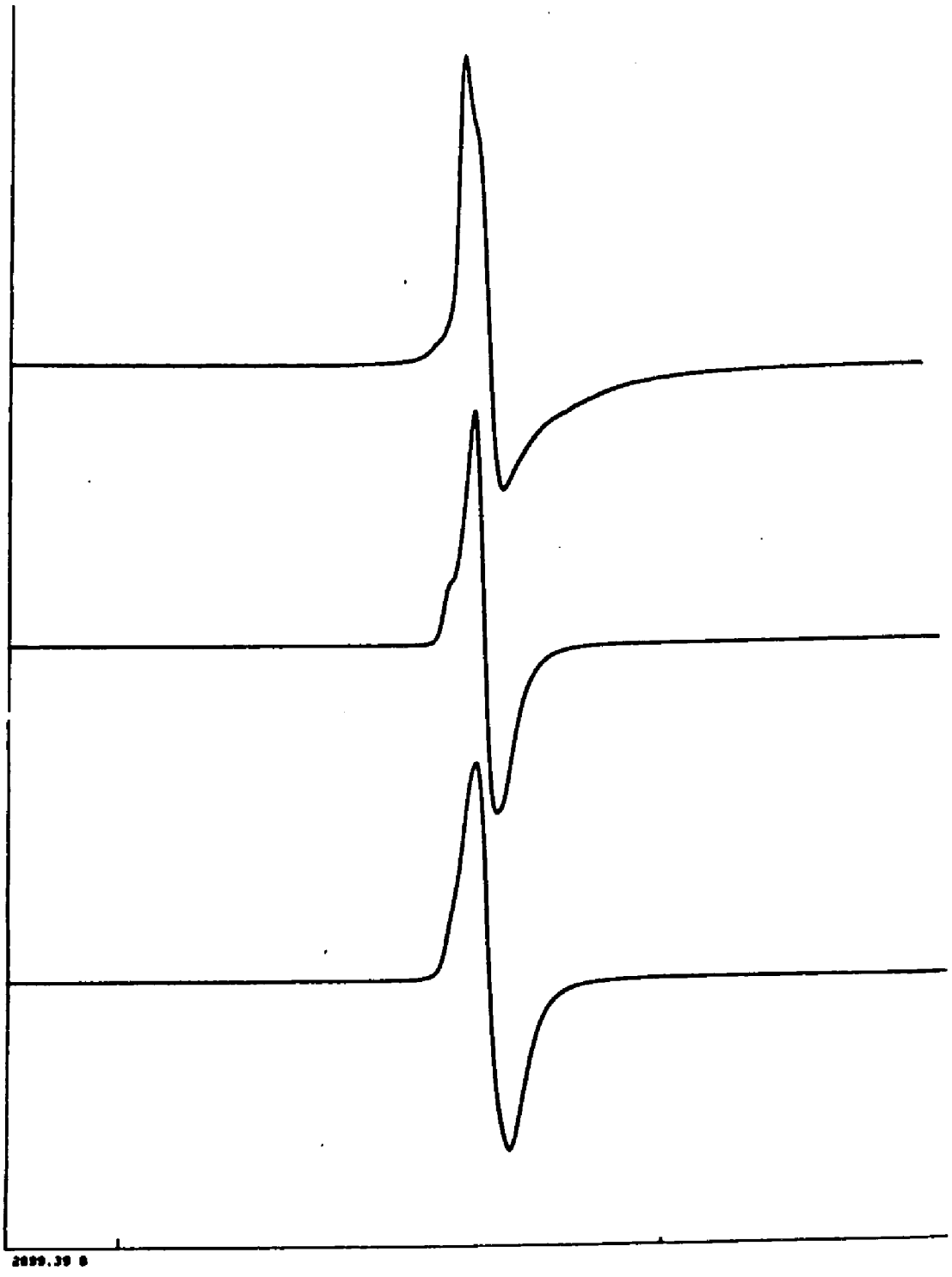

Figure IL. EPR spectrum of dithionite reduced bands I, II and III for ferricyanide treated Clostridium acidi-urici

Conditions: ca. 2-3 mg/ml protein in 0.10 M potassium phosphate buffer , pH 7.5, temperature, $15^{o}K$.

top spectrum - band I eluted with 0.10M NaCl
middle spectrum - band II eluted with 0.20M NaCl
bottom spectrum - band III eluted with 0.35M NaCl

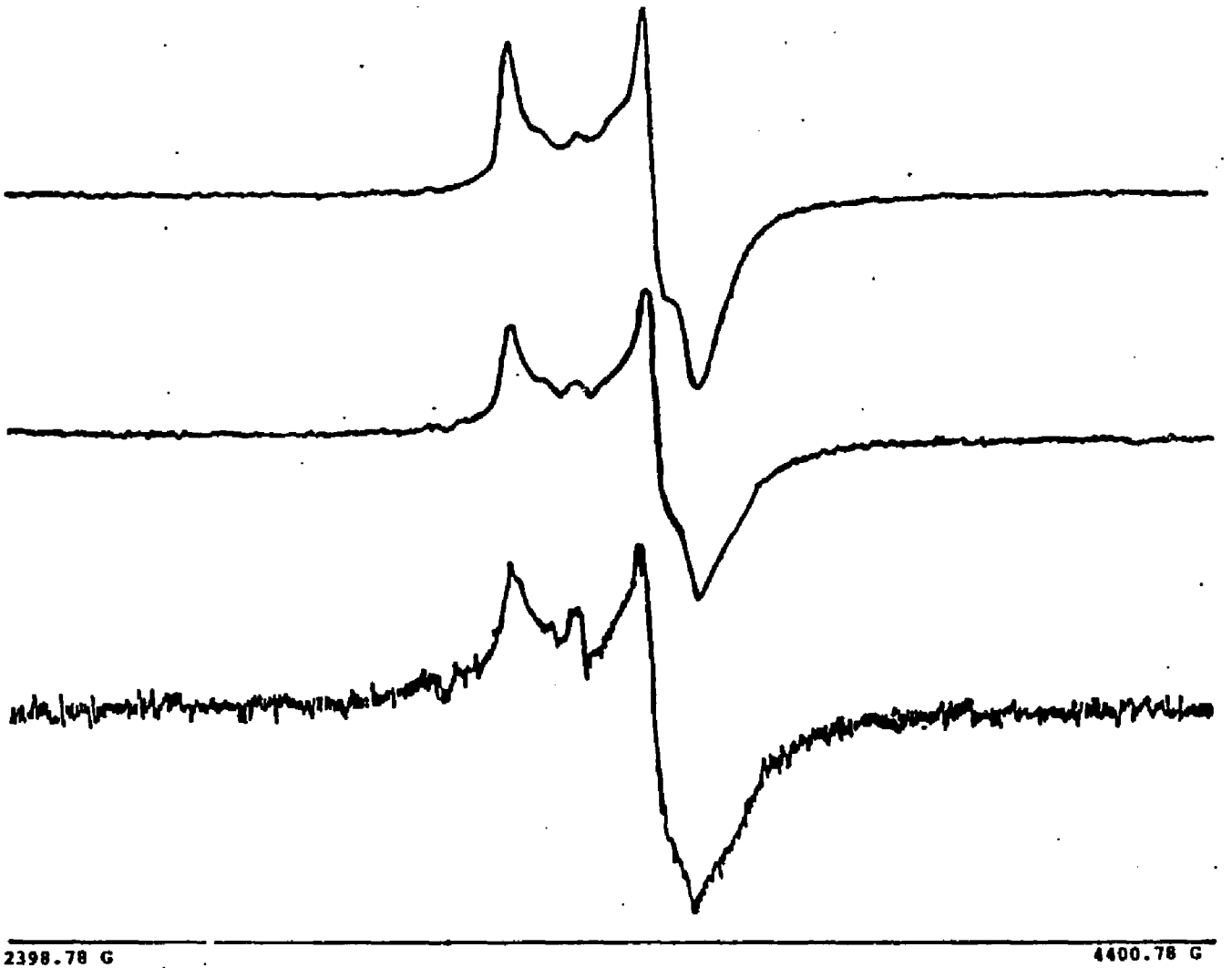
2398.78 G
4400.78 G

Figure L. Resonance Raman spectra of bands I, II and III for ferricyanide treated *Clostridium acidi-urici*

Conditions: 2-3 mg/ml protein in 0.10 M potassium phosphate buffer, pH 7.5, 50% glycerol

A - Band I eluted with 0.10M NaCl

B - Band II eluted with 0.20 M NaCl

C - Band III eluted with 0.35M NaCl

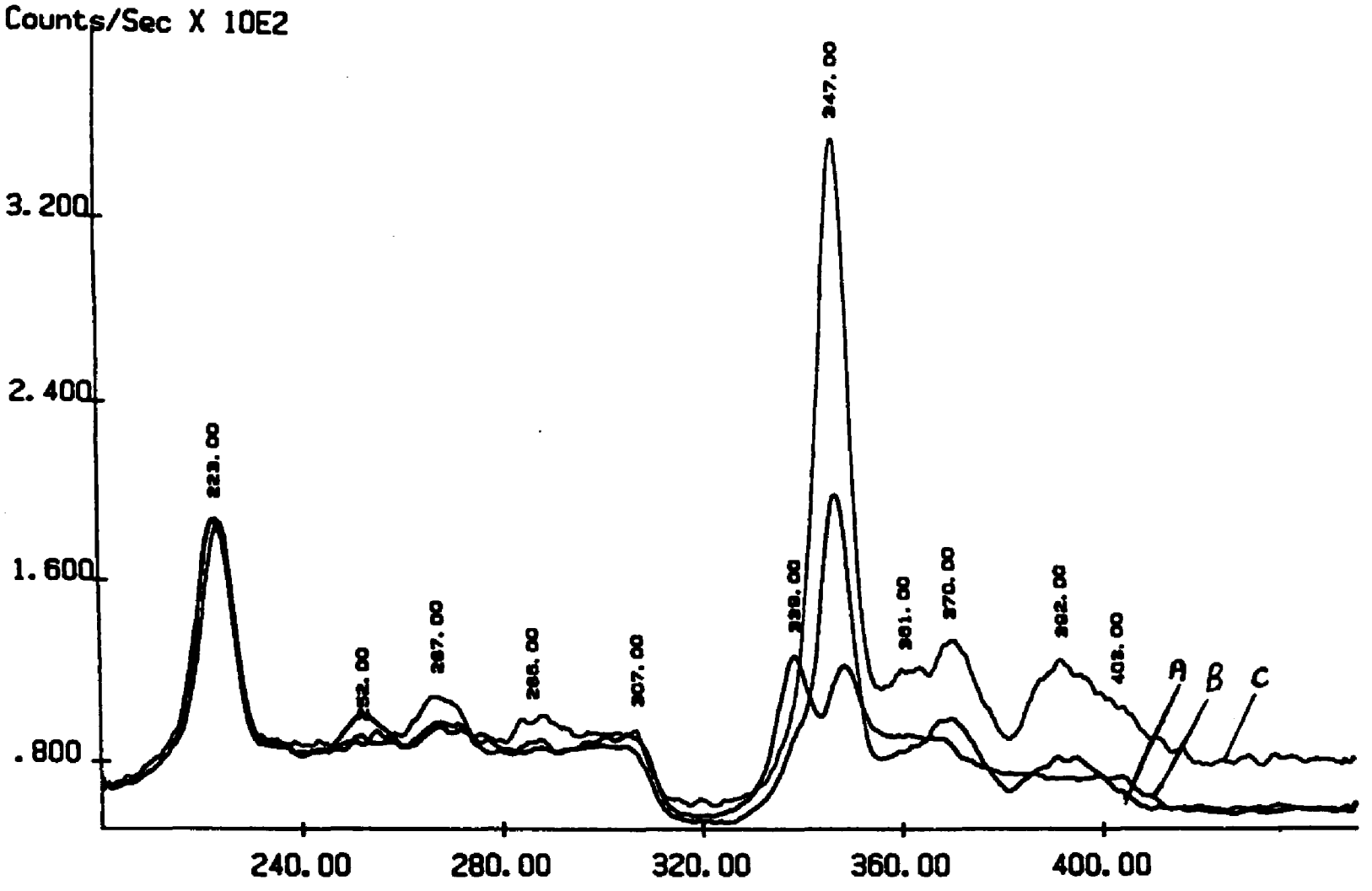
Counts/Sec X 10E2
3.200
2.400
1.600
.800
223.00
252.00
287.00
298.00
307.00
336.00
347.00
361.00
370.00
392.00
408.00
A
B
C
240.00
280.00
320.00
360.00
400.00

Figure LI. Low temperature MCD spectra for bands I, II and III for ferricyanide treated Clostridium acidi-urici

Conditions: 2-3 mg/ml protein in 0.10 M potassium phosphate buffer, pH 7.5, 50% glycerol

A - Band I eluted with 0.10M NaCl

B - Band II eluted with 0.20 M NaCl

C - Band III eluted with 0.35M NaCl

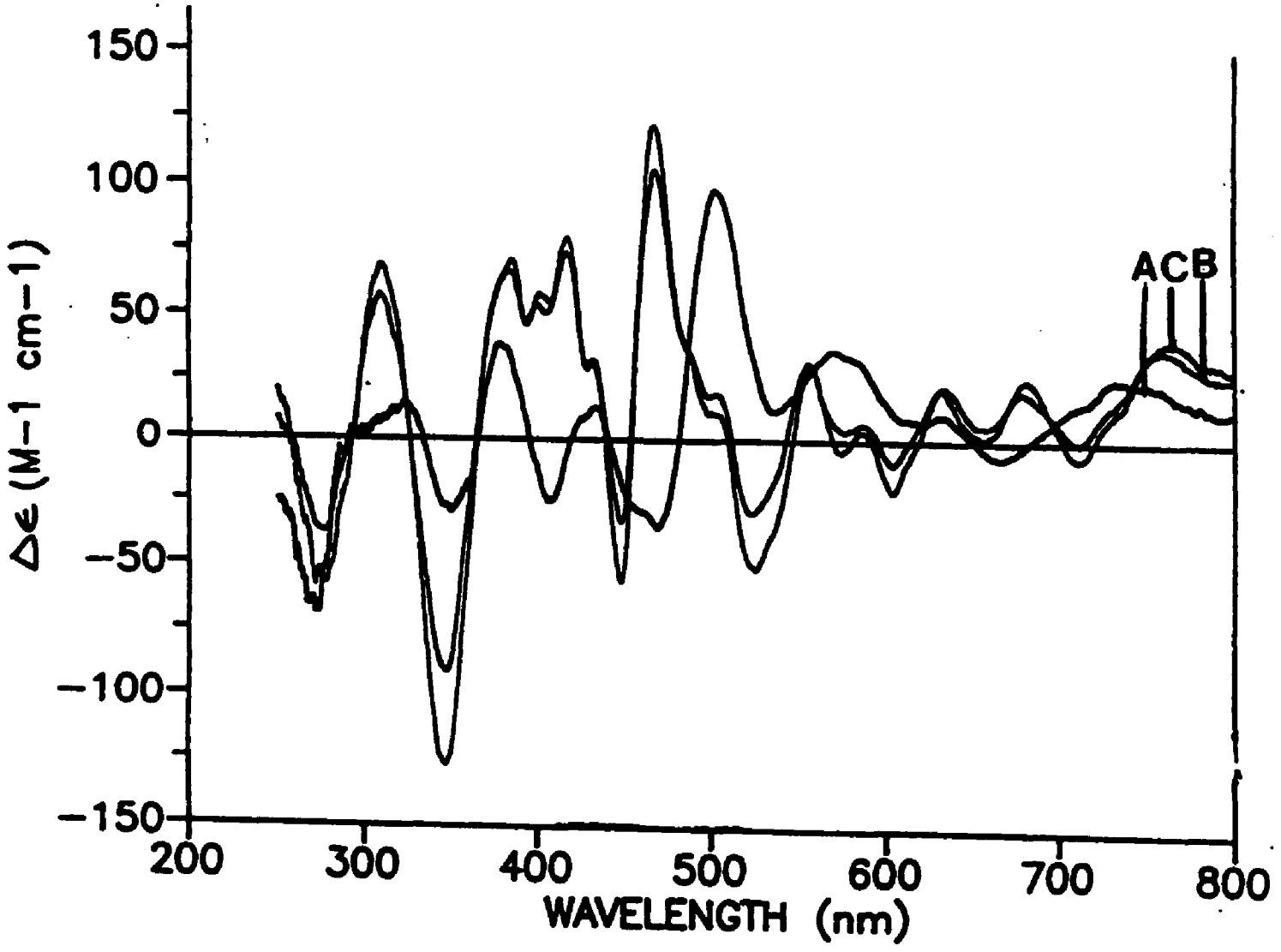
150
100
50
0
−50
−100
−150
Δε (M−1 cm−1)
200
300
400
500
600
700
800
WAVELENGTH (nm)
ACB

Figure LII. Low temperature MCD spectra of dithionite reduced bands I, II and III for ferricyanide treated Clostridium acidi-urici 8Fe ferredoxin

Conditions: 2-3 mg/ml protein in 0.10 M potassium phosphate buffer, pH 7.5, 50% glycerol

A - Band I eluted with 0.10M NaCl

B - Band II eluted with 0.20 M NaCl

C - Band III eluted with 0.35M NaCl

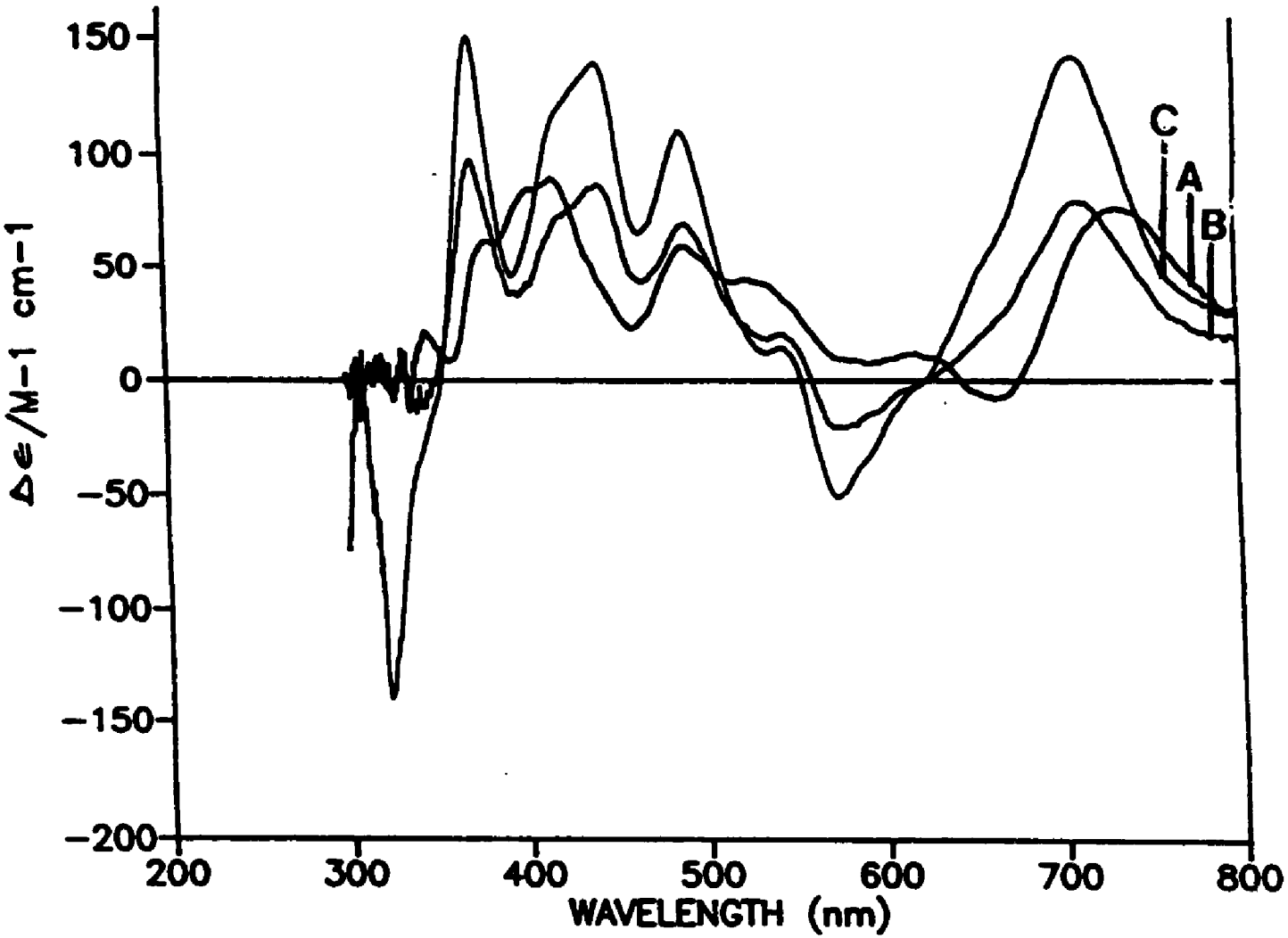
150
100
50
0
−50
−100
−150
−200
Δε/M−1 cm−1
200
300
400
500
600
700
800
WAVELENGTH (nm)
C
A
B

ferricyanide treated ferredoxin was first applied to a Sephacel G-75 column to ascertain the approximate molecular weights of the products formed after ferricyanide oxidation. By this method four different bands are observed at approximate molecular weights of 64000, 35000, 15000 and 6000, respectively. Further purification of the bands on Whatman-DEAE showed additional protein bands as well. When the 64000 MW band is applied to DEAE it resolves into two bands, I and II, at 0.20M and 0.35M NaCl, respectively. The 35000 MW band also resolves into two bands , III and IV, at the same salt elutions. The 15000 MW band shows only one band, V , eluted at 0.20M NaCl, whereas the 6000 MW band resolves into two bands, VI and VII, at 0.125M and 0.20M NaCl , respectively. These results , in agreement with those obtained for CAU 8Fe Fd, show that ferricyanide treatment can result in the formation of multiple products containing peptide of variable molecular weight.

Gel electrophoresis was used to examine the purity of the bands separated by ion exchange chromatography, and to determine whether the increase in the molecular weight of the product was a result of covalent or non-covalent interactions. Bands III, IV and VII were applied to an electrophoretic gel in the presence of mercaptoethanol and SDS detergent (data not shown). When the protein bands are run in the presence of SDS one major band is resolved having a molecular weight of about 5200 , which

corresponds to the weight of one apoprotein molecule. The results indicate that the increased molecular weight seen in the ferricyanide treated products is due to non-covalent interactions between peptide molecules. The varying degree of molecular weight is likely to be due to different degrees of aggregation.

In contrast to ferricyanide oxidation, ambient exposure to oxygen leading to the formation of a 3Fe form appears to result in a less heterogeneous mixture of products. When run on a G-75 molecular weight exclusion column the protein elutes as one main band having a molecular weight of about 48000 . The UV-visible absorption spectrum of this protein was obtained and assayed with Bradford reagent (Bio-Rad) to ascertain the number of iron-sulfur centers in the protein aggregate. These results, shown in Table X indicate that there is one peptide for every iron-sulfur center present in the molecule. Therefore , the likely structure for this oxidation product is a octomer containing eight iron-sulfur centers. Unfortunately, it is not possible to determine how the iron-sulfur centers are distributed in this complex protein aggregate.

CONCLUSION

The data presented here provides evidence that oxidation of the 2(4Fe-4S) centers in CP and CAU 8Fe Fd, either by potassium ferricyanide or air leads to the

Table X. Tabulated data of Bio-Rad assay for air oxidized 3Fe converted Clostridium pasteurianum 8Fe ferredoxin

TABLE X

volume (ul) unknown ferredoxin	Bio-Rad A_{595} (1:155 diln)	ug unknown ferredoxin/ ml solution	moles ferredoxin/ L solution	A_{400}	E/ mole Fd
20	.135	2325	3.87×10^{-4}	5.6	14500
40	.270	2300	3.83×10^{-4}	5.6	14600
40	.249	2100	3.50×10^{-4}	5.6	16000

formation of a protein containing a 3Fe center. NMR spectroscopy indicates the ligand environment about this iron-sulfur center must be in a unique environment with respect to normal 3Fe centers. This difference might arise from different ligand conformations of the cysteinyl sulfurs around this iron-sulfur center. For potassium ferricyanide oxidized 8Fe ferredoxin it appears that a heterogeneous population of proteins are formed containing variable amounts of iron, sulfide and peptide. For air oxidized ferredoxin, a much less heterogeneous population is observed. It appears the major species formed under these conditions is likely to be a octomer containing eight iron-sulfur centers. The results also indicate that conversion of the 4Fe-4S center into a 3Fe center occurs spontaneously under normal aerobic conditions in the clostridial-type 8Fe ferredoxins.

V. NMR of Clostridium acidi-urici ferredoxin and rubredoxin

NMR spectroscopy has been widely used to characterize Fe-S proteins. This is due in large part to the paramagnetic Fe-S centers present in these proteins. The paramagnetic Fe-S center causes nearby protons to be downfield shifted out of the aliphatic and aromatic envelopes. In addition, a broadening is associated with these downfield resonances , due to a decreased proton relaxation time , which arises from paramagnetic contributions from the Fe-S center. Those protons close to the Fe-S center will be most downfield shifted.

Although the ^{1}H-NMR of many iron-sulfur proteins have been reported, little is known about the actual resonance assignments for these spectra. However, the ^{1}H-NMR is still of great value because it serves as a fingerprint that can in many cases differentiate the 2Fe, 3Fe and 4Fe centers in various ferredoxins (67,68,69). Although there have been papers citing theoretical NMR assignments, the only NMR assignment of any ferredoxin based on actual isotopic incorporation was reported (34) by Packer et al. , in 1977 in the 8Fe ferredoxin from Clostridium acidi-urici. The authors reported that the eight most downfield resonances arose from single beta-cysteinyl hydrogens bound to the 4Fe-4S center. However , the

assignments of all sixteen of the expected resonances could not be determined. In the same report, the assignments for the 3'-5'-^{2}H-tyrosine resonances were also made by isotopic incorporation. These resonances , as expected , fell in the aromatic envelope. The experiments presented in this section involve direct assignment of the alpha-cysteinyl hydrogens in the ^{1}H-NMR spectrum of Clostridium acidi-urici 8Fe ferredoxin in the oxidized form. Also presented in this section are experiments involving the isolation and characterization of a newly discovered rubredoxin protein from this bacteria.

RESULTS AND DISCUSSION

A. Assignment of alpha-cysteinyl resonances in the ^{1}H-NMR of Clostridium acidi-urici 8Fe ferredoxin

Clostridium acidi-urici bacteria will uptake alpha-^{2}H-DL-cystine from an enriched medium and incorporate it directly into the 2(4Fe-4S) ferredoxin as L-cysteine as indicated by ^{2}H-NMR (Figure LIII). The ^{2}H-NMR spectrum of the enriched protein shows a natural abundance water peak around 4.8 ppm and a very broad resonance from 6-10 ppm. This broad peak arises from the overlap of several resonances and gives clear evidence for direct isotope incorporation into the protein. To determine the actual resonances arising from alpha-cysteinyl hydrogens in the

Figure LIII. ^{2}H-NMR of alpha-^{2}H-L-cysteine labelled *Clostridium acidi-urici* 8Fe ferredoxin

Conditions: 3 mg/ml protein in .050 M K_2HPO_4 in deuterium depleted H_2O, pH 7.45 , temperature , 28^{o}C, 25000 scans, pulse delay ,0.100 seconds, Spectrum was referenced relative to the natural abundance water peak (4.80 ppm).

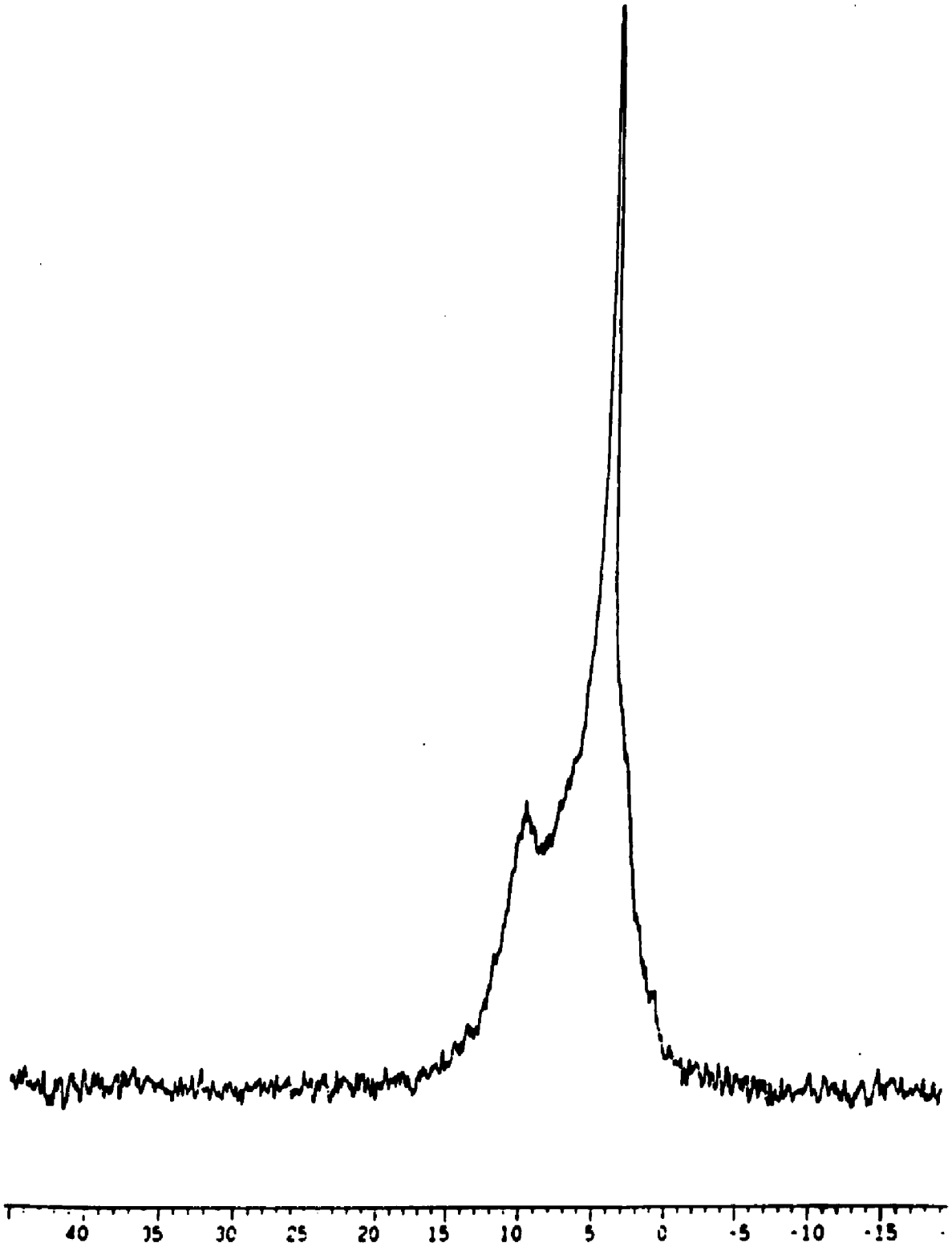
40
35
30
25
20
15
10
5
0
-5
-10
-15

^{1}H-NMR spectrum , the NMR spectrum of the enriched and the normal protein was acquired and compared (Figure LIV). In addition, the difference spectrum for normal and labeled ferredoxin is shown in Figure LV. Specifically, three downfield resonances are diminished in intensity. The most downfield peaks at 10.2 and 9.8 ppm diminish in intensity by about 40%. This indicates a 40% labeling of the protein. Since Packer (34) et al. , showed nearly full incorporation in similar experiments , it remains unclear as to why the level of incorporation in these experiments was lower. The narrow downfield peaks corresponding to single alpha-cysteinyl hydrogens are grouped within an envelope of resonances consisting of beta-cysteinyl hydrogens and exchangable hydrogens, presumably from amide protons. Another alpha-cysteinyl hydrogen is downfield shifted about 3 ppm from its normal expected position to 7.6 ppm. The remaining five resonances arising from the alpha-cysteinyl hydrogens are likely to be buried in the aliphatic envelope. These results are consistent with the beta-cysteinyl labeling experiments which showed that half of the beta-hydrogens were downfield shifted (34) .

B. Isolation and characterization of rubredoxin from Clostridium acidi-urici

In the course of characterizing the isotopically

Figure LIV. ^{1}H-NMR spectrum of native and alpha-2^{H}-L-cysteine labelled <u>Clostridium acidi-urici</u> 8Fe ferredoxin

Conditions: 6 mg/ml protein in 0.070 M K_2HPO_4/0.050 M NaCl in D_2O (99.9% atom), pH_{meter} 7.43, temperature 25°C, 5000 scans, pulse delay, 0.100 seconds. Spectra were referenced relative to DSS .

Arrows indicate resonances that have dimished in intensity and represent alpha-labelled cysteinyl hydrogens.

Top spectrum - unlabeled protein

bottom spectrum - labeled protein

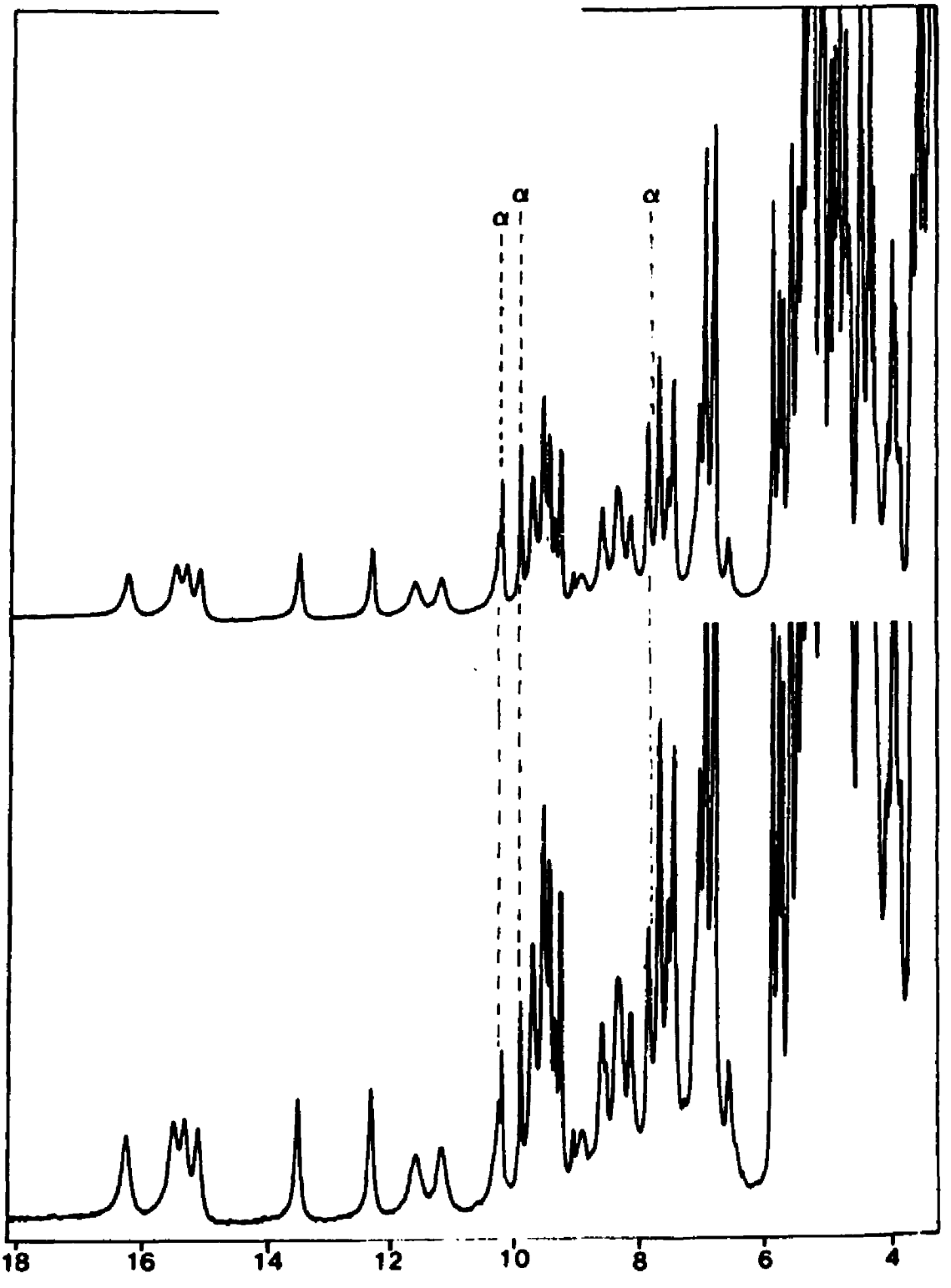
α
α
α
18
16
14
12
10
8
6
4
PPM

Figure LV. Difference spectrum for native and ^{2}H-L-cysteine labelled Clostridium acidi-urici 8Fe ferredoxin.

Bottom spectra (labelled protein) is subtracted from normal native protein.

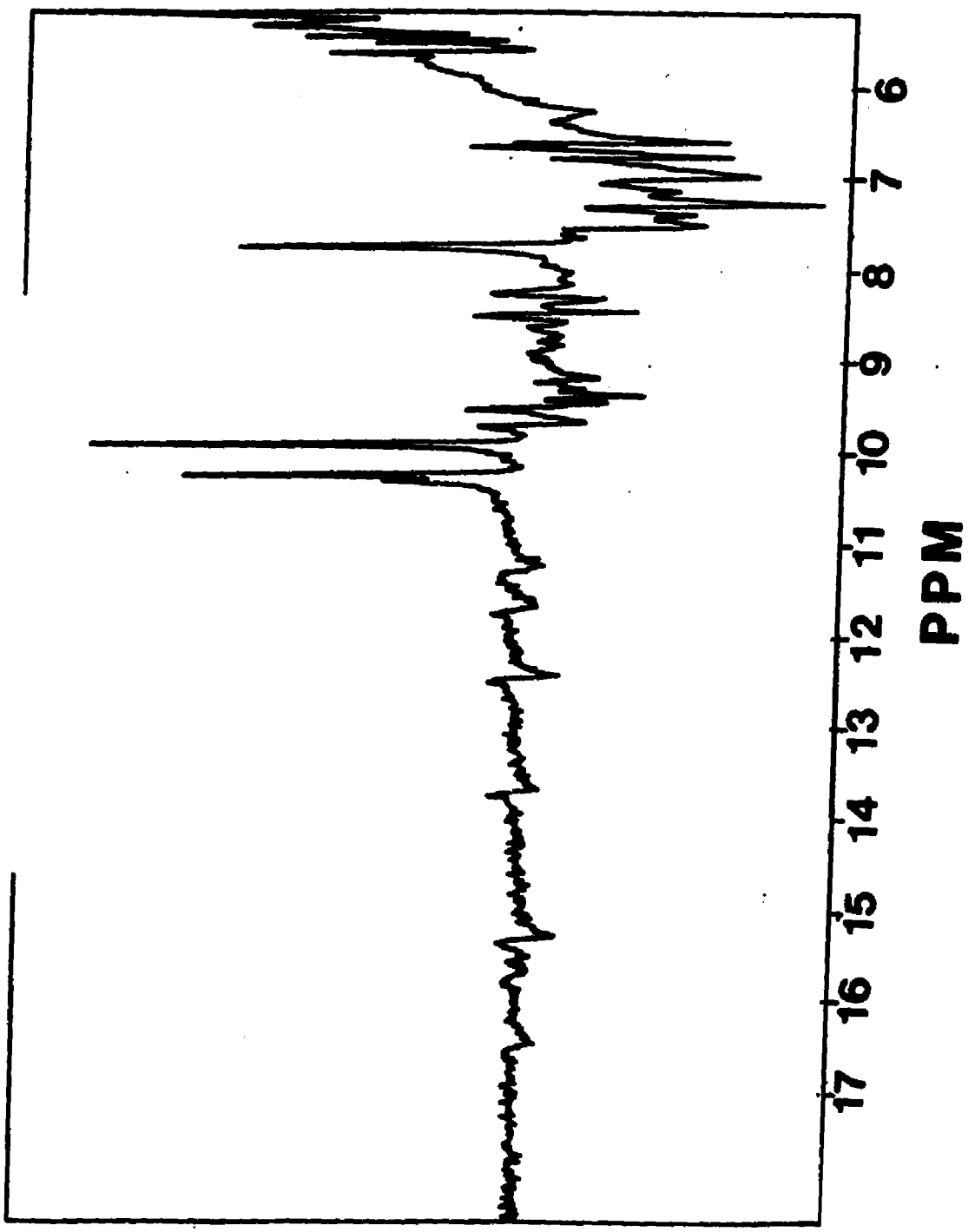
6
7
8
9
10
11
12
13
14
15
16
17
PPM

labeled ferredoxin from Clostridium acid-urici , it was discovered that the bacteria produced a rubredoxin protein. The isolation of this protein has never been reported in the literature. Although rubredoxin is produced it is produced in such small amounts under the growth conditions described that detecting the protein was only possible during large protein isolations. The separation and purification of this protein is identical to the procedure used for the isolation of rubredoxin from Clostridium pasteurianum. The UV-visible spectrum for the oxidized form of the protein is shown in Figure LVII , along with rubredoxin from Clostridium pasteurianum (Figure LVI). The spectral features of these proteins are virtually identical. The purity ratio A_{280}/A_{490} , for CAU rubredoxin was 2.73, as compared to 2.55 for CP rubredoxin. The molecular weight of CAU rubredoxin as determined by molecular gel-exclusion chromatography was approximately 6000 daltons, identical to that of CP rubredoxin. The ^{1}H-NMR spectra of oxidized and reduced CAU rubredoxin are shown in Figures LVIII and LIX , respectively. The general spectral features of CAU rubredoxin are very similar but not identical to CP rubredoxin (Figures LX and LXI). These results are likely to indicate similar chemical environments around the iron atoms in the two proteins.

Figure LVI. UV-visible absorption spectrum of oxidized rubredoxin protein from Clostridium pasteurianum

Conditions: 0.10 mg/ml protein in 0.10M Tris/ 0.10M NaCl, pH 7.4, spectral width 700-250 nm.

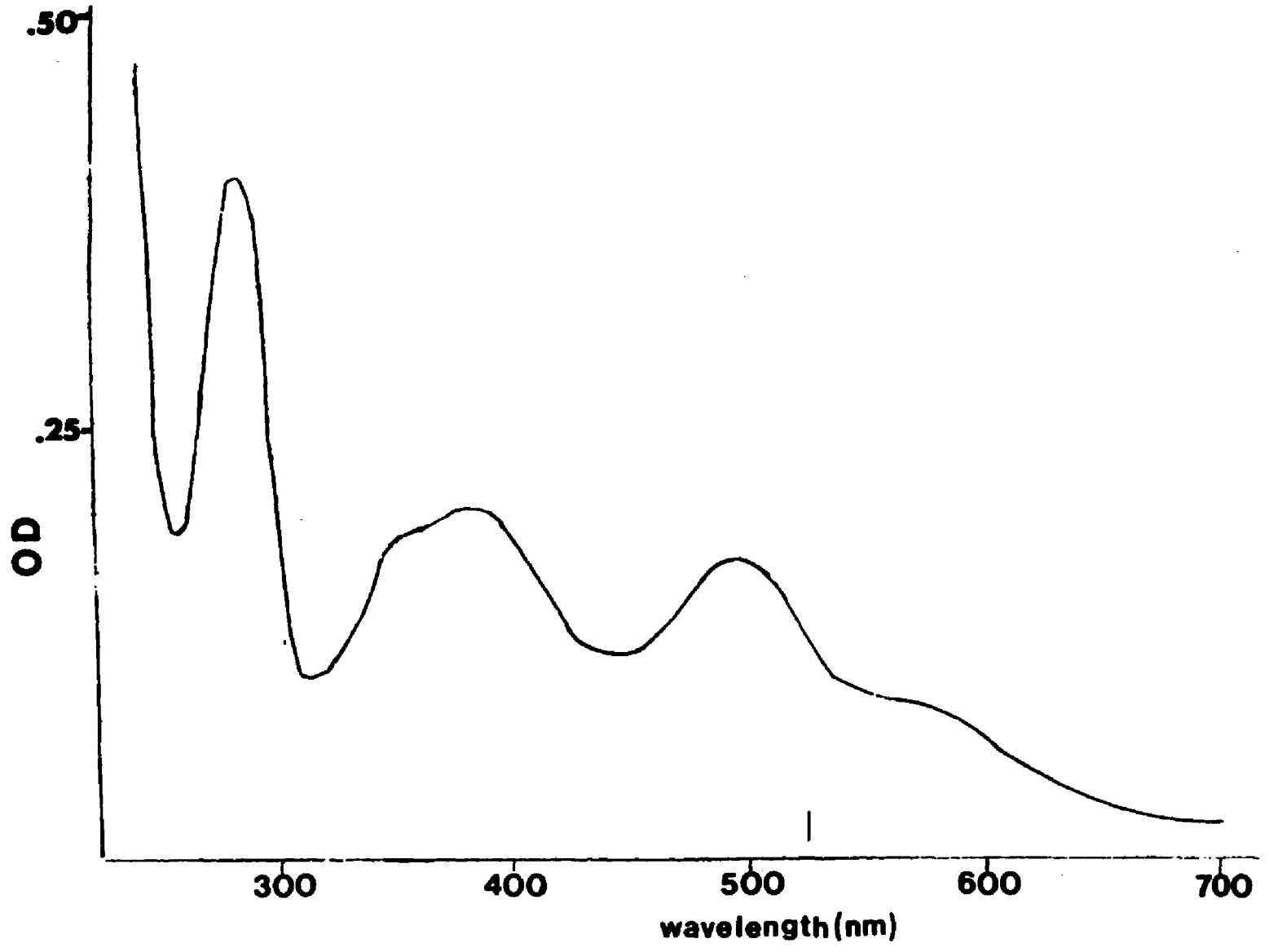
.50
.25
OD
300
400
500
600
700
wavelength (nm)

Figure LVII. UV-visible absorption spectrum of oxidized rubredoxin protein from Clostridium acidi-urici

Conditions: 0.10 mg/ml protein in 0.10M Tris/ 0.10M NaCl, pH 7.4, spectral width 700-250 nm.

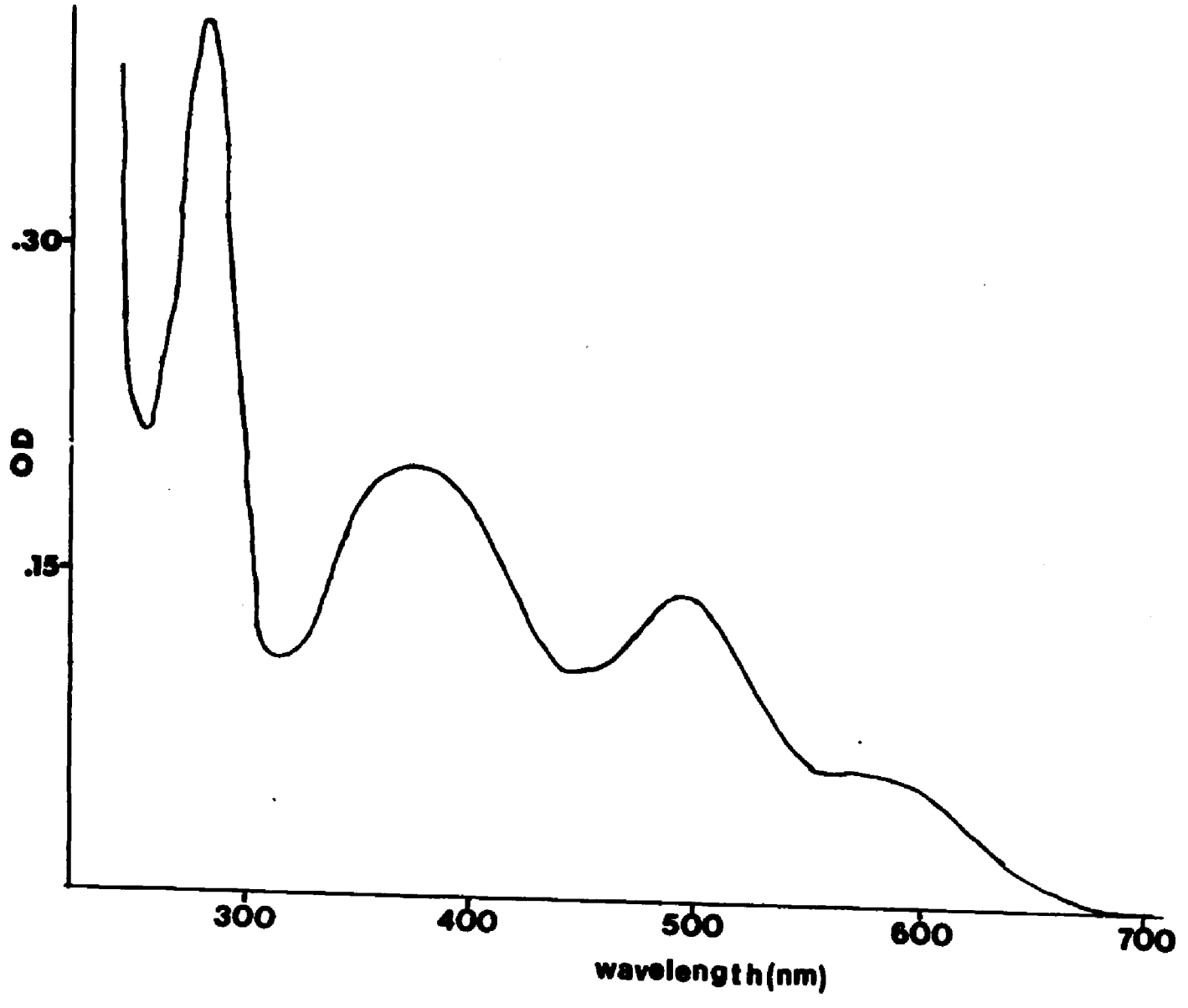
.30
OD
.15
300
400
500
600
700
wavelength(nm)

Figure LVIII. 400 MHz ^{1}H-NMR spectrum of oxidized rubredoxin from Clostridium acidi-urici

Conditions: 6 mg/ml protein in 0.050 M K_2HPO_4/ 0.050 M NaCl in D_2O (99.9% atom), pH_{meter} 7.38 , temperature 25°C, 5000 scans, 32000 points, pulse delay 0.10 seconds, acquisition time, 0.568 sec. Spectra were referenced relative to water (4.80 ppm).

PPM
12 11 10 9 8 7 6 5 4 3 2 1 0 -1 -2 -3 -4 -5 -6 -7 -8 -9 -10 -11 -12
17 16 15 14 13 12 11 10 9 8 7 6 5 4 3 2 1 0

Figure LIX. ^{1}H-NMR spectrum of dithionite reduced *Clostridium acidi-urici* rubredoxin protein

Conditions: same as Figure LVIII

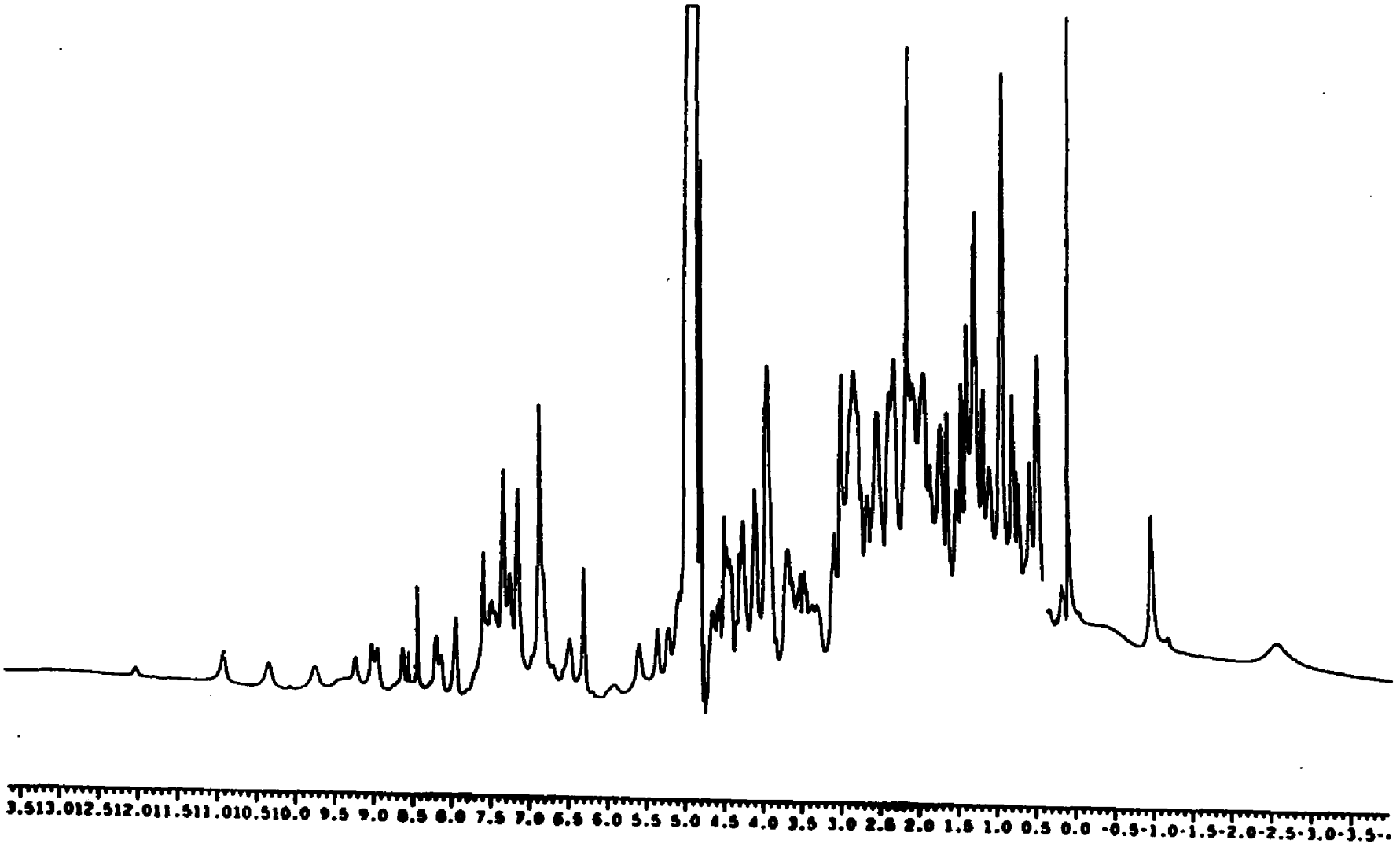
221
3.513.012.512.011.511.010.510.0 9.5 9.0 8.5 8.0 7.5 7.0 6.5 6.0 5.5 5.0 4.5 4.0 3.5 3.0 2.5 2.0 1.5 1.0 0.5 0.0 -0.5-1.0-1.5-2.0-2.5-3.0-3.5-

Figure LX. ^{1}H-NMR spectrum of oxidized Clostridium pasteurianum rubredoxin

Conditions: 8 mg/ml protein in .040 M K_2HPO_4/ 0.050 M NaCl in D_2O (99.9 % atom), pH 7.40 , temperature , 25°C, 5000 scans, 32000 points, pulse delay, 0.100 seconds, acquisition time , 0.568 seconds. Spectrum was referenced relative to water (4.80 ppm).

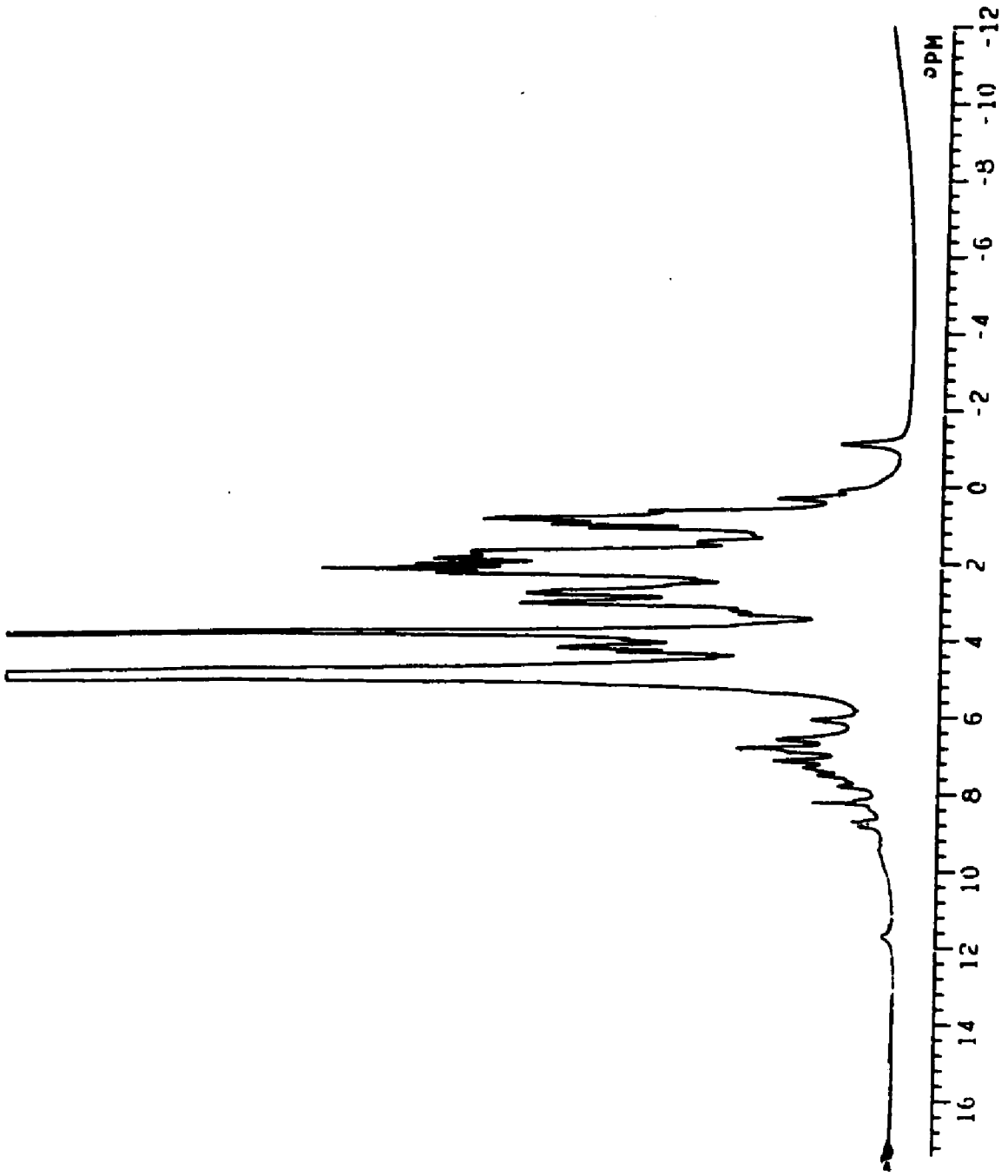
PPM
16
14
12
10
8
6
4
2
0
-2
-4
-6
-8
-10
-12

Figure LXI. ^{1}H-NMR spectrum of dithionite reduced *Clostridium pasteurianum* rubredoxin protein

Conditions: same as Figure LX

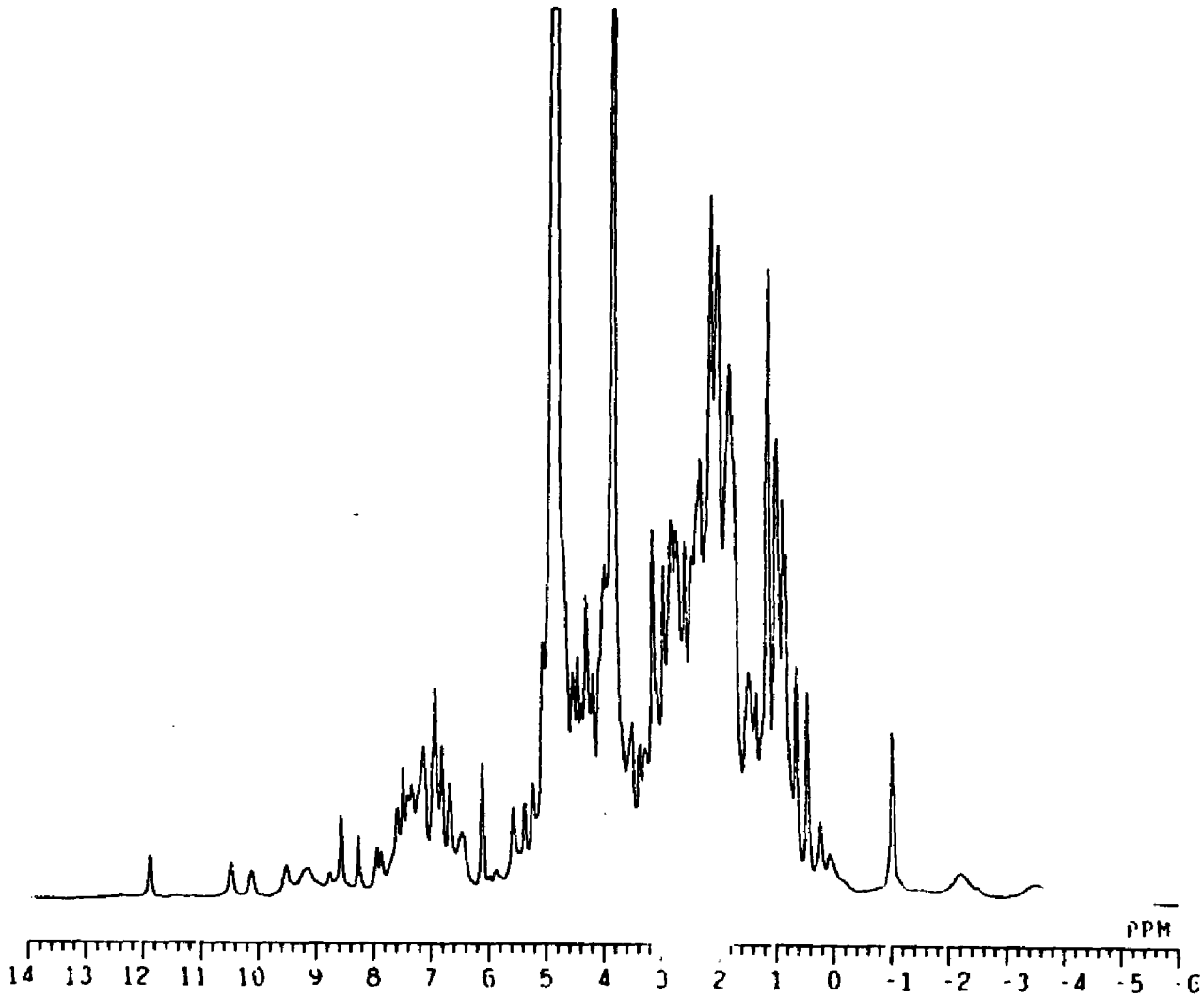
PPM
14 13 12 11 10 9 8 7 6 5 4 3 2 1 0 -1 -2 -3 -4 -5 -6

SUMMARY

This dissertation presented an examination of various chemical, physical and spectroscopic properties of the 2(4Fe-4S) ferredoxins from Clostridium acidi-urici and Clostridium pasteurianum. The major focus of this manuscript concerned itself with chemical modification experiments involving reductive methylation of Clostridium pasteurianum 8Fe ferredoxin using $^{13}CH_2O$ and $NaCNBH_3$.

^{13}C-NMR titrations of the methylated amines revealed the pKa values for the N-terminal alanine residue were virtually identical in the oxidized and reduced ferredoxin, as were the values obtained for the Lys^3 residue. The results indicate the amines do not play a role in oxidation-state dependent proton binding and therefore provide additional evidence against the existence of a pH dependent midpoint reduction potential in this protein. Subsequently, a reexamination of previous experiments reporting a pH dependent E_m showed that the original conclusions reached were in error and that it is unlikely a pH dependence exists in Clostridium pasteurianum 8Fe ferredoxin.

Reductive methylation also revealed that the N-terminal alanine with a pKa of 9.4 is in an ion pair and is likely to be responsible in part for maintaining the intrinsic stabilty of the protein. In addition, the well resolved chemical shift differences between the N-terminal

^{13}C-resonance in oxidized and apoferredoxin made it possible to assign a quantitative relationship between the UV-visible absorption purity ratio, A_{390}/A_{280}, with the amounts of native and denatured protein in mixtures of partially denatured protein.

Additional chemical modification experiments are also presented which examine the effects on Clostridium pasteurianum and Clostridium acidi-urici 8Fe ferredoxin when the protein is chemically modified using $K_3Fe(CN)_6$. The results indicate that $K_3Fe(CN)_6$ treatment can lead to the formation of a heterogeneous population of altered 3Fe proteins containing varying amounts of peptide and iron. A similar conversion of the 4Fe-4S centers into the 3Fe type was observed by prolonged exposure to air. This conversion, however, led to the formation of a more homogeneous population of peptide whose Fe-S content and molecular weight analysis is consistent with an octomer containing eight iron-sulfur centers. The ^1H-NMR spectrum of the ferricyanide treated ferredoxin showed the 3Fe center formed in the interconversion process has a different chemical enviroment around the Fe-S center compared with other proteins containing known 3Fe-4S centers.

Finally, experiments whereby Clostridium acidi-urici was grown on L-alpha-^2H-cysteine and the 8Fe ferredoxin isolated was subjected to ^2H and ^1H-NMR spectroscopic analysis were presented. Direct assignment of three of

the eight alpha-cysteinyl proton resonances at 10.2, 9.8 and 7.8 ppm , respectively, were identified. The remaining five resonances were presumably buried within the aliphatic envelope and could not be identified. Also presented is a preliminary report on the isolation and partial characterization of a rubredoxin protein isolated from Clostridium acidi-urici. The molecular weight, UV-visible and ^{1}H-NMR spectra of this protein are very similar to rubredoxin isolated from Clostridium pasteurianum , for which an x-ray structure is known.

REFERENCES

1. Lovenberg, W., ed., (1977) Iron-Sulfur Proteins , Vols. 1, 2, 3., Academic Press, New York .

2. Dreyer, Jean-Luc. (1982) Experimentia 38,521-529.

3. Yoch, D.C. and Carithers, R.P. (1979) Microbiol. Rev. 43, 384-421 .

4. Kerschier, L. and Oesterhelt, D. (1977) FEBS Lett. 83 , 197-201 .

5. Meyer, J., Bruschi, M.H., Bonicel, J.J., and Gisele E. Bovier-Lapierre (1986) Biochemistry 25 , 6054-6061.

6. Brintzinger, Hans., Palmer, G. and Sands, Richard H., (1966) Biochemistry 5 , 397-404 .

7. Johnson, C.E., Commack, R., Roa, K.K., and Hall, D.O. (1971) Biochem. Biophys. Res. Commun. 43 , 564-571.

8. Tsukihara, T., Fukuyama, K., Nakamura, M., Katsube, Y., Tanaka, N., Kakudo, M., Wada, K., Hase, T. and Matsubara, Hiroshi (1981) J. Biochem. 90 , 1763-1773.

9. Johnson, M.K., Bennett, D.E., Morningstar, J.E., Adams, M.W.W., and Mortenson, L.E. (1985) J. Biol. Chem. 260 , 5456-5463.

10. Nagayama, K., Ohmori, D., Imai, T., and Oshima, T. (1983) FEBS 158 , 208-212.

11. Stout, G.H., Turley, S., Sieker, L.C., and Jensen, L.H. (1988) Proc. Natl. Acad. Sci. USA 85 , 1020-1022.

12. Robbins, A.H., and Stout, Charles D. (1985) J. Biol. Chem. 260 , 2328-2333.

13. Thompson, C.L., Johnson, C.E., Dickson, D.P.E., Commack, R., Hall, D.O., Weser, V. and Roa, K.K. (1974) Biochem J. 139 , 97-103 .

14. Adams, M.W.W., Johnson, M.K., Zambrano, I.C., and Mortenson, L.E. (1986) Biochimie 68 , 35-41 .

15. Paech, C., Reynolds, J.G., Singer, T.P., and Holms, Richard H. (1981) J. Biol. Chem. 256 , 3167-3170 .

16. Carter, C.C., Kraut, J., Freer, S.T. and Alden, Richard A. (1974) J. Biol. Chem. 249 , 6339-6346 .

17. Mortenson, L.E., Valentine, R.C. and Carnahan, J.E. (1962) Biochem. Biophys. Res. Commun. 7 , 448-452 .

18. Valentine, R.C., Brill, W.J.,and Jagers, R.D. (1963) Biochem. Biophys. Res. Commun. 12 , 315-321 .

19. Tanaka, M., Nakashima, T., Benson, A., Mower, H. and Kerry, T. (1966) Biochemistry 5 , 1666-1680 .

20. Rall, S.C., Bolinger, R.E. and Cole, David E. (1969) Biochemistry 8 , 2486-2498 .

21. Tsunoda, J.N., Yasunobu, K.T., and Whiteley, H.R. (1968) J. Biol. Chem. 243 , 6262-6272 .

22. Orne-Johnson, W.H. (1973) Ann. Rev. Biochem. 42 , 159-204 .

23. Raeburn, S. and Rabinowitz, Jesse C. (1971) Archives of Biochem. and Biophys. 146 , 9-20.

24. Telser, J., Benecky, M.J., Adams, M.W.W., Mortenson, L.E. and Hoffman, B.M. (1987) J. Biol. Chem. 262 , 6589-6594 .

25. Lode, E.T., Murray, C.L., Sweeney, W.V. and Rabinowitz, Jesse C. (1974) Proc. Natl. Acad. Sci. USA 71 , 1361-1365 .

26. Lode, E.T., Murray, C.L. and Rabinowitz, J.C. (1976) J. Biol. Chem. 251 , 1683-1689 .

27. Magliozzo, R.S., McKintosh, B.A. and Sweeney, W.V. (1982) J. Biol. Chem. 257 , 3506-3509 .

28. Johnson, M.K., Spiro, T.G. and Mortenson, L.E. (1982) J. Biol. Chem. 257 , 2447-2452 .

29. Lutz, Marc., Moulis, J.M. and Meyer, J. (1983) FEBS 163 , 212-216 .

30. Macor, K.A., Czernuszewicz, R.S., Adams, M.W.W. and Spiro, T.G. (1987) J. Biol. Chem. 262 , 9945-9947.

31. Thomson, A.J., Robinson, A.E., Johnson, M.K., Commack, R., Roa, K.K. and Hall, D.O. (1981) Biochimica et Biophysica Acta. 637 , 423-432 .

32. Johnson, M.K., Bennett, D.E., Fee, J.A. and Sweeney, W.V. (1987) Biochimica et Biophysica Acta. 911 , 81-94 .

33. Mathews, R., Charlton, S., Sands, R. and Palmer, G. (1974) J. Biol. Chem. 249 , 4326-4336 .

34. Packer, E.L., Sweeney, W.V., Rabinowitz, J.C., Sternlicht, H. and Shaw, Elliot N. (1977) 25 , 2245-2253 .

35. Thompson, C.L., Johnson, C.E., Dickson, D.P.E., Cammack, R., Hall, D.O., Weser, V. and Roa, K.K. (1974) J. Biochem. 139 , 97-106 .

36. Carter, C.W., Kraut, J., Freer, S.T., Alden, R.A., Sieker, L.C., Adman, E.T. and Jensen, Lyle H. (1976) Proc. Natl. Acad. Sci. USA 69 , 3526-3535 .

37. Stombaugh, N.A., Sundquist, J.E., Burris, R.H. and Orne-Johnson, W.H. (1976) Biochemistry 15 , 2633-2641 .

38. Mizrahi, I.A., Wood, F.E. and Cusanovich, M.A. (1976) Biochemistry 15 , 343-349 .

39. Sweeney, W.V. and McIntosh, B.A. (1979) J. Biol. Chem. 254 , 4499-4501 .

40. Packer, E.L., Sternlicht, H., Lode, E.T. and Rabinowitz, J.E. (1975) J. Biol. Chem. 260 , 2062-2072.

41. Hong, J.S. and Rabinowitz , J.C. (1970) J. Biol. Chem. 245 , 4982-4987 .

42. Sweeney, W.V. (1974) BBRC 59 , 188-194 .

43. Kent, T.A., Dreyer, J.L., Kennedy, M.C., Huynh, B.H., Emptage, M.H., Beinert, H. and Munck, E. (1982) Proc. Natl. Acad. Sci. USA 79 , 1096-1100 .

44. Chen, J.S. and Mortenson , Leonard E. (1974) Biochim. et Biophysica Acta. 371 , 283-298 .

45. Chen, J.S. and Blanchard , D.K. (1978) Biochem. Biophys. Res. Commun. 84 , 1144-1150 .

46. Adman, E.T., Sieker, L.C. and Jensen, L.H. (1973) J. Biol. Chem. 248 , 3978-3996 .

47. Rabinowitz , Jesse C. (1972) Methods in Enzymology 24 , 431-446 .

48. Jentoft, N. and Dearborn , D.G. (1983) Methods in Enzymology 91 , 570-579 .

49. Wood, J.L., and DuVigneaud, V. (1939) J. Biol. Chem. 131 , 267-274.

50. Adzamli, I.K. , Henderson, R.A., Sinclair-Day, J.D. and Sykes, A.G. (1984) Inorg. Chem. 23 , 3069-3073.

51. Job, R.C. and Bruice, T.C. (1975) Proc. Natl. Acad. Sci. USA 72 , 2478-2482 .

52. Tanaka, K., Moriya, M. and Tanaka, T. (1986) Inorg. Chem. 25 , 835-838 .

53. Tsai, H., Sweeney, W.V.S. and Coyle, C.L. (1985) Inorg. Chem. 24 , 2796-2798.

54. Ingledew, W.J. and Ohnishi, T. (1980) Biochem. J. 186 , 111-117 .

55. Prince, R. and Adams, M.W.W. (1988) J. Biol. Chem. 262 , 5125-5128 .

56. Gerken, T.A., Jentoft, J.E., Jentoft, N. and Dearborn, D.G. (1982) J. Biol. Chem. 257 , 2894-2900.

57. Jentoft, J.E., Gerkin, T.A., Jentoft, N. and Dearborn, D.G. (1981) J. Biol. Chem. 256 , 231-236.

58. Jentoft, J.E., Jentoft, N., Gerkin, T.A. and Dearborn, D.G. (1979) J. Biol. Chem. 254 , 4366-4370.

59. Bradbury, J.H. and Brown, L.R. (1973) Eur. J. Biochem. 40 , 565-576 .

60. Gerken, T.A. (1984) Biochemistry 23 , 4688-4697 .

61. Sherry, A.D. and Teherani, J. (1983) J. Biol. Chem. 258 , 8663-8669 .

62. Goux, W.J., Teherani, J. and Sherry, A.D. (1984) Biophys. Chem. 19 , 363-373 .

63. Sherry, A.D., Keepers, J., James, T.L. and Teherani, J. (1984) Biochemistry 23 , 3181-3185 .

64. Hong, J.S. and Rabinowitz, J.C. (1970) J. Biol. Chem. 245 , 4982-4987 .

65. Adman, E.T., Sieker, L.C. and Jensen, L.H. (1976) J. Biol. Chem. 251 , 3801-3806 .

66. Fee, J.A., Mayhem, S.G. and Palmer, G. (1971) Biochem. Biophys. Acta. 245 , 196-200 .

67. Adman, E.T., Sieker, L.C. and Jensen, L.H. (1973) J. Biol. Chem. 248 , 3978-3996 .

68. Poe, M., Phillips, W.O., McDonald, C.C. and Lovenberg, W. (1970) Proc. Natl. Acad. Sci. USA 65 , 797-804 .

69. Nagayama, K., Imai, T., Ohmori, D. and Oshina, T. (1984) FEBS 169 , 79-84 .

70. Nagayama, K., Ozaki, Y., Kyogoku, Y., Hase, T. and Matsubara, H. (1983) J. Biochem. 94 , 893-902 .

71. Stephens, P.J., Morgan, J.V. and Burgess, B.K. (1986) Frontiers of Bioinorganic Chemistry (Xavier, A.V. ed.), pgs. 637-646 VCH Publishers, Weinhein .

72. Emptage, M.H., Dreyer, J.L., Kennedy, M.C. and Beinhart, H. (1985) J. Biol. Chem. 258 , 11106-11111.